

# Spatiotemporal cat: a chaotic field theory

P Cvitanović and H Liang

Center for Nonlinear Science, School of Physics, Georgia Institute of Technology,  
Atlanta, GA 30332-0430, USA

E-mail: [predrag.cvitanovic@physics.gatech.edu](mailto:predrag.cvitanovic@physics.gatech.edu)

1 December 2020

## Abstract.

While the global dynamics of an extended, spatiotemporally turbulent system can be extraordinarily complex, the local dynamics, observed through small spatiotemporal windows, can be thought of as a visitation sequence through a finite repertoire of finite patterns. To compute spatiotemporal expectation values of observables from the defining equations of such systems, one needs to know how often a given pattern occurs. Here we address this fundamental question by constructing a spatiotemporal cat, a classical  $d$ -dimensional chaotic lattice field theory. Treating the temporal and spatial directions on equal footing, we abandon initial state evolution, local in time, and enumerate instead global solutions compatible with system's defining equations. In such field theory any spatiotemporal state is labeled by a unique  $d$ -dimensional lattice block of symbols from a finite alphabet, a state of the system over a finite spatiotemporal region is specified uniquely and with exponential precision by a finite blocks of such symbols, and the likelihood of such state occurring is given by the Hill determinant of its spatiotemporal orbit Jacobian matrix.

PACS numbers: 02.20.-a, 05.45.-a, 05.45.Jn, 47.27.ed

Submitted to: *Nonlinearity*

A temporally chaotic system is exponentially unstable with time: double the time, and exponentially more orbits are required to cover its strange attractor to the same accuracy. For large spatial extents, the complexity of the spatial shapes also needs to be taken into account; double the spatial extent, and exponentially as many distinct spatiotemporal patterns will be required to describe the repertoire of system's shapes to the same accuracy. The systems whose temporal and spatial correlations decay sufficiently fast, and whose “physical” dimension [67, 87] grows with system size, are said to be “spatiotemporally chaotic.”

Our goal here is to make this “spatiotemporal chaos” tangible and precise, by offering the reader what we believe is its simplest explicit example, the *spatiotemporal cat* [96, 99] (a screened Poisson or Yukawa equation)

$$(\square - d(s - 2)) \Phi = -M,$$

a classical field theory on a  $d$ -dimensional hyper-cubic lattice, with an “anti-harmonic” rotor  $\phi_z$  at each site  $z$  coupled to its nearest neighbors. In contrast to a field governed by its close relative, Helmholtz equation, with oscillatory solutions, spatiotemporal cat solutions are hyperbolic and ‘turbulent’, in the same sense that in contrast to stable oscillations of a harmonic oscillator, Bernoulli coin flip solutions are unstable and chaotic.

Spatiotemporally homogenous turbulent flows offer one physical motivation for considering such models: a very rough approximation to such flows is discretizing them into spatiotemporal cells, with each cell turbulent, and cells coupled to their nearest neighbors. Spatiotemporal cat is arguably the simplest such model, no closer to physical turbulence than the Lorenz model [152] is to weather, but still capturing the essential qualitative features of spatiotemporal chaos.

The main thrust of this paper is, however, more radical: we’ve been doing ‘turbulence’ all wrong, and we know that since Poincaré’s times. In “explaining” chaos we talk the talk as though we have never moved beyond Newton; here is an initial state of a system, local in time, and here are the differential equations that evolve it forward in time. But when we -all of us- do the work, we do something altogether different, closer to Lagrange, and to the 20th century ‘spacetime’ physics. This paper realigns the theory to what we actually *do* when solving “chaos” equations, using not much more than linear algebra. In this formulation, there is no time, and there is no “Lyapunov” horizon; every solution  $\Phi$  is a global solution of a spatiotemporal fixed point condition  $F[\Phi] = 0$ , and there is no exponential blowup of anything.

As we shall here have to traverse territory unfamiliar to many, we follow Mephistopheles pedagogical dictum “You have to say it three times” [90], and sing our song thrice.

The first time, for a reader too busy [53] to read the book [58], we disguise a brief course on chaos theory as something everyone understands, a Bernoulli coin toss, section 1. In section 1.2 we introduce the ‘temporal Bernoulli’, a lattice reformulation of the Bernoulli map. The deep insight here is the realization that the *Hill determinant*, i.e., the volume (16) of the *orbit Jacobian matrix* (figure 2, 3 and 4) counts all global solutions of given defining equations.

The second time, as a ‘temporal cat’, a 1-dimensional lattice of rotors that all dynamicists understand, section 2. In section 2.1 we review the traditional cat map in its Hamiltonian formulation (but relegate to Appendix C the explicit Adler-Weiss generating partition of the cat map phase space). In section 2.2 we introduce the ‘temporal cat’, a lattice reformulation of the cat map. The periodic orbits theory of cat maps can be developed in either formulation: both the forward-in-time Hamiltonian cat map, Appendix C.2, and the Lagrangian temporal cat lead to the same topological zeta function (68) count of *prime* periodic orbits, with the two formulations related by Hill’s formula (67).

The third time, herding cats all over spacetime, as a field theory similar to ones studied by statistical mechanics and field theorists, section 3. In section 3.1 we

review the traditional coupled map lattice model discretizations of dissipative PDEs, as well as many-body Hamiltonian models, section 3.2. In section 3.3 we generalize the temporal cat model to the  $d$ -dimensional *spatiotemporal* cat, and in section 3.5 show that the system admits a  $d$ -dimensional symbolic code with a finite alphabet. We then turn to study of admissible finite spatiotemporal symbol blocks. The key to solution counting problem is the enumeration of *prime* periodic orbits, with the notion of ‘prime’ now subtler than what it was for 1-dimensional lattices, different for the integer lattice coordinate system, section 3.6, from periodic orbits, i.e., the fields over these coordinates, section 3.7. Section 3.8 illustrates our periodic orbit spatiotemporal cat solutions by several explicit examples. In section 3.10 we use the spatiotemporal cat symbolic dynamics to show that spatiotemporal periodic orbits that share finite spatiotemporal symbol blocks shadow each other to exponential precision (the symbolic dynamics definitions used throughout the paper are collected in Appendix F).

Section 4 tabulates our prime periodic orbits counts. Hill’s formula for the 2-dimensional lattice spatiotemporal cat is derived in section 5.3. We evaluate and cross-check Hill determinants by two methods, either the ‘fundamental fact’ evaluation, section Appendix A.4.3, or by the discrete Fourier transform diagonalization, Appendix A.

The results are summarized and some open questions discussed in the section 6.

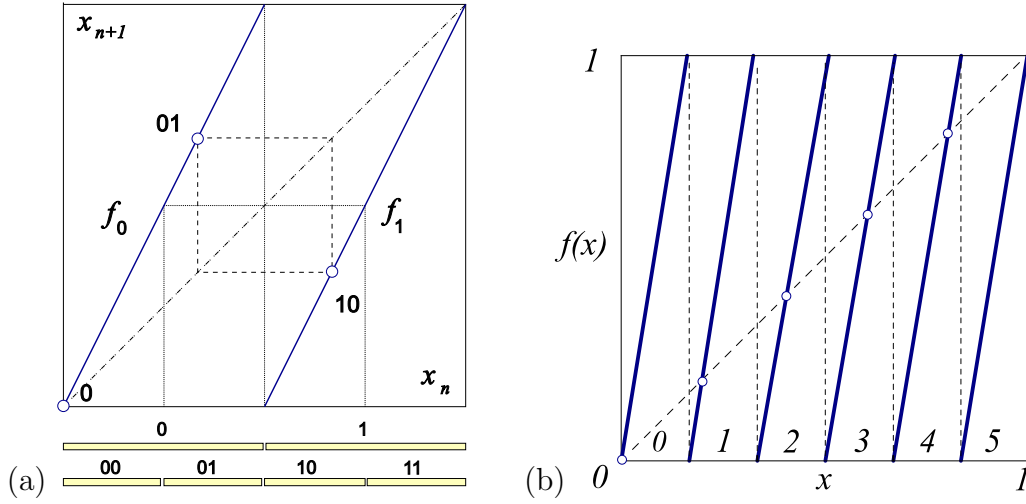


**Figure 1.** (a) The ‘coin toss’ map (1), together with the  $\bar{0}$  fixed point, and the  $\bar{01}$  2-cycle. Preimages of the critical point  $x_c = 1/2$  partition the unit interval into  $\{\mathcal{M}_0, \mathcal{M}_1\}$ ,  $\{\mathcal{M}_{00}, \mathcal{M}_{01}, \mathcal{M}_{10}, \mathcal{M}_{11}\}$ ,  $\dots$ , subintervals. (b) The base- $s$  Bernoulli map, here with the ‘dice throw’ stretching parameter  $s = 6$ , partitions the unit interval into 6 subintervals  $\{\mathcal{M}_m\}$ , labeled by the 6-letter alphabet (5). As the map is a circle map,  $x_5 = 1 = 0 = x_0 \pmod{1}$ .

## 1. A fair coin toss

The very simplest example of a deterministic law of evolution that gives rise to ‘chaos’ is the *Bernoulli* map, figure 1(a), which models a **coin toss**. Starting with a random initial state, the map generates, deterministically, a sequence of tails and heads with the 50-50% probability.

We introduce the model in its conventional, time-evolution dynamical formulation, than reformulate it as a lattice ‘field theory’, solved by enumeration of all admissible *lattice states*, field configurations that satisfy a global fixed point condition, and use this simple setting to motivate (1) the *fundamental fact*: for a given lattice period, the *Hill determinant* of stabilities of global solutions counts their number, and (2) the topological zeta function counts their symmetry orbits, with a *prime* lattice state per each orbit.

### 1.1. Bernoulli map

The base-2 *Bernoulli* shift map,

$$x_{t+1} = \begin{cases} f_0(x_t) = 2x_t, & x_t \in \mathcal{M}_0 = [0, 1/2) \\ f_1(x_t) = 2x_t \pmod{1}, & x_t \in \mathcal{M}_1 = [1/2, 1) \end{cases}, \quad (1)$$

is shown in figure 1(a). If the linear part of such map has an integer-valued slope, or ‘stretching’ parameter  $s \geq 2$ ,

$$x_{t+1} = sx_t \pmod{1} \quad (2)$$

that maps state  $x_t$  into a state in the ‘extended state space’, outside the unit interval, the (mod 1) operation results in the base- $s$  Bernoulli circle map,

$$\phi_{t+1} = s\phi_t \pmod{1}, \quad (3)$$

sketched as a **dice throw** in figure 1 (b). The (mod 1) operation subtracts  $m_{t+1} = \lfloor s\phi_t \rfloor$ , the integer part of  $s\phi_t$ , or the circle map *winding number*, to keep  $\phi_{t+1}$  in the unit interval  $[0, 1)$ , and partitions the unit interval into  $s$  subintervals  $\{\mathcal{M}_m\}$ ,

$$\phi_{t+1} = s\phi_t - m_{t+1}, \quad \phi_t \in \mathcal{M}_{m_t}, \quad (4)$$

where  $m_t$  takes values in the  $s$ -letter alphabet

$$m \in \mathcal{A} = \{0, 1, 2, \dots, s-1\}. \quad (5)$$

The Bernoulli map is a highly instructive example of a hyperbolic dynamical system. Its symbolic dynamics is simple: the base- $s$  expansion of the initial point  $\phi_0$  is also its temporal itinerary, with symbols from alphabet (5) indicating that at time  $t$  the orbit visits the subinterval  $\mathcal{M}_{m_t}$ . The map is a ‘shift’: a multiplication by  $s$  acts on the base- $s$  representation of  $\phi_0 = .m_1m_2m_3\cdots$  (for example, binary, if  $s = 2$ ) by shifting its digits,

$$\phi_1 = f(\phi_0) = .m_2m_3\cdots. \quad (6)$$

Periodic points can be counted by observing that the preimages of critical points  $\{\phi_{c1}, \phi_{c2}, \dots, \phi_{c,s-1}\} = \{1/s, 2/s, \dots, (s-1)/s\}$  partition the unit interval into  $\{\mathcal{M}_0, \mathcal{M}_1, \dots, \mathcal{M}_{s-1}\}$ ,  $\{\mathcal{M}_{m_1m_2}\}$ ,  $\dots$ ,  $s^n$  subintervals, each containing *one* unstable period- $n$  periodic point  $\phi_{m_1m_2\cdots m_n}$ , with stability multiplier  $s^n$ , see figure 1. The Bernoulli map is a full shift, in the sense that every itinerary is admissible, with one exception: on the circle, the rightmost fixed point is the same as the fixed point at the origin,  $\phi_{s-1} = \phi_0 \pmod{1}$ , so these fixed points are identified and counted as one, see figure 1. The total number of periodic points of period  $n$  is thus

$$N_n = s^n - 1. \quad (7)$$

## 1.2. Temporal Bernuolli

To motivate our formulation of a spatiotemporal chaotic field theory to be developed below, we now recast the local initial value, time-evolution Bernoulli map problem as a *temporal lattice* fixed point condition, the problem of enumerating and determining all global solutions.

‘Temporal’ here refers to the state (field)  $\phi_t$ , and the winding number (source)  $m_t$  taking their values on the lattice sites of a 1-dimensional *temporal* lattice  $t \in \mathbb{Z}$ . Over a finite lattice segment, these can be written compactly as a *lattice state* and the corresponding *symbol block*

$$\Phi^\top = (\phi_{t+1}, \dots, \phi_{t+n}), \quad \mathbf{M}^\top = (m_{t+1}, \dots, m_{t+n}), \quad (8)$$

where  $(\cdots)^\top$  denotes a transpose. The Bernoulli equation (4), rewritten as a first-order difference equation

$$\phi_t - s\phi_{t-1} = -m_t, \quad \phi_t \in [0, 1), \quad (9)$$

takes the matrix form

$$\mathcal{J}\Phi = -\mathbf{M}, \quad \mathcal{J} = \mathbf{1} - s\sigma^{-1}, \quad (10)$$

where the  $[n \times n]$  matrix

$$\sigma_{jk} = \delta_{j+1,k}, \quad \sigma = \begin{pmatrix} 0 & 1 & & & \\ & 0 & 1 & & \\ & & & \ddots & \\ & & & 0 & 1 \\ 1 & & & & 0 \end{pmatrix}, \quad (11)$$

implements the shift operation (6), a cyclic permutation that translates forward in time the lattice state  $\Phi$  by one site,  $(\sigma\Phi)^\top = (\phi_2, \phi_3, \dots, \phi_n, \phi_1)$ . The time evolution law (4) must be of the same form for all times, so the shift operator  $\sigma$  has to be time-translation invariant, with  $\sigma_{n+1,n} = \sigma_{1n} = 1$  matrix element enforcing the periodicity. After  $n$  shifts, a lattice state returns to the initial state,

$$\sigma^n = \mathbf{1}. \quad (12)$$

As the temporal Bernoulli condition (10) is a linear relation, a given block  $\mathbf{M}$ , or ‘code’ in terms of alphabet (5), corresponds to a unique temporal lattice state  $\Phi$ . That is why Percival and Vivaldi [176] refer to such symbol block  $\mathbf{M}$  as a *linear code*.

### 1.3. Orbit Jacobian matrix

The temporal lattice reformulation gives us deep insights into how to enumerate and determine all global solutions of such systems. The temporal Bernoulli condition (10) can be viewed as a search for zeros of the function

$$F[\Phi] = \mathcal{J}\Phi + \mathbf{M} = 0, \quad (13)$$

with the entire periodic *lattice state*  $\Phi_{\mathbf{M}}$  treated as a single fixed *point*  $(\phi_1, \phi_2, \dots, \phi_n)$  in the  $n$ -dimensional state space unit hyper-cube  $\Phi \in [0, 1]^n$ , where the  $[n \times n]$  matrix  $\mathcal{J}$  is given by (10).

The  $F[\Phi] = 0$  fixed point condition (13) is central to the theory of global methods for finding periodic orbits. Instead of requiring forward-in-time numerical integrations, in multi-shooting searches for periodic orbits one discretizes a periodic orbit into  $n$  segments [41, 60, 67–69, 93, 136], and lists a point for each segment

$$\Phi^\top = (\phi_1, \phi_2, \dots, \phi_n). \quad (14)$$

Starting with an initial guess for  $\Phi$ , the zero of function (13) is then found by Newton iteration, which requires an evaluation of the  $[n \times n]$  *orbit Jacobian matrix*

$$\mathcal{J}_{ij} = \frac{\delta F[\Phi]_i}{\delta \phi_j}. \quad (15)$$

For the particularly simple, linear case at hand, the orbit Jacobian matrix (10) is the same for all lattice states of period  $n$ .

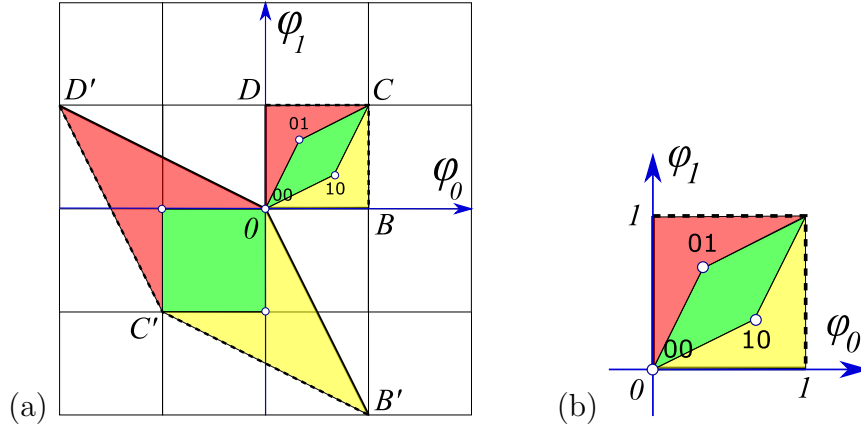


**Figure 2.** (a) The Bernoulli map (1) periodic points  $\Phi_M = (\phi_0, \phi_1)$  of period 2 are the  $\bar{0} = (0, 0)$  fixed point, and the 2-cycle  $\Phi_{01} = (1/3, 2/3)$ , see figure 1 (a). They all lie within the unit square  $[0BCD]$ , which is mapped by the orbit Jacobian matrix  $\mathcal{J}$  (17) into the fundamental parallelepiped  $[0B'C'D']$ . Periodic points  $\Phi_M$  are mapped by  $\mathcal{J}$  onto the integer lattice,  $\mathcal{J}\Phi_M \in \mathbb{Z}^n$ , and are sent back into the origin by integer translations  $M$ , in order to satisfy the fixed point condition (13). Note that this fundamental parallelepiped is covered by 3 unit area quadrilaterals, hence  $|\text{Det } \mathcal{J}| = 3$ . (b) Conversely, in the flow conservation sum rule (27) sum over all lattice states  $M$  of period  $n$ , the inverse of the Hill determinant defines the ‘neighborhood’ of a lattices state as the corresponding fraction of the unit hypercube volume.

#### 1.4. Fundamental fact

The orbit Jacobian matrix  $\mathcal{J}$  stretches the state space unit hyper-cube  $\Phi \in [0, 1]^n$  into the  $n$ -dimensional *fundamental parallelepiped*, and maps each periodic point  $\Phi_M$  into an integer lattice  $\mathbb{Z}^n$  site, which is then translated by the winding numbers  $M$  into the origin, in order to satisfy the fixed point condition (13). Hence  $N_n$ , the total number of the solutions of the fixed point condition equals the number of integer lattice points within the fundamental parallelepiped, a number given by what Baake *et al* [14] call the ‘fundamental fact’,

$$N_n = |\text{Det } \mathcal{J}|, \quad (16)$$

i.e., fact that the number of integer points in the fundamental parallelepiped is equal to its volume, or, what we refer to as the ‘Hill determinant’ below. In two dimensions this formula is known since 1899 as **Pick’s theorem**, in higher dimensions it was given by Nielsen [33, 172] in 1920, and rederived several times since in different contexts, for example by Baake *et al* [14]. For the task at hand, Barvinok [18] **lectures** offer a clear and simple introduction to integer lattices, and a proof of (16).

The action of orbit Jacobian matrix  $\mathcal{J}$  for the period-2 lattice states (periodic points) of the Bernoulli map of figure 1 (a), suffices to convey the idea. In this case, the  $[2 \times 2]$  orbit Jacobian matrix (10), the unit square basis vectors, and their images are

$$\mathcal{J} = \begin{pmatrix} 1 & -2 \\ -2 & 1 \end{pmatrix}$$

$$\Phi^{(B)} = \begin{pmatrix} 1 \\ 0 \end{pmatrix} \rightarrow \Phi^{(B')} = \mathcal{J} \Phi^{(B)} = \begin{pmatrix} 1 \\ -2 \end{pmatrix}, \quad \dots$$

i.e., the columns of the orbit Jacobian matrix are the edges of the fundamental parallelepiped,

$$\mathcal{J} = \left( \Phi^{(B')} \Phi^{(D')} \right), \quad (17)$$

see figure 2(a), and  $N_2 = |\text{Det } \mathcal{J}| = 3$ , in agreement with the periodic orbit count (7).

In general, the unit vectors of the state space unit hyper-cube  $\Phi \in [0, 1]^n$  point along the  $n$  axes; orbit Jacobian matrix  $\mathcal{J}$  maps them into a fundamental parallelepiped basis vectors  $\Phi^{(j)}$ , each one given by a column of the  $[n \times n]$  matrix

$$\mathcal{J} = \left( \Phi^{(1)} \Phi^{(2)} \dots \Phi^{(n)} \right). \quad (18)$$

The Hill determinant is then

$$\text{Det } \mathcal{J} = \text{Det} \left( \Phi^{(1)} \Phi^{(2)} \dots \Phi^{(n)} \right), \quad (19)$$

the volume of the fundamental parallelepiped whose edges are basis vectors  $\Phi^{(j)}$ . Note that the unit hypercubes and fundamental parallelepipeds are half-open, as indicated by dashed lines in figure 2(a), so that their translates form a partition of the extended state space (2). For further examples of fundamental parallelepipeds, see figure 3 and (120).

Note that in the temporal lattice reformulation, the Bernoulli system exhibits two unrelated lattices:

- (i) In the latticization of a time continuum, one replaces *any* dynamical system's time-dependent field  $\phi(t) \in \mathbb{R}$  at time  $t \in \mathbb{R}$  by a discrete set of its values  $\phi_t = \phi(t\Delta T)$  at time instants  $t \in \mathbb{Z}$ . Here the index  $t$  is a *coordinate* over which the field  $\phi$  is defined.
- (ii) Specific to the Bernoulli system is the fact that the *state*  $\phi_t$  (3) is confined to the unit interval  $[0, 1)$ , imparting integer lattice structure onto the intermediate calculational steps in the extended state space (2) on which the orbit Jacobian matrix  $\mathcal{J}$  (10) acts.

### 1.5. Counting temporal Bernoulli lattice states

To evaluate the Hill determinant (16), observe that from (10) it follows that

$$\text{Det}(-\mathcal{J}) = \text{Det}(s/\sigma) \text{Det}(1 - \sigma/s),$$

where  $|\text{Det}(s/\sigma)| = s^n$ . Expand  $\ln \text{Det}(1 - \sigma/s) = \text{Tr} \ln(1 - \sigma/s)$  as a series in  $1/s$ ,

$$\text{Tr} \ln \left( 1 - \frac{\sigma}{s} \right) = - \sum_{k=1}^{\infty} \frac{1}{k} \frac{\text{Tr}(\sigma^k)}{s^k}. \quad (20)$$

It follows from  $\sigma^n = 1$  that  $\text{Tr} \sigma^k = n\delta_{k, rn}$  is non-vanishing if  $k$  is a multiple of  $n$ , 0 otherwise:

$$\ln \text{Det}(1 - \sigma/s) = - \sum_{r=1}^{\infty} \frac{1}{r} \frac{1}{s^{nr}} = \ln(1 - s^{-n}).$$



So for the temporal Bernoulli the volume is

$$N_n = |\text{Det } \mathcal{J}(s)| = s^n - 1, \quad (21)$$

in agreement with the time-evolution count (7); all itineraries are allowed, except that the periodicity of  $\sigma^n = 1$  accounts for  $\bar{0}$  and  $\overline{s-1}$  fixed points (see figure 1) being a single periodic point.

### 1.6. Stability of an orbit vs. its time-evolution stability

The orbit Jacobian matrix  $\mathcal{J}_{ij}$  (15) is a high-dimensional linear stability matrix for a *zero* of function  $F[\Phi_M] = 0$ , evaluated on the lattice state  $\Phi_M$ . How is the stability so computed related to the conventional dynamical systems, forward-in-time stability? To motivate the answer, consider a temporal lattice with a set of  $d$  fields  $\phi_t = \{\phi_{t,1}, \phi_{t,2}, \dots, \phi_{t,d}\}$  on each lattice site  $t$ , and time evolution given by a  $d$ -dimensional map  $\phi_{t+1} = f(\phi_t)$ . The 1-time step  $[d \times d]$  Jacobian matrix of this dynamical system is

$$J(\phi_t)_{ij} = \left. \frac{\partial f(\phi)_i}{\partial \phi_j} \right|_{\phi_i = \phi_{t,i}}. \quad (22)$$

[2020-02-16 Predrag] Recheck - is this called something like ‘characteristic function’ in integer lattice and other lattice literature?

Bernoulli systems stretch uniformly, so for the example at hand it suffices to consider the case of a Jacobian matrix not depending on the field value  $\phi_t$  or time  $t$ ,  $J(\phi_t) = J$ . For a  $n$ -periodic lattice state  $\Phi_M$ , the orbit Jacobian matrix (15) is now a  $[nd \times nd]$  matrix function of the  $[d \times d]$  block matrix  $J$ ,

$$\mathcal{J}(J) = \begin{pmatrix} \mathbf{1} & & & -J \\ -J & \mathbf{1} & & \\ & -J & \ddots & \\ & & \mathbf{1} & \\ & & -J & \mathbf{1} \end{pmatrix}, \quad (23)$$

where  $\mathbf{1}$  is a  $d$ -dimensional identity matrix.

The evaluation of the Hill determinant of this orbit Jacobian matrix proceeds as in the Bernoulli case, the only difference being that the Bernoulli Hill determinant is replaced by a function of a matrix,  $\text{Det } \mathcal{J}(s) \rightarrow \text{Det } \mathcal{J}(J)$ , resulting in (21) being replaced by  $|\text{Det } \mathcal{J}(J)| = |\det(\mathbf{1} - J_M)|$ . (Were the 1-step Jacobian matrix  $J_t$  varying with time  $t$ , by chain rule the period- $n$  Jacobian matrix would be of form  $J_M = \prod_{t=1}^n J_t$ ). The orbit Jacobian matrix evaluated on a lattice state  $\Phi_M$ , and the dynamical, forward in time Jacobian matrix are related by *Hill’s formula*

$$|\text{Det } \mathcal{J}_M| = |\det(\mathbf{1} - J_M)|, \quad (24)$$

of which (21) is the simplest example. We work that out in detail in section 5.3.

### 1.7. Periodic orbit theory

How come that a ‘Det’ in (16) counts lattice states?

For a general, nonlinear fixed point condition  $F[\Phi] = 0$ , expansion (20) in terms of traces is a cycle expansion [11, 52, 58], with support on *periodic orbits*. Ozorio de Almeida and Hannay [4] were the first to relate the number of periodic points to a Jacobian matrix generated volume; in 1984 they used such relation as an illustration of their ‘principle of uniformity’: “periodic points of an ergodic system, counted with their natural weighting, are uniformly dense in phase space.” In periodic orbit theory [52, 56] this principle is stated as a **flow conservation** sum rule, a sum over all lattice states  $\mathbf{M}$  of period  $n$ ,

$$\sum_{|\mathbf{M}|=n} \frac{1}{|\det(\mathbf{1} - J_{\mathbf{M}})|} = 1, \quad (25)$$

or, by Hill’s formula (24),

$$\sum_{|\mathbf{M}|=n} \frac{1}{|\text{Det } \mathcal{J}_{\mathbf{M}}|} = 1. \quad (26)$$

For the Bernoulli system the ‘natural weighting’ takes a particularly simple form, as the Hill determinant of the orbit Jacobian matrix is the same for all periodic points of period  $n$ ,  $\text{Det } \mathcal{J}_{\mathbf{M}} = \text{Det } \mathcal{J}$ , whose number is thus given by (16). For example, the sum over the  $n = 2$  lattice states is,

$$\frac{1}{|\text{Det } \mathcal{J}_{00}|} + \frac{1}{|\text{Det } \mathcal{J}_{01}|} + \frac{1}{|\text{Det } \mathcal{J}_{10}|} = 1, \quad (27)$$

see figure 2(b). Furthermore, for any piece-wise linear system all curvature corrections [55] for orbits of periods  $k > n$  vanish, leading to explicit lattice state-counting formulas of kind reported in this paper.

### 1.8. Shadowing

As the temporal Bernoulli condition (10) is a linear relation, a given block  $\mathbf{M}$ , or ‘code’ in terms of alphabet (5), corresponds to a unique temporal lattice state  $\Phi$  given by the temporal lattice Green’s function

$$\Phi_{\mathbf{M}} = \mathbf{g} \mathbf{M}, \quad \mathbf{g} = \frac{\sigma/s}{1 - \sigma/s}. \quad (28)$$

For an infinite lattice  $t \in \mathbb{Z}$ , this Green’s function can be expanded as a series in  $\Lambda^{-k}$ ,

$$\mathbf{g} = \frac{\sigma/\Lambda}{1 - \sigma/\Lambda} = \sum_{k=1}^{\infty} \frac{\sigma^k}{\Lambda^k}, \quad (29)$$

where  $\Lambda = s$  is the 1-time step stability multiplier for the Bernoulli system. From (28) it follows that the influence of a source  $m_{t'}$  back in the past, at site  $t'$ , falls off exponentially with the temporal lattice distance  $t - t'$ ,

$$\phi_t = \sum_{t'=-\infty}^{t-1} g_{tt'} m_{t'}, \quad g_{tt'} = \frac{1}{\Lambda^{t-t'}}, \quad t > t', \quad 0 \text{ otherwise}. \quad (30)$$

That means that an ergodic lattice state segment of length  $n$  (or a periodic lattice state of a longer period) is shadowed by the periodic lattice state (8) with the same  $n$ -sites symbol block  $\mathbf{M}$ ,

[2020-02-16 Predrag] Do I need to derive this?

$$\phi_t = \frac{1}{1 - 1/\Lambda^n} \left( \frac{m_1}{\Lambda} + \frac{m_2}{\Lambda^2} + \cdots + \frac{m_{n-1}}{\Lambda^{n-1}} + \frac{m_n}{\Lambda^n} \right), \quad (31)$$

with exponentially decreasing shadowing error of order  $O(1/\Lambda^{n+1})$ . The error is controlled by the (24) prefactor  $1/|\text{Det } \mathcal{J}| = 1/|\det(1 - J_{\mathbf{M}})|$ , with the determinant arising from inverting the orbit Jacobian matrix  $\mathcal{J}$  to obtain the Green's function (10).

This error estimate is deeper than what it might seem at the first glance. In fluid dynamics, pattern recognition, neuroscience and other high or  $\infty$ -dimensional settings distances between ‘close solutions’ (let's say pixel images of two faces in a face recognition code) are almost always measured using some arbitrary yardstick, let's say a Euclidean  $L_2$  norm, even though the state space that has no Euclidean symmetry. Not so in the periodic orbit theory: here  $1/|\text{Det } \mathcal{J}|$  is the *intrinsic, coordinatization and norm independent* measure of the distance between similar spatiotemporal states.

### 1.9. Topological zeta function

Now that we have the numbers of lattice states  $N_n$  for any period  $n$ , we can combine them all into a single generating function by substituting  $N_n$  into the *topological* or *Artin-Mazur* zeta function [10, 55],

[2020-02-16 Predrag] Do I need to derive this, rather than refer to ChaosBook?

$$1/\zeta_{\text{top}}(z) = \exp \left( - \sum_{n=1}^{\infty} \frac{z^n}{n} N_n \right), \quad (32)$$

which, when expanded as a Taylor series in  $z$ , is built from *primitive* (or *prime*), i.e., non-repeating lattice states [52]. Conversely, given the topological zeta function, the number of periodic points of period  $n$  is given by the logarithmic derivative of the topological zeta function (see ChaosBook [55])

$$\sum_{n=1}^{\infty} N_n z^n = - \frac{1}{1/\zeta_{\text{top}}} z \frac{d}{dz} (1/\zeta_{\text{top}}). \quad (33)$$

For a Bernoulli system (21),

$$\begin{aligned} 1/\zeta_{\text{top}}(z) &= \exp \left( - \sum_{n=1}^{\infty} \frac{z^n}{n} (s^n - 1) \right) = \exp [\ln(1 - sz) - \ln(1 - z)] \\ &= \frac{1 - sz}{1 - z}. \end{aligned} \quad (34)$$

The numerator  $(1 - sz)$  says that a Bernoulli system is a full shift [55]: there are  $s$  fundamental lattice states, in this case fixed points  $\{\phi_0, \phi_1, \dots, \phi_{s-1}\}$ , and every other

lattice state is built from their concatenations and repeats. The denominator  $(1 - z)$  compensates for the single overcounted lattice state, the fixed point  $\phi_{s-1} = \phi_0 \pmod{1}$  of figure 1 and its repeats.

### 1.10. Counting temporal Bernoulli prime periodic orbits

Substituting the Bernoulli map topological zeta function (34) into (33) we obtain

$$\begin{aligned} \sum_{n=1} N_n z^n = & z + 3z^2 + 7z^3 + 15z^4 + 31z^5 + 63z^6 + 127z^7 \\ & + 255z^8 + 511z^9 + 1023z^{10} + 2047z^{11} \dots, \end{aligned} \quad (35)$$

in agreement with the lattice states count (21). The number of *prime* cycles of period  $n$  is given recursively by subtracting repeats of shorter prime cycles [55],

$$M_n = \frac{1}{n} \left( N_n - \sum_{d|n, d < n} d M_d \right), \quad (36)$$

where  $d$ 's are all divisors of  $n$ , hence

$$\begin{aligned} \sum_{n=1} M_n z^n = & z + z^2 + 2z^3 + 3z^4 + 6z^5 + 9z^6 + 18z^7 \\ & + 30z^8 + 56z^9 + 99z^{10} + 186z^{11} \dots, \end{aligned} \quad (37)$$

in agreement with the usual numbers of binary symbolic dynamics prime cycles [55].

### 1.11. Bernoulli as a continuous time dynamical system

The discrete time derivative of a lattice state  $\Phi$  evaluated at the lattice site  $t$  is given by the *difference operator* [77]

$$\dot{\Phi}_t = \left[ \frac{\partial \Phi}{\partial t} \right]_t = \frac{\phi_t - \phi_{t-1}}{\Delta t} \quad (38)$$

The temporal Bernoulli condition (9) can be thus viewed as a time-discretized, first-order ODE dynamical system

$$\dot{\Phi} = v(\Phi), \quad (39)$$

where the ‘velocity’ vector field  $v$  is given by

$$v(\Phi) = (s - 1) \sigma^{-1} \Phi - \mathbf{M},$$

with the time increment set to  $\Delta t = 1$ , and perturbations that decay (or grow) with rate  $(s - 1)$ . By inspection of figure 1 (a), it is clear that for *shrinking*,  $s < 1$  parameter values the orbit is stable forward in time, with a single linear branch, 1-letter alphabet  $\mathcal{A} = \{0\}$ , and the only periodic lattice states being the single fixed point  $\phi_0 = 0$ , and its repeats  $\Phi = (0, 0, \dots, 0)$ . However, for *stretching*,  $s > 1$  parameter values Bernoulli systems that we study here, every periodic lattice state  $\Phi_{\mathbf{M}}$  is unstable, and there is a periodic orbit solution for each symbol block  $\mathbf{M}$ .

As far as the time-evolution stability is concerned, the  $|\text{Det } \mathcal{J}_M| = |\det(1 - J_M)|$  formula (24) is correct for all first-order difference equations (systems whose evolution laws are first order in time), for any  $[d \times d]$  one-time-step Jacobian matrix. For the Bernoulli system that is a  $[1 \times 1]$  matrix  $J = s$ , with the periodic points count (21) trivially verified.

The orbit Jacobian matrix  $\mathcal{J} = \partial/\partial t - (s - 1)\sigma^{-1}$  is a differential operator whose determinant one usually computes by a Fourier transform diagonalization (see Appendix A). The Fourier discretization approach goes all the way back to Hill's 1886 paper [102]; in the limit of  $n \rightarrow \infty$  multi-shooting steps (14), this is a remarkable formula, relating a field-theoretic,  $\infty$ -dimensional *functional* Hill determinant  $\text{Det } \mathcal{J}_M$  to a determinant of the finite,  $[d \times d]$  matrix  $J_M$ , and it took Poincaré [182] to prove that Hill's Fourier modes calculation is correct in the continuum limit. Historically, in periodic orbit theory calculations one always computes  $J_M$ . However, as we shall show here, and in more generality in section 5, it is the Hill determinant  $\text{Det } \mathcal{J}$  that is the computationally robust quantity that one should evaluate.

**A fair coin toss, summarized.** We refer to the *global* temporal lattice condition (10) as the ‘*temporal* Bernoulli’, in order to distinguish it from the one-time step Bernoulli evolution *map* (3), in preparation for the study of *spatiotemporal* systems to be undertaken in section 3. In the lattice formulation, a *global* temporally periodic lattice state  $\Phi_M$  is determined by the requirement that the *local* temporal lattice condition (9) is satisfied at every lattice site. For temporal Bernoulli there is no need for forward-in-time searches for the returning periodic points. Instead, one determines each global temporally periodic lattice state  $\Phi_M$  at one go, by solving the fixed point condition (13), and one determines the total number of lattice states by computing the Hill determinant (16) of the *orbit Jacobian matrix*. The most importantly for what follows, this calculation requires no recourse to any *explicit coordinatization of system's state space* (as, for example, the Adler-Weiss partition of figure C1 below), and *no explicit symbolic dynamics*. This is the ‘periodic orbit theory’. And if you don't know, **now you know**.

The observation that a Bernoulli system can be viewed as a discretization of a first-order in time ODE, eq. (39), with solutions whose temporal global linear stability is described by the orbit Jacobian matrix  $\mathcal{J}_{ij} = \delta F[\Phi]_i / \delta \phi_j$ , has profound implications for dissipative spatiotemporal systems such as Navier-Stokes and Kuramoto-Sivashinsky [94]. However, the goal here is to formulate a classical spatiotemporally chaotic field theory, Hamiltonian and energy conserving, because (a) that is physics, and (b) cannot do quantum theory without it. We need a system as simple as the Bernoulli map, but mechanical. So, we move on from running in circles, to a mechanical rotor to kick.

## 2. A kicked rotor

The 1-degree of freedom maps that describe kicked rotors subject to discrete time sequences of angle-dependent impulses  $P(q_t)$ ,  $t \in \mathbb{Z}$ ,

$$q_{t+1} = q_t + p_{t+1} \pmod{1}, \quad (40)$$

$$p_{t+1} = p_t + P(q_t), \quad (41)$$

with  $2\pi q$  the angle of the rotor,  $p$  the momentum conjugate to the angular coordinate  $q$ , and the angular pulse  $P(q) = P(q+1)$  periodic with period 1, play a key role in the theory of classical and quantum chaos in atomic physics, from the Taylor, Chirikov and Greene standard map [40, 145], to the cat maps discussed below. The equations are of the canonical Hamiltonian form: (40) is  $\dot{q} = p/m$  in terms of discrete time derivative (38), i.e., the configuration trajectory starting at  $q_t$  reaches  $q_{t+1} = q_t + p_{t+1}\Delta t/m$  in one time step  $\Delta t$ , and (41) is the time-discretized  $\dot{p} = -\partial V(q)/\partial q$ : at each kick the angular momentum  $p_t$  is accelerated to  $p_{t+1}$  by the force pulse  $P(q_t)\Delta t$ , with the time step set to  $\Delta t = 1$ , and the rotor mass  $m$  set to 1.

For an atomic physics kicked rotor, the values of the angle  $q$  differing by integers are identified, but the momentum  $p$  is unbounded. As for the Bernoulli map (2), one compactifies the momentum by adding (mod 1) to (41). This reduces the phase space to a square  $[0, 1) \times [0, 1)$  of unit area, with the opposite edges identified.

### 2.1. Cat map

The simplest kicked rotor is subject to a force is proportional to displacement, that is, Hooke's law force  $P(q) = Kq$  linear in the angular displacement  $q$ . The (mod 1) added to (41) makes the map a discontinuous 'sawtooth,' unless  $K$  is an integer. In the integer  $K$  case, the map (40,41) is of form

$$\begin{pmatrix} q_{t+1} \\ p_{t+1} \end{pmatrix} = J \begin{pmatrix} q_t \\ p_t \end{pmatrix} \pmod{1}, \quad J = \begin{pmatrix} a & c \\ d & b \end{pmatrix}, \quad (42)$$

where  $a, b, c, d$  are integers whose precise values do not matter, as long as  $\det J = 1$ , i.e., the map is area-preserving. The map is then a Continuous Automorphism of the Torus, or a 'cat map', a linear area-preserving map on the unit 2-torus phase space, with the field at the temporal lattice site  $t$ ,  $\phi_t = (q_t, p_t) \in (0, 1] \times (0, 1]$  interpreted as the angular position and its conjugate momentum at time instant  $t$ .

[2020-02-20 Predrag] A matrix  $J$  is called hyperbolic when it has no eigenvalue on the unit circle.

We consider the case of stability multipliers  $(\Lambda, \Lambda^{-1})$  real, with a positive Lyapunov exponent  $\lambda > 0$ ,

$$\Lambda = e^\lambda = (s + \sqrt{(s-2)(s+2)})/2, \quad s = \text{tr } J = \Lambda + \Lambda^{-1}. \quad (43)$$

The eigenvalues are functions of the single stretching parameter  $s$ , and for  $|s| > 2$  the cat map (42) is a fully chaotic Hamiltonian dynamical system. Cat maps with the same

$s$  are equivalent up to a similarity transformation, so it suffices to work out a single convenient realization, as we shall do here for the Percival-Vivaldi example (45).

Cat maps are beloved by ergodicists and statistical mechanics because, even though the field  $(q_t, p_t)$  is 2-dimensional, for integer values of the stretching parameter  $s$ , a cat map has a finite alphabet linear code, just like the Bernoulli map, and its unit torus can be tiled by two rectangles (see figure C1 (a)), in analogy with the forward-in-time Bernoulli map subinterval partitioning of figure 1. From this it follows that all admissible symbol blocks can be generated as shifts of finite type, and all periodic points determined and counted.

As all that is well known, and a side issue for this paper, we relegate the details of the Hamiltonian cat map dynamics and periodic orbit counting to Appendix C. Here we focus on reformulating the cat dynamics as a temporal lattice (or discrete Lagrangian) problem, as we have done for the Bernoulli system in section 1.2.

## 2.2. Temporal cat

To motivate our formulation of a spatiotemporal chaotic field theory to be developed in section 3, we again recast the local initial value, time-evolution cat map (42) as a global *temporal lattice* condition that we shall refer to as the *temporal cat*.

The discrete time Hamilton's equations (40,41) induce forward-in-time evolution on a 2-torus  $(q_t, p_t)$  *phase space*. For the problem at hand, it pays to go from the Hamiltonian (configuration, momentum) phase space formulation to the discrete Lagrangian  $(\phi_{t-1}, \phi_t)$  formulation. If the momentum is replaced by the discrete time velocity,

$$(q_t, p_t) \rightarrow \left( \phi_t, \frac{\phi_t - \phi_{t-1}}{\Delta t} \right), \quad (44)$$

and the time step set to  $\Delta t = 1$ , a cat map can be brought to the Percival-Vivaldi 'two-configuration representation' [176]

$$\begin{pmatrix} \phi_t \\ \phi_{t+1} \end{pmatrix} = J_{PV} \begin{pmatrix} \phi_{t-1} \\ \phi_t \end{pmatrix} - \begin{pmatrix} 0 \\ m_t \end{pmatrix}, \quad J_{PV} = \begin{pmatrix} 0 & 1 \\ -1 & s \end{pmatrix}, \quad (45)$$

with matrix  $J_{PV}$  acting on the 2-dimensional space of successive configuration points  $(\phi_{t-1}, \phi_t)^\top$ . As was case for the Bernoulli map (9), the cat map (mod 1) condition (42) is enforced by integers  $m_t \in \mathcal{A}$ , where for a given integer stretching parameter  $s$  the alphabet  $\mathcal{A}$  ranges over  $|\mathcal{A}| = s+1$  possible values for  $m_t$ ,

$$\mathcal{A} = \{\underline{1}, 0, \dots, s-1\}, \quad (46)$$

necessary to keep  $\phi_t$  for all times  $t$  within the unit interval  $[0, 1)$ . We find it convenient to have symbol  $\underline{m}_t$  denote  $m_t$  with the negative sign, i.e., ' $\underline{1}$ ' stands for symbol ' $-1$ '. As for the Bernoulli system,  $m_t$  can be interpreted as 'winding numbers' [131], or, as they shepherd stray points back into the unit torus, as 'stabilising impulses' [176]. Here we shall refer to them as a 'code', or, in the field-theoretical parlance, as 'sources'.

Written out as a second-order difference equation, the Percival-Vivaldi map (45) takes a particularly elegant, *temporal cat* form

$$\phi_{t+1} - s\phi_t + \phi_{t-1} = -m_t, \quad (47)$$

or, in terms of a lattice state  $\Phi$ , the corresponding symbol block  $\mathbf{M}$  (8), and the  $[n \times n]$  shift operator  $\sigma$  (11),

$$(\sigma - s\mathbf{1} + \sigma^{-1})\Phi = -\mathbf{M}, \quad (48)$$

very much like the temporal Bernoulli condition (10). ‘Temporal’ again refers to the global lattice state (field)  $\Phi$ , and the winding numbers (sources)  $\mathbf{M}$  taking their values on the lattice sites of a 1-dimensional *temporal* lattice  $t \in \mathbb{Z}$ .

For a finite lattice segment  $\Phi$ , one needs to specify the boundary conditions (bc’s). The companion article [96] tackles the Dirichlet bc’s, a difficult, time-translation symmetry breaking, and from the periodic orbit theory perspective, a wholly unnecessary, self-inflicted pain. All that one needs to solve the temporal cat is the  $n$ -periodic, time-translation invariant bc’s used here.

[2020-02-08 Predrag] Complain about that stupidity clearly both in the intro and in conclusions.

### 2.3. Orbit Jacobian matrix

Again, the temporal lattice reformulation gives us a different perspective into how to enumerate and determine global solutions of such systems. The temporal cat condition (48) can be viewed as a search for zeros (13) of the function

$$F[\Phi] = \mathcal{J}\Phi + \mathbf{M} = 0, \quad (49)$$

with the entire periodic *lattice state*  $\Phi_{\mathbf{M}}$  treated as a single fixed *point*  $(\phi_1, \phi_2, \dots, \phi_n)$  in the  $n$ -dimensional phase space unit hyper-cube  $\Phi \in [0, 1]^n$ , where the  $[n \times n]$  orbit Jacobian matrix  $\mathcal{J}$  is now given by

$$\mathcal{J} = \sigma - s\mathbf{1} + \sigma^{-1} \quad (50)$$

a tri-diagonal Toeplitz matrix (constant along each diagonal,  $\mathcal{J}_{k\ell} = j_{k-\ell}$ ) of circulant form,

$$\mathcal{J} = \begin{pmatrix} -s & 1 & 0 & 0 & \dots & 0 & 1 \\ 1 & -s & 1 & 0 & \dots & 0 & 0 \\ 0 & 1 & -s & 1 & \dots & 0 & 0 \\ \vdots & \vdots & \vdots & \vdots & \ddots & \vdots & \vdots \\ 0 & 0 & \dots & \dots & \dots & -s & 1 \\ 1 & 0 & \dots & \dots & \dots & 1 & -s \end{pmatrix}. \quad (51)$$



#### 2.4. Integer lattices

As in section 1.4, the fundamental parallelepiped given the stretching of the  $n$ -dimensional phase space unit hyper-cube  $\Phi \in [0, 1)^n$  by the orbit Jacobian matrix counts periodic lattice states, with the admissible lattice states of period  $n$  constrained to field values within  $0 \leq \phi_t < 1$ . The fundamental parallelepiped contains images of all periodic lattice states  $\Phi_{\mathbf{M}}$ , which are then translated by integer winding numbers  $\mathbf{M}$  into the origin, in order to satisfy the fixed point condition (49). The total number of periodic lattice states is again, as for the Bernoulli system (16), given by the ‘fundamental fact’

$$N_n = |\text{Det } \mathcal{J}|. \quad (52)$$

Period-1, or fixed point lattice states are easy to count: the orbit Jacobian matrix is a 1-dimensional matrix, so it follows from (47) that

$$N_1 = s - 2, \quad (53)$$

[2020-06-10 Predrag] to Han: If the alphabet (46) is really  $|\mathcal{A}| = s+1$  letters, how come there are only  $s - 2$  fixed point lattice states? Where did the extra 3 letters go?

[2020-06-12 Han] The fixed point lattice states with the other 3 letters are not admissible. The fixed point solution satisfies:

$$(s - 2)\phi_t = m_t.$$

Since  $\phi_t \in [0, 1)$ , the range of  $m_t$  is  $m_t \in [0, s - 2)$ . So the letter  $\underline{1}$ ,  $s - 2$  and  $s - 1$  are not in the admissible range, as the corresponding fields of these 3 letters are  $-1/(s - 2)$ ,  $1$  and  $(s - 1)/(s - 2)$  respectively.

The action of the temporal cat orbit Jacobian matrix is harder to visualize than the 2-dimensional fundamental parallelepiped of forward-in-time cat map of Appendix C.2: a period-2 solution temporal cat is a 2-torus, period-3 solution a 3-torus, etc.. Still, the fundamental parallelepiped for the period-2 and period-3 lattice states, figure 3, should suffice to convey the idea. The fundamental parallelepiped basis vectors (18) are the columns of  $\mathcal{J}$ . The  $[2 \times 2]$  orbit Jacobian matrix (51) and its Hill determinant are

$$\mathcal{J} = \begin{pmatrix} -s & 2 \\ 2 & -s \end{pmatrix}, \quad N_2 = \text{Det } \mathcal{J} = (s - 2)(s + 2), \quad (54)$$

(compare with the lattice states count (69)), with the resulting fundamental parallelepiped shown in figure 3(a). The period-3 lattice states for  $s = 3$  are contained in the half-open fundamental parallelepiped of figure 3(b), defined by the columns of  $[3 \times 3]$  orbit Jacobian matrix

$$\mathcal{J} = \begin{pmatrix} -s & 1 & 1 \\ 1 & -s & 1 \\ 1 & 1 & -s \end{pmatrix}, \quad N_3 = |\text{Det } \mathcal{J}| = (s - 2)(s + 1)^2, \quad (55)$$

again in agreement with the periodic orbit count (69).



**Figure 3.** (a) For  $s = 3$ , the temporal cat (48) has 5 period-2 lattice states  $\Phi_M = (\phi_0, \phi_1)$ :  $\Phi_{00}$  fixed point and 2-cycles  $\{\Phi_{01}, \Phi_{10}\}$ ,  $\{\Phi_{12}, \Phi_{21}\}$ . They lie within the unit square  $[0BCD]$ , and are mapped by the  $[2 \times 2]$  orbit Jacobian matrix  $\mathcal{J}$  (54) into the fundamental parallelepiped  $[0B'C'D']$ , as in, for example, Bernoulli figure 2. The images of periodic points  $\Phi_M$  land on the integer lattice, and are sent back into the origin by integer translations  $M = m_0 m_1$ , in order to satisfy the fixed point condition  $\mathcal{J}\Phi_M + M = 0$ . (b) A 3-dimensional [blue basis vectors] unit-cube stretched by  $\mathcal{J}$  (55) into the [red basis vectors] fundamental parallelepiped. For  $s = 3$ , the temporal cat (48) has 16 period-3 lattice states: a  $\Phi_{000}$  fixed point at the vertex at the origin, [pink dots] 3 period-3 orbits on the faces of the fundamental parallelepiped, and [blue dots] 2 period-3 orbits in its interior. An  $n$ -dimensional phase space unit hyper-cube  $\Phi \in [0, 1]^n$  and the corresponding fundamental parallelepiped are half-open, as indicated by dashed lines, so the integer lattice points on the far corners, edges and faces do not belong to it.

The 16 period-3 lattice states  $\Phi_M = (\phi_0, \phi_1, \phi_3)$  are the  $\Phi_{000}$  fixed point at the vertex at the origin, 3 period-3 orbits on the faces of the fundamental parallelepiped, and 2 period-3 orbits in its interior, all five of form  $\{\Phi_{m_0 m_1 m_2}, \Phi_{m_1 m_2 m_0}, \Phi_{m_2 m_0 m_1}\}$ .

Note that in the temporal lattice reformulation, the temporal cat happens to involve two unrelated lattices:

- (i) In the latticization of a time continuum, one replaces a time-dependent field  $\phi(t)$  at time  $t \in \mathbb{R}$  of *any* dynamical system by a discrete set of its values  $\phi_t = \phi(t\Delta T)$ ,  $t \in \mathbb{Z}$ . Here the index ' $t$ ' is a *coordinate* over which the field  $\phi$  lives.
- (ii) A peculiarity of the temporal cat is that the *field*  $\phi_t$  (45) is confined to the unit interval  $[0, 1)$ , imparting a  $\mathbb{Z}^1$  lattice structure onto the computationally intermediate fundamental parallelepiped  $\mathcal{J}$  basis vectors (18).

### 2.5. Counting temporal cat lattice states (unwritten)

We now count the number of periodic lattice states (67) in the temporal cat (or, 'discrete Lagrangian') formulation (for counting using the Hamiltonian formulation, see Appendix C.2).

[...] one can write the Hill determinant compactly as

$$N_n = |\det(\mathcal{J})| = 2 T_n(s/2) - 2, \quad (56)$$

where  $T_n(s/2)$  is the Chebyshev polynomial of the first kind.

## 2.6. Counting temporal cat lattice states (experimental)

The temporal cat equation (47) is a linear 2nd-order inhomogeneous difference equation (a 3-term recurrence relation) with constant coefficients that can be solved by standard methods [77] that parallel the theory of linear differential equations.

[2020-06-10 Predrag] Comparing with (??) we see that we need to solve a second-order inhomogeneous difference equation with a constant forcing term  $2(s-2)$ .

Inserting a solution of form  $\phi_t = \Lambda^t$  into the associated ( $m_t=0$ ) homogenous 2nd-order difference equation

$$\phi_{t+1} - s\phi_t + \phi_{t-1} = 0 \quad (57)$$

yields the characteristic equation

$$\Lambda^2 - s\Lambda + 1 = 0, \quad (58)$$

which, for  $|s| > 2$ , has two real roots  $\{\Lambda, \Lambda^{-1}\}$ ,

$$\Lambda = \frac{1}{2}(s + \sqrt{(s-2)(s+2)}), \quad (59)$$

and the so-called *complementary* solution of form

$$\phi_{c,t} = a_1 \Lambda^t + a_{-1} \Lambda^{-t}. \quad (60)$$

A difference of any pair of solutions to the temporal cat inhomogenous equation (47) is a solution of the homogenous difference equation (57), so the general solution is a sum of the complementary solution (60) and a *particular* solution  $\phi_p$ ,

$$\phi_t = \phi_{c,t} + \phi_{p,t}. \quad (61)$$

Eq. (57) is time-reversal invariant,  $\phi_t = \phi_{-t}$ , so  $a_1 = a_{-1} = a$ . To determine the particular solution, assume that both the source  $m_t = m$  and  $\phi_{p,t} = \phi_p$  in (47) are site-independent,

$$\phi_p - s\phi_p + \phi_p = -m, \quad (62)$$

so  $\phi_p = m/(s-2)$ . Hence the solution is

$$\phi_t = \phi_{c,t} + \phi_{p,t} = a(\Lambda^t + \Lambda^{-t}) + m/(s-2), \quad (63)$$

with  $a_i$  determined by fields at two lattice sites,

$$\phi_0 = 2a + m/(s-2), \quad \phi_1 = a(\Lambda + \Lambda^{-1}) + m/(s-2), \quad .$$

Temporal cat starts with  $N_0 = 0$ , and according to (53),  $N_1 = s-2$ , so  $a = 1$ ,  $m = -2(s-2)$ , and the number of temporal lattice states of period  $n$  is

$$N_n = \Lambda^n + \Lambda^{-n} - 2. \quad (64)$$

### 2.7. Shadowing

As the relation between the symbol blocks  $\mathbf{M}$  and the corresponding lattice states  $\Phi_{\mathbf{M}}$  is linear, for  $\mathbf{M}$  an admissible symbol block, the corresponding lattice state  $\Phi_{\mathbf{M}}$  is given by the Green's function

$$\Phi_{\mathbf{M}} = \mathbf{g} \mathbf{M}, \quad \mathbf{g} = \frac{1}{-\sigma + s\mathbf{1} - \sigma^{-1}}, \quad (65)$$

as in the Bernoulli case (28).

As in section 1.8, the Green's function (65) decays exponentially with the distance from the origin, a fact that is essential in establishing the 'shadowing' between lattice states sharing a common sub-block  $\mathbf{M}$ . For an infinite temporal lattice  $t \in \mathbb{Z}$ , the lattice field at site  $t$  is determined by the sources  $m_{t'}$  at all sites  $t'$ , by the Green's function  $g_{tt'}$  for one-dimensional discretized heat equation [161, 176],

$$\phi_t = \sum_{t'=-\infty}^{\infty} g_{tt'} m_{t'}, \quad g_{tt'} = \frac{1}{\Lambda - \Lambda^{-1}} \frac{1}{\Lambda^{|t-t'|}}, \quad (66)$$

with  $\Lambda$  is the expanding stability multiplier defined in (43).

Suppose there is a non-vanishing point source  $m_0 \neq 0$  only at the present,  $t' = 0$  temporal lattice site. Its contribution to  $\phi_t \sim \Lambda^{-|t|}$  decays exponentially with the distance from the origin. More generally, as in the Bernoulli case (31), if two lattice states  $\Phi$ ,  $\Phi'$  share a common sub-block  $\mathbf{M}$  of length  $n$ , they shadow each other with accuracy of order of  $O(1/\Lambda^n)$ .

### 2.8. Topological zeta function

The number of lattice states of period  $n$  is given by the area of the fundamental parallelepiped (52) (Hill's formula)

$$N_n = |\text{Det } \mathcal{J}| = |\det(J^n - \mathbf{1})| = \Lambda^n + \Lambda^{-n} - 2, \quad (67)$$

where the  $\Lambda$  is the stability multiplier (43) of the one-time-step evolution matrix  $J$  (42).

Substituting the numbers of lattice states  $N_n$  into the *topological zeta function* (32) we obtain

$$\begin{aligned} 1/\zeta_{\text{top}}(z) &= \exp \left( - \sum_{n=1}^{\infty} \frac{z^n}{n} N_n \right) = \exp \left( - \sum_{n=1}^{\infty} \frac{z^n}{n} (\Lambda^n + \Lambda^{-n} - 2) \right) \\ &= \exp [\ln(1 - z\Lambda) + \ln(1 - z\Lambda^{-1}) - 2\ln(1 - z)] \\ &= \frac{(1 - z\Lambda)(1 - z\Lambda^{-1})}{(1 - z)^2} = \frac{1 - sz + z^2}{(1 - z)^2}, \end{aligned} \quad (68)$$

in agreement with Isola [115], as well as the Adler-Weiss generating partition topological zeta function (C.4). Topological zeta functions count *prime orbits*, i.e., time invariant *sets* of equivalent lattice states related by translations (cyclic permutations), and other symmetries [55].

Conversely, given the topological zeta function, the generating function for the number of temporal lattice states of period  $n$  is given by the logarithmic derivative of the topological zeta function (33),

$$\begin{aligned} \sum_{n=0}^{\infty} N_n z^n &= \frac{2 - sz}{1 - sz + z^2} - \frac{2}{1 - z} \\ &= (s - 2) \left[ z + (s + 2)z^2 + (s + 1)^2 z^3 \right. \\ &\quad \left. + (s + 2)s^2 z^4 + (s^2 + s - 1)^2 z^5 + \dots \right], \end{aligned} \quad (69)$$

which is indeed the generating function for  $T_n(s/2)$ , the Chebyshev polynomial of the first kind of (56).

### 2.9. Temporal cat as a continuous time dynamical system

Recall how the Bernoulli first-order difference equation could be viewed as a time-discretization of the first-order linear ODE (39). The second-order difference equation (47) can be interpreted as the second order discrete time derivative  $d^2/dt^2$ , or the temporal lattice Laplacian,

$$\square \phi_t \equiv \phi_{t+1} - 2\phi_t + \phi_{t-1} = (s - 2)\phi_t - m_t, \quad (70)$$

with the time step set to  $\Delta t = 1$ . But that is nothing but Newton's Second Law: "acceleration equals force," so Percival and Vivaldi [176] refer to this formulation as 'Newtonian', while Allroth [3], Mackay, Meiss, Percival, Kook & Dullin [75, 134, 154, 155, 160], and Li and Tomsovic [143] refer to it as the 'Lagrangian' formulation.

In other words, for a cat map the force pulse  $P(q) = (s - 2)q$  in (41) is linear in the angular displacement  $q$ , so the temporal lattice equation takes form

$$(-\square + (s - 2)1) \Phi = \mathbf{M}. \quad (71)$$

For small stretching parameter values,  $s < 2$ , this equation describes a set of coupled penduli, with oscillatory solutions, known as the discrete Helmholtz equation or the tight-binding model, with Hamiltonian [76]

$$H = \sum_{\ell} |\ell\rangle \epsilon_0 \langle \ell| + \sum_{\ell m} |\ell\rangle V_{\ell m} \langle m|, \quad V_{\ell m} = \begin{cases} V & \text{if } \ell, m \text{ nearest neighbors} \\ 0 & \text{otherwise} \end{cases}$$

corresponding to the stretching factor  $s = -\epsilon_0/V$  in eq. (71).

Here we study the strong stretching,  $s > 2$  case, known as the discrete *screened Poisson equation* (hyperbolic, damped solutions) [70, 78, 187]. We refer to eq. (71) as the '*temporal cat*', both to distinguish it from the forward-in-time Hamiltonian cat *map* (42), and in the anticipation of the spatiotemporal cat of section 3.

**Temporal cat, summarized.** In the spatiotemporal formulation a *global* temporal lattice state

$$\Phi^\top = (\phi_t, \phi_{t+1}, \dots, \phi_{t+k}) \quad (72)$$

is not determined by a forward-in-time ‘cat map’ evolution (42), but rather by the fixed point requirement (49) that the *local*, 3-term discrete temporal lattice condition (47) is satisfied at every lattice point. The Lagrangian formulation requires only temporal lattice states and their actions, replacing the phase space ‘cat map’ (42) by a ‘temporal cat’ lattice (71). The temporal cat has no generating partition analogue of the Adler-Weiss partition for a Hamiltonian cat map (see section Appendix C.1).

As we have shown here, no funky Hamiltonian phase space partitioning magic (such as figure C1) is needed to count the periodic lattice states of a temporal cat. Not only are no such partitions needed to solve the system, but the Lagrangian, temporal 1-dimensional lattice formulation is the bridge that takes us from the single cat map (42) to the higher-dimensional coupled infinity “multi-cat” spatiotemporal lattices (80).

And did you know that the cute Arnold cat is but the screened Poisson equation in disguise?

### 3. Spatiotemporal cat

The *temporal cat* of section 2 is a 1-dimensional example of the simplest spatiotemporally chaotic, or ‘turbulent’ field theory, the *spatiotemporal cat* to which we turn now. Spatiotemporal cat lives on a  $d$ -dimensional discretized spacetime, a spatiotemporal  $\mathbb{Z}^d$  integer lattice, with a cat map (a ‘rotor’) on each site, coupled to its nearest neighbors. Another way of visualizing a spatiotemporal cat is as a lattice of locally hyperbolic ‘anti’ oscillators, as opposed to the classical free field theory, with an oscillator at each site (‘Gaussian model’ [82, 122]).

The temporal cat lives on a 1-dimensional temporal integer lattice  $\mathbb{Z}$ , with very simple ‘tilings’. For every integer temporal period  $T$ , we first determine  $N_T$ , the number of all periodic *lattice state*  $\Phi_M$  solutions on a tile of length  $T$ . However, if  $T = mT_p$ , the  $T$ -tile can be tiled by  $m$  repeats of a smaller  $T_p$ -tile, so some of  $T$ -periodic orbit solutions are repeats of the already determined shorter  $T_p$  *prime* solution  $\Phi_p$ . Furthermore, due to the time invariance of the defining equations, there are  $T_p$  physically equivalent copies of a given solution in the time orbit of every  $\Phi_p$ . So all we really have to do is to enumerate  $M_T$  *prime orbits* of the time-invariance equivalent periodic orbit solutions, whose generating function is the analytically elegant topological zeta function.

For the  $d$ -dimensional spatiotemporal cat the repertoire of periodic tilings is richer. In  $d = 2$  and 3 the basic facts are well known both from crystallography, and from the number theory of integer lattices. In this paper we systematically construct and enumerate distinct  $d = 2$  tilings, or Bravais lattices  $[L \times T]_S$ , of increasing spacetime periodicities, and determine  $N_{[L \times T]_S}$ , the number of *doubly periodic lattice state* solutions, by evaluating the associated Hill determinants. For  $d = 2$  and higher-dimensional lattices counting the spatiotemporal ‘prime’ tilings requires some thought. We determine  $M_{[L \times T]_S}$ , the numbers of doubly-periodic prime orbits, invariant under spacetime translations. We, however, fail to find an analytic form for the associated doubly-periodic topological zeta function.

We start by a brief review of physical origin of coupled map lattices (CMLs) models. The impatient reader should proceed directly to the spatiotemporal cat, introduced in section 3.3, and solved in section 3.8.

#### 3.1. Coupled map lattices

In order to solve a partial differential equation (PDE) on a computer, one represents it by a finite number of computational elements. The simplest discretization of a scalar spacetime field  $\phi(\vec{q}, \tau)$  is by specifying its values  $\phi_{n_1 n_2 \dots n_{d-1} t} = \phi(q_n, \tau_t)$  on lattice points  $(\vec{n}, t) \in \mathbb{Z}^d$ . Once spatial and temporal derivatives are replaced by their discretizations, the PDE is reduced to dynamics of a coupled map lattice, a spatially extended system with discrete time, discrete space, and a set of continuous fields on each site. For many PDEs, CML conceptual advantage is not only numerical, but also that the technical problems such as existence and uniqueness of the field theory are regularized away, and the essence of spatiotemporal chaos is revealed in a transparent form.

Often one starts out by coupling neighbors harmonically, and thinks of this starting, free field theory formulation as a spring mattress [226] to which weakly coupled nonlinear terms are then added. Similarly, the conventional CML models, mostly motivated by discretizations of dissipative PDEs, start out with chaotic on-site dynamics weakly coupled to neighboring sites, with a strong space-time asymmetry. An example are the diffusive coupled map lattices introduced by Kaneko [123, 124], with time evolution given by

$$\begin{aligned}\phi_{n,t+1} &= (1 + \epsilon \square)g(\phi_{nt}) \\ &= g(\phi_{nt}) + \epsilon[g(\phi_{n-1,t}) - 2g(\phi_{nt}) + g(\phi_{n+1,t})],\end{aligned}\tag{73}$$

where the individual spatial site's dynamical system  $g(x)$  is a 1-dimensional map, such as the logistic map, coupled to its nearest neighbors by  $\square$ , the spatial version of the Laplacian (70) for the discretized second order *spatial* derivative  $d^2/dx^2$  (we always set the lattice spacing constant equal to unity).

The form of time-step map  $g(\phi_{nt})$  is the same for all times, i.e., the law of temporal evolution is invariant under the group of discrete *time translations*. Spatially homogenous lattice models also invariant under discrete *space translations* were studied by Bunimovich and Sinai [34] in the case when  $g(\phi_{nt})$  is a one-dimensional expanding map.

The observation that for spatiotemporally chaotic systems space and time should be considered on the same footing goes back to the ‘chronotopic’ program of Politi and collaborators [84, 139, 140, 185] who, in their studies of propagation of spatiotemporal disturbances in extended systems, discovered that the spatial stability analysis can be combined with the temporal stability analysis, with orbit weights depending exponentially both on the space and the time variables,  $t_p \propto e^{-LT\lambda_p}$ . Politi and Torcini [183] study of periodic orbits of *spatiotemporal Hénon*, a (1+1)-spacetime lattice of Hénon maps with solutions periodic both in space and time is the closest to the present investigation. They explain why the dependence of the lattice field at time  $\phi_{t+1}$  on the two previous time steps prevents an interpretation of dynamics as the composition of a local chaotic evolution with a diffusion process (73). In the CML tradition, they study the weak coupling regime  $\epsilon \approx 0$ , but note that the  $b = -1$  case could be an interesting example of a nonlinear Hamiltonian lattice field theory.

### 3.2. Hamiltonian coupled map lattices

For quantum mechanics and statistical mechanics applications, one needs the dynamics to be Hamiltonian, motivating models such as coupled standard map lattice [125] and  $\phi^4$  lattice [105]. Lattice recurrence relations [169] of the type studied below arise in the Frenkel-Kontorova lattice, Hamiltonian lattice models for ferromagnetism, many-body quantum chaos [97–99, 170, 197], and in discretizations of elliptic PDEs.

Pesin and Sinai [178] were the first to study such lattices, with chains of coupled Anosov maps. In order to establish rigorously the desired statistical properties of coupled map lattices, such as the continuity of their SRB measures, they, and most



of the subsequent statistical mechanics literature, relied on the structural stability of Anosov automorphisms under small perturbations. For such lattices the neighboring sites have to be coupled sufficiently weakly (small  $\epsilon$  in (73)) so that the site cat maps could be conjugated to a lattice of uncoupled Anosov automorphisms, with a finite Markov partition, the key ingredient required for the proofs.

This exploration, as well as the companion paper [96] for Dirichlet bc's, starts with the study of a coupled  $L$ -body Hamiltonian system undertaken by Gutkin and Osipov [99]. If the reader wants to quantize an  $L$ -body Hamiltonian system, Gutkin and Osipov article covers the formalism in depth, so we do not review the Hamiltonian formulation here.

### 3.3. Spatiotemporal cat

In their paper, Gutkin and Osipov also note that if the single ‘body’ dynamics is described by a cat map coupled to its nearest spatial neighbors, and if the spatial coupling strength is taken to be the same as temporal coupling strength, one obtains a spatiotemporally symmetric 5-term recurrence relation

$$\phi_{n,t+1} + \phi_{n,t-1} - 2s\phi_{nt} + \phi_{n+1,t} + \phi_{n-1,t} = -m_{nt}, \quad (74)$$

that adds one spatial lattice direction to the temporal cat 3-term recurrence relation (47). As these equations are symmetric under interchange of the ‘space’ and the ‘time’ directions, their temporal and spatial dynamics are strongly coupled, corresponding to  $\epsilon \approx O(1)$  in (73), in contrast to the traditional spatially weakly coupled CML [34].

Now that we have mastered the *temporal cat* (47), a generalization to the *spatiotemporal cat* (74) is immediate. Consider a 1-dimensional spatial lattice, with field  $\phi_{nt}$  (the angle of a kicked rotor (40) at instant  $t$ ) at spatiotemporal site  $z = (n, t) \in \mathbb{Z}^2$ . If each site couples only to its nearest spatial neighbors  $\phi_{n\pm 1,t}$ , and if we require (1) invariance under spatial translations, (2) invariance under spatial reflections, and (3) invariance under the space-time exchange, we arrive at the 2-dimensional Euclidean lattice difference equations (74).

Gutkin and Osipov –for reasons that make sense in context of  $L$ -body quantum systems– call this recurrence relation a ‘non-perturbed coupled cat map’. A well-established name [70, 78] for this system is the ‘discrete screened Poisson equation’. We, however, find a ‘*spatiotemporal cat*’ more descriptive for our field-theoretic purposes. While the generalization of (74) to  $d$ -dimensional hypercubic  $\mathbb{Z}^d$  lattice is immediate, it suffices to work out the  $d = 2$  spatiotemporal cat in some detail to develop intuition about the general case.

The spatiotemporal cat equation (74) can be written compactly as

$$\mathcal{J} \Phi = -\mathbf{M}, \quad \mathcal{J} = \sigma_1 + \sigma_2 - 2s1 + \sigma_2^{-1} + \sigma_1^{-1}, \quad (75)$$

where  $\sigma_1, \sigma_2$  are shift operators (11) which translate the field by one lattice spacing in the spatial, temporal direction, respectively. The inverses  $\sigma_i^{-1}$  translate the field in the

opposite directions. The block  $\mathbf{M} = \{m_{nt}\}$  is composed of symbols from alphabet

$$m_{nt} \in \mathcal{A}, \quad \mathcal{A} = \{\underline{3}, \underline{2}, \underline{1}, 0, \dots, 2s-2, 2s-1\}, \quad (76)$$

where symbol  $\underline{m}_{nt}$  denotes  $m_{nt}$  with the negative sign, i.e., ‘ $\underline{3}$ ’ stands for symbol ‘ $-3$ ’. In our explicit computational examples, we shall always set  $s$  to

$$s = 5/2 \quad \Rightarrow \quad \mathcal{A} = \{\underline{3}, \underline{2}, \underline{1}, 0, 1, 2, 3, 4\}, \quad (77)$$

the smallest value of the ‘stretching’ parameter  $s$  for which the orbit Jacobian matrix  $\mathcal{J}$  is an integer-valued matrix, and the system is hyperbolic.

As for the temporal Bernoulli (10) and the temporal cat (49), one can view the spatiotemporal cat condition (75) as a zero of the function

$$F[\Phi] = \mathcal{J}\Phi + \mathbf{M} = 0, \quad (78)$$

with the entire periodic lattice state  $\Phi_{\mathbf{M}} = \{\phi_z\}$  treated as a single fixed point within the  $(\ell_1 \ell_2 \cdots \ell_d)$ -dimensional state space unit hyper-cube  $\Phi \in [0, 1)^{\ell_1 \ell_2 \cdots \ell_d}$ , where  $\ell_j$  is the lattice period in direction  $j$ , and the  $(\ell_1 \ell_2 \cdots \ell_d)^2$ -dimensional orbit Jacobian matrix  $\mathcal{J}_{zz'}$  is given by

$$\mathcal{J} = \sum_{j=1}^d (\sigma_j - s\mathbf{1} + \sigma_j^{-1}). \quad (79)$$

Here  $\sigma_i$  is a shift operator (11) which translates the field in the  $i$ th direction by one lattice spacing. Its inverse  $\sigma_i^{-1}$  translates the field in the negative  $i$ th direction.

In multi-index, or ‘tensorial’ notation, the spatiotemporal cat equation (75) can be written as

$$\begin{aligned} (\mathcal{J}\phi)_z &= \sum_{z'} \sum_{i=1}^d (\sigma_i - s\mathbf{1} + \sigma_i^{-1})_{zz'} \phi_{z'} = -m_z, \quad m_z \in \mathcal{A}, \\ z &= (n_1, n_2, n_3, \dots, n_d) \in \mathbb{Z}^d \\ \mathcal{A} &= \{-2d+1, -2d+2, \dots, 2s-2, 2s-1\}, \end{aligned} \quad (80)$$

with field  $\phi_z$  and source  $m_z$  labelled by the  $d$  indices of lattice site  $z$ . Sources  $m_z \in \mathcal{A}$  keep the field (‘rotor angle’  $\phi_z$ ) within the unit interval on every site. The orbit Jacobian matrix  $\mathcal{J}$ , labelled by  $d$  pairs of indices, acts on the lattice state  $\Phi$  by usual matrix multiplication. We illustrate how that works by working out in detail an example in [Appendix A.4.3](#). As yet another notational choice, in (117) we recast the orbit Jacobian matrix (75) as a  $[LT \times LT]$  Kronecker product block matrix.

In the lattice formulation, the spatiotemporal cat happens to involve two quite distinct lattices:

- (i) In the latticization of a spacetime continuum, one replaces a time-dependent field  $\phi(x, t)$  at spacetime point  $(x, t) \in \mathbb{R}^d$  of *any* field theory by a discrete set of its values  $\phi_z = \phi(n\Delta L, t\Delta T)$  on lattice sites, where the index  $z \in \mathbb{Z}^d$  is a discrete  $d$ -dimensional spacetime *coordinate* over which the field  $\phi$  lives. We describe the properties of this integer lattice  $\mathbb{Z}^d$  and its sublattices in [Sections 3.4 to 3.6](#).

- (ii) A peculiarity of the spatiotemporal cat is that the *field*  $\phi_z$  (74) is confined to the unit interval  $[0, 1)$ , imparting a  $\mathbb{Z}^1$  lattice structure –in any spacetime dimension  $d$ – onto the computationally intermediate fundamental parallelepiped  $\mathcal{J}$  basis vectors (see, for example, (120)). The lattice structure of periodic orbits  $\Phi$  is discussed in Sections 3.7 to 5.

### 3.4. Symmetries of the integer lattice

The spatiotemporal cat equation (75) is *equivariant* under the discrete spacetime translations; the space  $\sigma_x$  and time  $\sigma_y$  reflections  $n \rightarrow -n$ ,  $t \rightarrow -t$ ; as well as under  $\sigma_a$  exchange  $n \longleftrightarrow t$  of space and time. Spatiotemporal cat thus has the point-group symmetries of the square lattice: rotations by  $\pi/2$ , and reflection across  $x$ -axis,  $y$ -axis, and diagonals  $a$  and  $b$ ,

$$C_{4v} = D_4 = \{E, C_{4z}^+, C_{4z}^-, C_{2z}, \sigma_y, \sigma_x, \sigma_a, \sigma_b, \}. \quad (81)$$

In the international crystallographic notation, the square lattice space group of symmetries is referred to as  $p4mm$  [72].

### 3.5. Bravais lattices

For the 1-dimensional temporal lattices considered so far, a sublattice is tiled by repeats of a block of temporal period  $T$ .

For a  $d$ -dimensional integer lattice  $\mathbb{Z}^d$ , a  $d$ -periodic sublattice that tiles the spacetime is called a *Bravais lattice*.

For a  $d$ -dimensional integer lattice  $\mathbb{Z}^d$ , the primitive unit cell of a  $d$ -dimensional Bravais lattice tiles the spacetime.

A 2-dimensional Bravais lattice  $\Lambda$  is an infinite array of points

$$\Lambda = \{n_1 \mathbf{a}_1 + n_2 \mathbf{a}_2 \mid n_i \in \mathbb{Z}\}, \quad (82)$$

generated by the group of discrete translations  $R = n_1 \mathbf{a}_1 + n_2 \mathbf{a}_2$ , where  $\{n_1, n_2\}$  are any integers, and  $(\mathbf{a}_1, \mathbf{a}_2)$  is a pair of  $\mathbb{Z}^2$  integer lattice vectors that span the Bravais lattice as a set of basis.

The primitive unit cell of a Bravais lattice can be chosen in different ways. In this paper we will always choose the primitive unit cell uniquely corresponding to the basis vectors:

$$C(\mathbf{a}_1, \mathbf{a}_2) = \{m_1 \mathbf{a}_1 + m_2 \mathbf{a}_2 \mid 0 \leq m_i < 1\}, \quad (83)$$

and call  $C(\mathbf{a}_1, \mathbf{a}_2)$  the *Bravais cell* of Bravais spanned by basis vectors  $(\mathbf{a}_1, \mathbf{a}_2)$ .

A given Bravais *lattice*  $\Lambda$  can be defined by any of the infinity of Bravais cells, each defined by a different pair of basis vectors  $(\mathbf{a}_1, \mathbf{a}_2)$ , but equivalent under unimodular,  $SL_2(\mathbb{Z})$  transformation [137].

[2020-09-05 Predrag] recheck Lang [137] *Linear Algebra*, or replace! It is possible that it does not reference modular group at all...

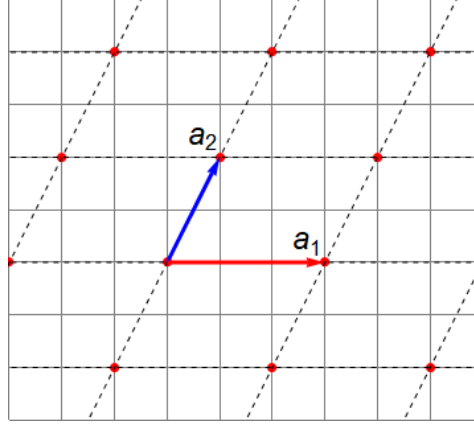


**Figure 4.** (Color online) The intersections of the (light grey) solid lines form the square lattice on which the discrete field  $\phi_z$  is defined. The (red) basis vector  $\mathbf{a}_1 = (3, 0)$  and the (blue) basis vector  $\mathbf{a}_2 = (1, 2)$  form a  $[L \times T]_S = [3 \times 2]_1$  Bravais cell. The intersections (red points) of the black dashed lines form the Bravais lattice  $\Lambda$ .

Each such family contains a unique Bravais cell of the *Hermite normal form* [48], which, for a 2-dimensional square lattice, can be chosen to have the first basis vector pointing in the spatial direction [149]

$$\mathbf{a}_1 = \begin{pmatrix} L \\ 0 \end{pmatrix}, \quad \mathbf{a}_2 = \begin{pmatrix} S \\ T \end{pmatrix}, \quad (84)$$

where  $L, T$  are respectively the spatial, temporal lattice periods, and the ‘tilt’ [173]  $0 \leq S < L$  imposes the relative-periodic ‘shift’ bc’s [58] (in the integer lattices literature these are also referred to as ‘helical’ [144] vs. ‘toroidal’ [119]; ‘twisted’ and ‘twisting factor’ [144]; ‘screw’ bc’s). We label Bravais cell (84) and the corresponding Bravais lattice  $\Lambda$  by  $[L \times T]_S$ . An example is the  $[3 \times 2]_1$  Bravais lattice is shown in figure 4.

For each width  $L$ , height  $T$ , the number of (tilted) Hermite normal form Bravais cells is

$$\#_{[L \times T]} = \sum_{S=0}^{L-1} 1 = L, \quad (85)$$

and a Bravais lattices-counting zeta function (see Lind [149] Example 3.1) can be constructed by substituting  $\#_{[L \times T]}$  into

$$\begin{aligned} 1/\zeta(z) &= \exp \left( - \sum_{L=1}^{\infty} \sum_{T=1}^{\infty} \#_{[L \times T]} \frac{z^{LT}}{LT} \right) = \exp \left( - \sum_{L=1}^{\infty} \sum_{T=1}^{\infty} \frac{(z^L)^T}{T} \right) \\ &= \exp \left( \sum_{L=1}^{\infty} \ln(1 - z^L) \right) = \prod_{L=1}^{\infty} (1 - z^L). \end{aligned} \quad (86)$$

[2020-09-05 Predrag] As long as I do not understand the logic of this zeta function, we will have to drop it from the paper...

### 3.6. Prime Bravais lattices

It might be possible to tile a given Bravais lattice  $\Lambda$  by a finer lattice  $\Lambda_p$ . Lattice  $\Lambda_p$ , defined by a Bravais cell

$$\mathbf{a}_1^p = \begin{pmatrix} L_p \\ 0 \end{pmatrix}, \quad \mathbf{a}_2^p = \begin{pmatrix} S_p \\ T_p \end{pmatrix}, \quad (87)$$

is a *prime* Bravais lattice, if there is no finer Bravais cell, other than the unit volume  $[1 \times 1]_0$  Bravais cell, that can tile it.

[2020-07-15 Predrag] In *siminos/spatiotemp/chapter/integLatt.tex* Dudgeon and Mersereau [74] explain clearly that if  $\det \Lambda$  is a prime number, then  $\Lambda$  is a *prime matrix*. If  $\Lambda$  is neither prime nor unimodular, it is *composite*, and can be decomposed, nonuniquely - up to a unimodular transformation - into a product of two non-unimodular matrices  $\Lambda = PQ$ . Then one can “quotient”  $Q$  by “dividing” by  $P$ .

In order to determine all prime lattices  $\Lambda_p$  (87) that tile a given Bravais lattice  $\Lambda$  (84),

$$\begin{aligned} \mathbf{a}_1 &= k \mathbf{a}_1^p + \ell \mathbf{a}_2^p \\ \mathbf{a}_2 &= m \mathbf{a}_1^p + n \mathbf{a}_2^p, \end{aligned}$$

observe that a prime tile  $(\mathbf{a}_1^p, \mathbf{a}_2^p)$  tiles the larger tile only if larger tile’s width  $L$  is a multiple of  $L_p$ , the height  $T$  is a multiple of  $T_p$ , and the two tile ‘tilts’ satisfy

$$\mathbf{a}_2 = m \mathbf{a}_1^p + \frac{T}{T_p} \mathbf{a}_2^p \quad \rightarrow \quad S = mL_p + \frac{T}{T_p} S_p.$$

Hence a prime lattice  $\Lambda_p$  tiles the given lattice  $\Lambda$  only if the area spanned by the two ‘tilted’ basis vectors

$$\mathbf{a}_2 \times \mathbf{a}_2^p = ST_p - TS_p \quad (88)$$

is a multiple of the prime tile area  $L_p T_p$ .

### 3.7. Lattice states

A *lattice state* is a set of all field values  $\Phi = \{\phi_z\}$  over the  $d$ -dimensional lattice  $z \in \mathbb{Z}^d$  that satisfies the spatiotemporal cat equation (75), with all field values constrained to  $0 \leq \phi_z < 1$ .

While the spatiotemporal cat equation (75) is *equivariant* under the integer lattice *space group*  $p4mm$  symmetry operations (81), the individual lattice states either have no symmetry at all (they are, after all, ‘turbulent’), or are invariant under subgroups of space group  $p4mm$ . In what follows we quotient only the translational symmetries, and postpone dazzling the captive reader with the full  $D_4$  point group reduction to a later, more ponderous publication.

Furthermore, inspection of the temporal cat figure 3 suggests that there is a *field symmetry* under inversion though the center of the  $0 \leq \phi_z < 1$  unit interval. Indeed, if

$\mathbf{M} = \{m_{nt}\}$ , composed of symbols from alphabet (76), corresponds to a 2-dimensional lattice state  $\Phi_{\mathbf{M}} = \{\phi_{nt}\}$ , its conjugation symmetry partner

$$\bar{\mathbf{M}} = \{\bar{m}_{nt}\}, \quad \bar{m}_{nt} = 2(s-2) - m_{nt}, \quad (89)$$

corresponds to lattice state  $\bar{\Phi}_{\bar{\mathbf{M}}} = \{1 - \phi_{nt}\}$ . So, every lattice state either belongs to a conjugate pair  $\{\Phi_{\mathbf{M}}, \bar{\Phi}_{\bar{\mathbf{M}}}\}$ , or is self-dual under conjugation.

While the action of orbit Jacobian matrix  $\mathcal{J}$  (80) maps fields  $\phi_{nt}$  to values outside the unit interval, such values that are then returned back to the unit interval by integer  $m_{nt}$ . This ‘ $\mathbb{Z}^1$  lattice action’ at every spatiotemporal lattice site is a peculiarity of the coupled Bernoulli and cat map lattice models, not a condition that a spatiotemporal discretization of a generic field theory would satisfy, and should never be confused with a discretization of spacetime continuum to integer lattice  $\mathbb{Z}^d$ .

For brevity, we shall refer to lattice state  $\Phi$  as a *periodic orbit* if it satisfies

$$\Phi(z + R) = \Phi(z) \quad (90)$$

for any discrete translation  $R = n_1 \mathbf{a}_1 + n_2 \mathbf{a}_2 \in \Lambda$ , where  $\{n_1, n_2\}$  are any integers, and  $(\mathbf{a}_1, \mathbf{a}_2)$  is a pair of  $\mathbb{Z}^2$  integer lattice vectors that define a *Bravais cell*. We shall always refer to a Bravais sublattice (sublattice of  $\mathbb{Z}^2$ ) by its unique Hermite normal form Bravais cell (84) (basis?), and denote it  $\Lambda = [L \times T]_S$ , a 2-dimensional doubly-periodic (relative) *periodic orbit*

$$\phi_{nt} = \phi_{n+L, t} = \phi_{n+L, t+T}, \quad (n, t) \in \mathbb{Z}^2 \quad (91)$$

with periods  $(L, T)$  and tilt  $S$ .

A correct definition of a *prime* periodic orbit [57] is subtler than for the 1-dimensional temporal lattice case. If a given periodic orbit over lattice  $\Lambda$  is not periodic under translations  $R \in \Lambda_p$  on any sublattice  $\Lambda_p$  (except for  $\Lambda$  itself), we shall refer to it here as a *prime periodic orbit*, a periodic orbit of the smallest periodicity in all spacetime directions.

[2020-09-08 Predrag] The  $\mathbb{Z}^d$  unit cell is always one of  $\Lambda_p$ , see table 2, do we say that anywhere?

We return to explicit construction of prime periodic orbits in section 4. Prime periodic orbits are the basic building blocks of topological zeta functions (see section 1.9 and 2.8).

Explicitly verifying the periodic lattice states counting formulas for several 2-dimensional spatiotemporal cat examples is now in order.

The simplest examples of periodic orbits are (i) spacetime equilibria over  $[1 \times 1]_0$ , (ii) space-equilibria over  $[1 \times T]_0$ , (iii) time-equilibria over  $[L \times 1]_0$ , and (iv) time-relative equilibria over  $[L \times 1]_S$ ,  $S \neq 0$ , stationary patterns in a time-reference frame [183] moving with a constant velocity  $S/T$ .

### 3.7.1. Spacetime equilibria over $[1 \times 1]_0$ .

*3.7.2. Time-equilibria over  $[L \times 1]_0$ .* Consider the time-equilibrium  $\phi_{nt} = \phi_{n1}$  for all spatial sites  $n$ , and all times  $t$ . To see that this is the 1-dimensional lattice temporal cat tiles of period  $L$  already counted in section 2.5, note that the 5-term recurrence relation (74) reduces to the 3-term recurrence

$$\phi_{n+1,1} - 2(s_2 - 1)\phi_{n1} + \phi_{n-1,1} = -m_{n1}, \quad (92)$$

where we have temporarily added index ‘2’ to the stretching parameter  $s_2$  to indicate that it refers to the 2-dimensional spatiotemporal cat. Comparing with the temporal cat (47),  $\phi_{t+1} - s_1\phi_t + \phi_{t-1} = -m_t$ , we see that we have already counted all lattice states on Bravais cells of form  $[L \times 1]_0$ , provided we replace  $s_1 \rightarrow 2(s_2 - 1)$  in (69). For the values chosen in our numerical examples,  $s_1 = 3$  and  $s_2 = 5/2$ , the two counts happen to be the same and given by (C.5).

However, already the smallest *relative*-periodic  $[L \times 1]_S$  Bravais lattices are new, and perhaps surprising.

*3.7.3. Relative  $[2 \times 1]_1$  periodic orbit.* Consider a  $[2 \times 1]_1$  periodic orbit with tilt periodic bc’s, periodic state  $\Phi_{m_1 m_2} = [\phi_1 \ \phi_2]$ , tiled by the Bravais lattice (82) with basis vectors  $\mathbf{a}_1 = \{2, 0\}$  and  $\mathbf{a}_2 = \{1, 1\}$ , see figure 5(a).

[2020-02-23 Predrag] This is wrong, it is written for the symmetric alphabet that we do not use. Fix.

$$\Phi_{\underline{m}m} = \frac{1}{9} \begin{bmatrix} -m & m \end{bmatrix}, \quad m \in \mathcal{A}, \quad (93)$$

for example

$$\mathbf{M} = \begin{bmatrix} -4 & 4 \end{bmatrix} \Rightarrow \Phi_{\underline{44}} = \frac{1}{9} \begin{bmatrix} -4 & 4 \end{bmatrix}.$$

Note that these are ‘periodic lattice state’ solutions: there is one *prime* periodic orbit for each set of period-2 periodic lattice states related by cyclic permutations,  $\overline{mm} = (\Phi_{\underline{m}m}, \Phi_{\underline{m}m})$ , and there are only 4 of those, as  $\Phi_{00} = \Phi_0$  is a repeat of the 1-block.

By (A.36) the number of  $[2 \times 1]_1$  relative periodic orbits with the given Bravais lattice bc’s is 9. Using the Green’s function method (102) one can verify that there are indeed 9 such periodic orbits, one periodic orbit solution for each letter of alphabet (76),

*3.7.4.  $[2 \times 1]_0$  periodic orbit.* As an illustration of the fundamental parallelepiped (16)  $s = 3$  cat map (45) acting on states  $\phi_t$  within the unit square  $(\phi_0, \phi_1) \in [0, 1) \times [0, 1)$ . In 2 time steps orbit Jacobian matrix  $\mathcal{J}$  unit square into the fundamental parallelepiped, with integer points within the fundamental parallelepiped corresponding to  $N_2 = 5$  periodic lattice states (C.5) of period 2. These integer-valued vertices over-count the number distinct lattice states, as already noted in the construction of the topological zeta function (C.4).

But the great thing about the spatiotemporal cat is that it is a field theory defined on a lattice, a theory that can be solved by the well-developed crystallographic methods: here we follow the notation of Dresselhaus *et al* [72].

To determine the *admissible* blocks,

(7) compute  $\Phi_p$  for each prime block  $M_p$ , and eliminate every  $\Phi_p$  which contains a lattice site or sites on which the value of the field violates the admissibility condition  $\phi_z \in [0, 1)$ .

For  $s = 5/2$  spatiotemporal cat the pruning turns out to be very severe. Only 52 of the prime  $[2 \times 2]_0$  blocks are admissible. As for the repeats of smaller blocks, there are 2 admissible  $[1 \times 2]_0$  blocks repeating in time and 2  $[2 \times 1]_0$  blocks repeating in space. There are 4 admissible 1/2-shift periodic boundary  $[1 \times 2]_0$  blocks. And there is 1 admissible block which is a repeat of letter 0. The total number of  $[2 \times 2]_0$  of periodic orbits is obtained by all cyclic permutations of admissible prime blocks,

$$\begin{aligned} N_{[2 \times 2]_0} &= 225 \\ &= 52 [2 \times 2]_0 + 2 [2 \times 1]_0 + 2 [1 \times 2]_0 + 4 [2 \times 1]_1 + 1 [1 \times 1]_0, \end{aligned} \quad (94)$$

summarized in table 1. This explicit list of admissible prime periodic orbits verifies the counting formula (A.33).

**3.7.5.  $[3 \times 2]_0$  periodic orbit.** For  $s = 5/2$  spatiotemporal cat only 850 prime  $[3 \times 2]_0$  blocks are admissible. There are 5 admissible repeating prime  $[3 \times 1]_0$  blocks, 2 admissible repeating prime  $[1 \times 2]_0$  blocks, and 1 admissible block which is a repeat of 0. The total number of admissible solutions obtained by all cyclic permutations of admissible prime blocks is:

$$N_{[3 \times 2]_0} = 5120 = 850 [3 \times 2]_0 + 5 [3 \times 1]_0 + 2 [1 \times 2]_0 + 1 [1 \times 1]_0, \quad (95)$$

summarized in table 1. The count is in agreement with the counting formula (A.33) for the  $[3 \times 2]_0$  periodic orbits.

**3.7.6. Relative  $[3 \times 2]_1$  periodic orbit.** Consider the Bravais lattice of figure 4, tiled by periodic orbit defined by the Bravais cell with basis vectors  $\mathbf{a}_1 = (3, 0)$  and  $\mathbf{a}_2 = (1, 2)$ , see figure 5(b). There are 6 independent field values in the repeating cell, which can be written as an  $[3 \times 2]$  array:

[2020-02-23 Predrag] Where is the source code for figure 5?

$$[3 \times 2]_1 = \begin{bmatrix} & \phi_{11} & \phi_{21} & \phi_{01} \\ \phi_{00} & \phi_{10} & \phi_{20} & \end{bmatrix}.$$

*Example:*  $[2 \times 2]_0$  Bravais lattices prime blocks.

Consider  $[2 \times 2]_0$  Bravais lattices prime block

$$M_p = \begin{bmatrix} m_{01} & m_{11} \\ m_{00} & m_{10} \end{bmatrix}, \quad (96)$$



According to (109), the number of prime  $[2 \times 2]_0$  lattice states is

$$M_{[2 \times 2]_0} = \frac{1}{2 \cdot 2} (N_{[2 \times 2]_0} - 2M_{[2 \times 1]_0} - 2M_{[1 \times 2]_0} - 2M_{[2 \times 1]_1} - M_{[1 \times 1]_0}) , \quad (97)$$

We can work this out explicitly as follows:

(3) The  $[2 \times 1]_1$  relative-periodic block (98) is counted as the  $[2 \times 2]_0$  periodic orbit.

(5) Throw away all blocks which are repeats of shorter blocks. There are three kinds of repeating small blocks:

$$[2 \times 1]_0 = \begin{bmatrix} a & b \\ a & b \end{bmatrix} , \quad [1 \times 2]_0 = \begin{bmatrix} b & b \\ a & a \end{bmatrix} , \quad [2 \times 1]_1 = \begin{bmatrix} & a & b \\ a & b & \end{bmatrix} .$$

the relative-periodic  $[2 \times 1]_1$  block with 1 site-shift periodic boundary, which is periodic after the second repeat in the time direction,

$$\mathbf{M}_p = \begin{bmatrix} & [m_{00} & m_{10}] \\ [m_{00} & m_{10}] & \end{bmatrix} . \quad (98)$$

*Example:*  $[3 \times 2]_0$  Bravais lattices prime blocks.

Consider the Bravais lattice

$$\mathbf{M} = \begin{bmatrix} m_{12} & m_{22} & m_{32} \\ m_{11} & m_{21} & m_{31} \end{bmatrix} . \quad (99)$$

According to (109), the number of prime  $[3 \times 2]_0$  lattice states is

$$M_{[3 \times 2]_0} = \frac{1}{3 \cdot 2} (N_{[3 \times 2]_0} - 3M_{[3 \times 1]_0} - 2M_{[1 \times 2]_0} - M_{[1 \times 1]_0}) , \quad (100)$$

Unlike the  $[2 \times 2]_0$  case (98), there no sub-blocks with relative-periodic boundary contributing to the  $[3 \times 2]_0$  blocks count, since  $[3 \times 1]_0$  and  $[1 \times 2]_0$  sub-blocks cannot fit into the  $[3 \times 2]_0$  doubly-periodic Bravais lattice without a shift.

### 3.8. Counting spatiotemporal cat lattice states

We now show how to count the number of periodic lattice states of a 2-dimensional spatiotemporal cat, and apply the method to counting periodic orbits of the 2-dimensional spatiotemporal cat.

Periodic lattice Hill determinants, such as (16), are usually evaluated by a Fourier transform diagonalization (see Appendix A). However, due to the uniformity of Bernoulli map stretching, in case at hand lattice points counting is a combinatorial problem. Counting of  $\mathbb{Z}^d$  integer lattice points within various convex domains is an important, highly developed field. For integer lattice counting powerful combinatorial methods are available, for example Barvinok multivariate generating functions algorithm for counting lattice points in convex lattice domains [20], and its online code implementations, such as the lattice point enumeration **LattE** code [63].

As in the temporal cat case (52), the total number of periodic lattice states is given by the volume of the fundamental parallelepiped

$$N_n = |\text{Det } \mathcal{J}| . \quad (101)$$

### 3.9. Periodic orbit theory

[2020-02-02 Predrag] Gutkin and Osipov [99] refer to an screened Poisson equation periodic orbit solution  $p$  as a ‘many-particle periodic orbit’, with  $\phi_{nt}$  ‘doubly-periodic’, or ‘closed,’

$$\phi_{nt} = \phi_{n+L_p, t+T_p}, \quad n = 0, 1, 2, \dots, L_p - 1; \quad t = 0, 1, 2, \dots, T_p - 1.$$

### 3.10. Shadowing

[2019-08-06 Predrag] Must emphasize *shadowing*? One of the main points of this and the companion papers is that periodic orbits shadowing generalizes to periodic orbits shadowing in higher spatiotemporal dimensions. Include 2d periodic orbits shadowing figures.

Add a shadowing sub-section here, the analogue to temporal cat Green’s function (66).

As we now show, the block  $\mathbf{M} = \{m_{nt} \in \mathcal{A}, (n, t) \in \mathbb{Z}^2\}$  can be used as a 2-dimensional symbolic representation of the lattice system state. By the linearity of equation (104), every solution  $\Phi$  can be uniquely recovered from its symbolic representation  $\mathbf{M}$ . Inverting (104) we obtain

$$\phi_z = \sum_{z' \in \mathbb{Z}^2} g_{zz'} m_{z'}, \quad g_{zz'} = \left( \frac{1}{-\square + 2(s-2)} \right)_{zz'}, \quad (102)$$

where  $g_{zz'}$  is the Green’s function for the 2-dimensional discretized screened Poisson equation. However, a given lattice block  $\mathbf{M}$  is *admissible* if and only if all  $\phi_z \in \Phi$  given by (102) fall into the interval  $[0, 1)$ .

For a given admissible source block  $\mathbf{M}$ , the periodic field can be computed by:

$$\Phi_{i_1 j_1} = \sum_{i_2=0}^2 \sum_{j_2=0}^1 g_{i_1 j_1, i_2 j_2} \mathbf{M}_{i_2 j_2}.$$

For example, if the source  $\mathbf{M}$  is:

$$\mathbf{M} = \begin{bmatrix} 0 & 2 & 0 \\ -1 & 0 & 0 \end{bmatrix},$$

the corresponding field is:

$$\Phi_{\mathbf{M}} = \begin{bmatrix} \phi_{01} & \phi_{11} & \phi_{21} \\ \phi_{00} & \phi_{10} & \phi_{20} \end{bmatrix} = \frac{1}{35} \begin{bmatrix} 5 & 17 & 6 \\ -1 & 5 & 3 \end{bmatrix}.$$

Substitute this solution into figure 5(b) we can see that (74) is satisfied everywhere.

### 3.11. Topological zeta function

### 3.12. Spatiotemporal cat as a continuous time dynamical system

$$(\square - 2(s-2)) \Phi = -\mathbf{M} \quad (103)$$

While the  $d = 2$  spatiotemporal cat does have a Hamiltonian formulation [99], its Lagrangian formulation as screened Poisson equation (103), in analogy with the temporal cat (71), is a natural departure point for what follows:

$$(\square - 2(s - 2)) \phi_{nt} = -m_{nt}, \quad \phi_{nt} \in [0, 1), \quad m_{nt} \in \mathcal{A}, \quad (n, t) \in \mathbb{Z}^2 \quad (104)$$

where  $\square$  is now the discrete 2-dimensional space-time Laplacian on  $\mathbb{Z}^2$ ,

$$\square \phi_{nt} = \phi_{n,t-1} + \phi_{n-1,t} - 4\phi_{nt} + \phi_{n,t+1} + \phi_{n+1,t}, \quad (105)$$

and the alphabet is given in (76).

[2019-01-04 Predrag] More generally, the same argument yields the screened Poisson equation (71) for the  $d$ -dimensional *spatiotemporal cat*

$$\begin{aligned} (\square - d(s - 2)) \phi_z &= -m_z, \quad \phi_z \in [0, 1), \quad m_z \in \mathcal{A}, \quad z \in \mathbb{Z}^d, \\ \mathcal{A} &= \{-2d + 1, -2d + 2, \dots, 2s - 2, 2s - 1\} \end{aligned} \quad (106)$$

where  $\square$  is the discrete  $d$ -dimensional Euclidean space-time Laplacian.

[2019-01-04 Predrag]

The  $d$ -dimensional spatiotemporal cat satisfies screened Poisson equation (80)

$$(\square - d(s - 2)) \phi_z = -m_z, \quad z \in \mathbb{Z}^d, \quad (107)$$

where  $\square$  is the discrete  $d$ -dimensional Laplacian (discrete Laplacians on 1-dimensional and 2-dimensional lattices are given in (70) and (105)). As in (??), a  $d$ -dimensional discrete Laplacian can be written as

$$\square = \sum_{i=1}^d (\sigma_i - 2\mathbf{1} + \sigma_i^{-1}), \quad (108)$$

**Spatiotemporal cat, summarized.** The key insight [34, 99] –an insight that applies to coupled-map lattices [179, 180, 184], and field theories modeled by them, not only the system considered here– is that a field  $\Phi = \{\phi_z\}$  over a  $d$ -dimensional spacetime lattice  $z \in \mathbb{Z}^d$  has to be described by a corresponding symbol block  $\mathbf{M} = \{m_z\}$ , over the same  $d$ -dimensional spacetime lattice  $z \in \mathbb{Z}^d$ , rather than a 1-dimensional temporal symbol sequence (??), as one does when describing a finite coupled “ $N$ -particle” system in the Hamiltonian formalism.

A key advantage of the spatiotemporal code  $\mathbf{M}$  is illustrated already by the  $d = 2$  case. While an Adler-Weiss type partition, forward-in time Hamiltonian evolution alphabet would grow exponentially with the “particle number”  $L$ , the number of letters (80) of the spatiotemporal code  $\mathcal{A}$  is finite and the same for any spatial extent  $L$ , including the  $L \rightarrow \infty$  spatiotemporal cat. For the spatiotemporal code, a field  $\Phi$  over a periodic spatiotemporal domain is encoded by a doubly periodic 2-dimensional block  $\mathbf{M}$  of symbols from a small alphabet, rather than by a 1-dimensional temporal string of symbols from the exponentially large (in  $L$ ) ‘ $L$ -particle’ alphabet  $\bar{\mathcal{A}}$ .

The spatiotemporal cat is arguably the simplest example of a chaotic (or ‘turbulent’) classical field theory for which the local degrees of freedom are hyperbolic (anti-harmonic, ‘inverted pendula’) rather than oscillatory (‘harmonic oscillators’). As we have shown here, it is also a field theory for which all admissible spatiotemporal patterns can be enumerated, and their recurrences (shadowing of a large periodic orbit by smaller periodic orbits) identified.

#### 4. Enumeration of prime periodic orbits

Here we show how to enumerate the total numbers of distinct periodic states in terms of prime periodic orbits.

The enumeration of spatiotemporal cat doubly-periodic lattice states proceeds in 3 steps:

- (i) Construct a hierarchy of 2-dimensional Bravais lattices  $\Lambda$ , starting with the smallest Bravais cells (84), list Bravais lattices by increasing  $[L \times T]_S$ , one per each set related by discrete symmetries (81).
- (ii) For each  $\Lambda = [L \times T]_S$  Bravais lattice, compute  $N_\Lambda$ , the number of doubly-periodic spatiotemporal cat lattice states, using the ‘fundamental fact’  $N_\Lambda = |\det \mathcal{J}(\Lambda)|$ .
- (iii) We have defined the *prime* Bravais lattice in section 3.6.
- (iv) The total number of (doubly) periodic blocks is the sum of all cyclic permutations of prime blocks,

$$N_\Lambda = \sum_p N_p [L_p \times T_p]_{S_p}$$

where the sum goes over prime tilings of the  $[L \times T]_S$  block.

The number of prime periodic orbits is given recursively by (see (36)),

$$M_p = \frac{1}{LT} \left( N_p - \sum_{p'} L_{p'} T_{p'} M_{p'} \right), \quad (109)$$

where the sum is over  $p'$ , the prime ‘divisors’ of  $p$  that satisfy tiling conditions (88).

The following expressions do not fit into table 2:

$$M_{[3 \times 3]_0} = 2(s-2) \frac{1}{9} (256s^8 + 512s^7 - 128s^6 - 640s^5 + 16s^4 + 320s^3 - 48s^2 - 72s + 9). \quad (110)$$

The last, currently unreduced formula exemplifies what is nonintuitive about the Fourier space results; it is not at all obvious that this

$$M_{[3 \times 3]_1} = M_{[3 \times 3]_2} = 2(s-2) \frac{1}{9} (1-2s)^2 \times \left\{ \left[ 2s+1-2\sin\left(\frac{\pi}{18}\right) \right]^2 \left[ 2s+1+2\cos\left(\frac{\pi}{9}\right) \right]^2 \right. \\ \left. \left[ \left( 2s+1-2\cos\left(\frac{2\pi}{9}\right) \right)^2 - 1 \right] \right\} \quad (111)$$

is an integer for any half-integer or integer  $s$ . **Predrag** to Han: can you evaluate this using the fundamental fact  $N_n = |\text{Det } \mathcal{J}|$ ?

Note that  $N_{[3 \times T]_1}(s) = N_{[3 \times T]_2}(s)$ , by reflection symmetry, as  $N_{[3 \times T]_2}(s) = N_{[3 \times T]_{-1}}(s)$ .

[2020-03-04 Predrag] Han, please recheck, complete.

**Table 1.** The numbers of the  $s = 5/2$  spatiotemporal cat  $[L \times T]_S$  periodic orbits:  $M_{[L \times T]_S}$  is the number of prime periodic orbits,  $N_{[L \times T]_S}$  is the number of doubly periodic lattice states, and  $R_{[L \times T]_S}$  is the number of prime periodic orbits in the  $D_4$  symmetries orbit.

$[L \times T]_S$	$M$	$N$	$R$
$[1 \times 1]_0$	1	1	1
$[2 \times 1]_0$	2	$5 = 2 [2 \times 1]_0 + 1 [1 \times 1]_0$	2
$[2 \times 1]_1$	4	$9 = 4 [2 \times 1]_1 + 1 [1 \times 1]_0$	
$[3 \times 1]_0$	5	$16 = 5 [3 \times 1]_0 + 1 [1 \times 1]_0$	
$[3 \times 1]_1$	16	$49 = 16 [3 \times 1]_1 + 1 [1 \times 1]_0$	
$[4 \times 1]_0$	10	$45 = 10 [4 \times 1]_0 + 2 [2 \times 1]_0 + 1 [1 \times 1]_0$	
$[4 \times 1]_1$	54	$225 = 54 [4 \times 1]_1 + 4 [2 \times 1]_1 + 1 [1 \times 1]_0$	
$[4 \times 1]_2$	60	$245 = 59 [4 \times 1]_2 + 2 [2 \times 1]_0 + 1 [1 \times 1]_0$	
$[2 \times 2]_0$	52	$225 = 52 [2 \times 2]_0 + 2 [2 \times 1]_0 + 2 [1 \times 2]_0 + 4 [2 \times 1]_1 + 1 [1 \times 1]_0$	1
$[2 \times 2]_1$	60	$245 = 60 [2 \times 2]_1 + 2 [1 \times 2]_0 + 1 [1 \times 1]_0$	
$[3 \times 2]_0$	850	$5120 = 850 [3 \times 2]_0 + 5 [3 \times 1]_0 + 2 [1 \times 2]_0 + 1 [1 \times 1]_0$	
$[3 \times 2]_1$	1012	$6125 = 1012 [3 \times 2]_1 + 16 [3 \times 1]_2 + 2 [1 \times 2]_0 + 1 [1 \times 1]_0$	
$[3 \times 3]_0$	68281	$614656 = 68281 [3 \times 3]_0 + 5 [3 \times 1]_0 + 16 [3 \times 1]_1 + 16 [3 \times 1]_2 + 5 [1 \times 3]_0 + 1 [1 \times 1]_0$	1
$[3 \times 3]_1$	70400	$633616 = 70400 [3 \times 3]_1 + 5 [1 \times 3]_0 + 1 [1 \times 1]_0$	

$$\begin{aligned}
\sum_{L=1} N_{[L \times 1]_0} z^L &= \frac{s-2z}{1-sz+z^2} - \frac{2}{1-z} \\
&= (s-2) + (s-2)z + (s-2)(s+2)z^2 + (s-2)(s+1)^2 z^3 \\
&\quad + (s-2)(s+2)s^2 z^4 + (s-2)(s^2+s-1)^2 z^5 \\
&\quad + \dots,
\end{aligned} \tag{112}$$

[2020-06-09 Predrag] explain table 2

**2020-06-09 Han** Figures 6 and 7 are the plots of the periodic blocks by color. The three figures in figure 6 are the blocks with periodicity  $[1 \times 3]_0$ ,  $[3 \times 1]_0$  and  $[3 \times 1]_1$ , which can show the periodicity of the space-equilibria, time-equilibria and time-relative equilibria. Figure 7 is the color coding of the periodic blocks with periodicity  $[2 \times 1]_1$ ,  $[3 \times 2]_1$  and  $[3 \times 2]_0$ .

**2020-10-03 Predrag** For periodic boundary conditions, the Laplacian  $\square$  in (71) and (104) has a translational zero mode,  $\lambda_0 = 0$ , corresponding to a constant eigenvector, so the matrix  $\square$  is singular. That is the reason why our counting formulas (69) and table 2 have a prefactor  $(s-2)$ ; in the Laplacian limit the corresponding determinant has a zero eigenvalue, and therefore vanishes.

**Table 2.** The numbers of spatiotemporal cat lattice states for Bravais lattices  $\Lambda = [L \times T]_S$  up to  $[3 \times 3]_2$ . Here  $N_\Lambda(s)$  is the number of doubly periodic lattice states,  $M_\Lambda(s)$  is the number of prime periodic orbits, and  $R_\Lambda$  is the number of prime periodic orbits in the  $D_4$  symmetries orbit. The stretching parameter  $s$  can take half-integer or integer values.

$\Lambda$	$N_\Lambda(s)$	$M_\Lambda(s)$	$R$
$[1 \times 1]_0$	$2(s-2)$	$2(s-2)$	1
$[2 \times 1]_0$	$2(s-2)2s$	$2(s-2)\frac{1}{2}(2s-1)$	2
$[2 \times 1]_1$	$2(s-2)2(s+2)$	$2(s-2)\frac{1}{2}(2s+3)$	
$[3 \times 1]_0$	$2(s-2)(2s-1)^2$	$2(s-2)\frac{4}{3}(s-1)s$	
$[3 \times 1]_1$	$2(s-2)4(s+1)^2$	$2(s-2)\frac{1}{3}(2s+1)(2s+3)$	
$[4 \times 1]_0$	$2(s-2)8(s-1)^2s$	$2(s-2)\frac{1}{2}(2s-3)(2s-1)s$	
$[4 \times 1]_1$	$2(s-2)8s^2(s+2)$	$2(s-2)\frac{1}{2}(s+2)(2s-1)(2s+1)$	
$[4 \times 1]_2$	$2(s-2)8(s+1)^2s$	$2(s-2)\frac{1}{2}(2s+3)(2s+1)s$	
$[4 \times 1]_3$	$2(s-2)8s^2(s+2)$	$2(s-2)\frac{1}{2}(s+2)(2s-1)(2s+1)$	
$[5 \times 1]_0$	$2(s-2)(4s^2-6s+1)^2$	$2(s-2)\frac{4}{5}(s-1)(2s-3)(2s-1)s$	
$[5 \times 1]_1$	$2(s-2)16(s^2+s-1)^2$	$2(s-2)\frac{1}{5}(2s-1)(2s+3)(4s^2+4s-5)$	
$[2 \times 2]_0$	$2(s-2)8s^2(s+2)$	$2(s-2)\frac{1}{2}(2s-1)(2s^2+5s+1)$	1
$[2 \times 2]_1$	$2(s-2)8s(s+1)^2$	$2(s-2)\frac{1}{2}(2s+1)(2s+3)s$	
$[3 \times 2]_0$	$2(s-2)2s(2s-1)^2(2s+3)^2$	$2(s-2)\frac{2}{3}(2s-1)(4s^3+10s^2+3s-5)s$	
$[3 \times 2]_1$	$2(s-2)32s^3(s+1)^2$	$2(s-2)\frac{1}{6}(2s-1)(2s+1)(8s^3+16s^2+10s+3)$	
$[3 \times 3]_0$	$2(s-2)16(s+1)^4(2s-1)^4$		
$[3 \times 3]_1$	$2(s-2)(2s-1)^2(8s^3+12s^2-1)^2$		

$x_1$	$x_2$	$x_1$	$x_2$	$x_1$	$x_2$
$x_2$	$x_1$	$x_2$	$x_1$	$x_2$	$x_1$
$x_1$	$x_2$	$x_1$	$x_2$	$x_1$	$x_2$
$x_2$	$x_1$	$x_2$	$x_1$	$x_2$	$x_1$
$x_1$	$x_2$	$x_1$	$x_2$	$x_1$	$x_2$
$x_2$	$x_1$	$x_2$	$x_1$	$x_2$	$x_1$

(a)

$x_{11}$	$x_{21}$	$x_{01}$	$x_{11}$	$x_{21}$	$x_{01}$
$x_{10}$	$x_{20}$	$x_{00}$	$x_{10}$	$x_{20}$	$x_{00}$
$x_{21}$	$x_{01}$	$x_{11}$	$x_{21}$	$x_{01}$	$x_{11}$
$x_{20}$	$x_{00}$	$x_{10}$	$x_{20}$	$x_{00}$	$x_{10}$
$x_{01}$	$x_{11}$	$x_{21}$	$x_{01}$	$x_{11}$	$x_{21}$
$x_{00}$	$x_{10}$	$x_{20}$	$x_{00}$	$x_{10}$	$x_{20}$

(b)

**Figure 5.** Examples of  $[L \times T]_S$  periodic orbits together with their spatiotemporal Bravais lattice tilings (82). (a)  $[2 \times 1]_1$ , basis vectors  $\mathbf{a}_1 = \{2, 0\}$  and  $\mathbf{a}_2 = \{1, 1\}$ ; (b)  $[3 \times 2]_1$ , basis vectors  $\mathbf{a}_1 = (3, 0)$  and  $\mathbf{a}_2 = (1, 2)$ . Rectangles enclose the Bravais cell and its Bravais lattice translations.

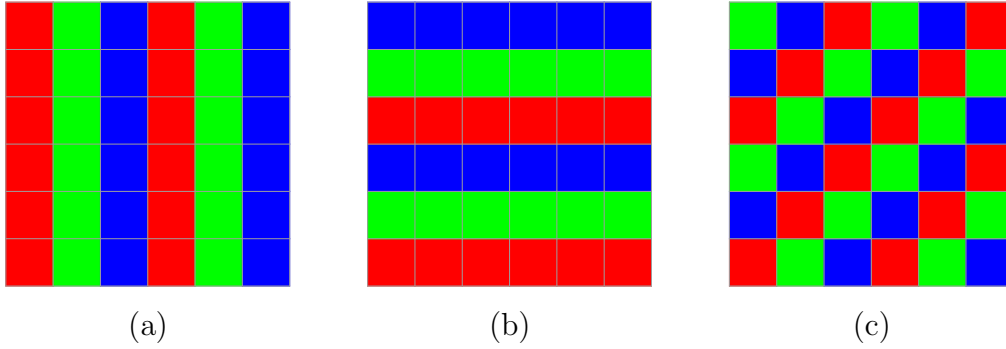


**Figure 6.** Examples of  $[L \times T]_S$  periodic blocks together with their spatiotemporal Bravais lattice tilings (82). (a)  $[3 \times 1]_0$ , basis vectors  $\mathbf{a}_1 = \{3, 0\}$  and  $\mathbf{a}_2 = \{0, 1\}$ ; (b)  $[1 \times 3]_0$ , basis vectors  $\mathbf{a}_1 = \{1, 0\}$  and  $\mathbf{a}_2 = \{0, 3\}$ ; (c)  $[3 \times 1]_1$ , basis vectors  $\mathbf{a}_1 = \{3, 0\}$  and  $\mathbf{a}_2 = \{1, 1\}$ ;

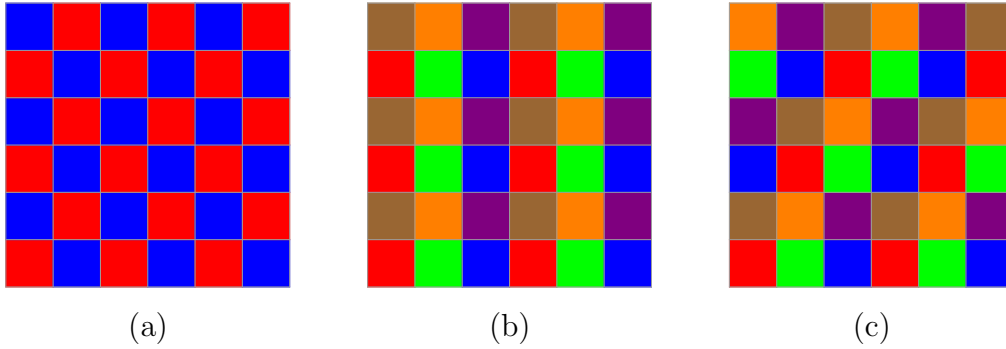


**Figure 7.** Examples of  $[L \times T]_S$  periodic blocks together with their spatiotemporal Bravais lattice tilings (82). (a)  $[2 \times 1]_1$ , basis vectors  $\mathbf{a}_1 = \{2, 0\}$  and  $\mathbf{a}_2 = \{1, 1\}$ ; (b)  $[3 \times 2]_0$ , basis vectors  $\mathbf{a}_1 = \{3, 0\}$  and  $\mathbf{a}_2 = \{0, 2\}$ ; (c)  $[3 \times 2]_1$ , basis vectors  $\mathbf{a}_1 = \{3, 0\}$  and  $\mathbf{a}_2 = \{1, 2\}$ ;

A hyper-cubic lattice consists of  $d$  intersecting one-dimensional lattices, with Laplacian eigenvalues being the sums of the eigenvalues of the Laplacian of the constituent one-dimensional lattices, hence for any dimension there is only one zero eigenvalue, and only a single power of the prefactor  $(s-2)$  in our counting formulas.

**2019-11-23 Predrag** We always reduce relative-shift symmetries, so I am not happy about the  $[2 \times 1]_1$  relative-periodic block (98) being counted as the  $[2 \times 2]_0$  periodic orbit. We'll have to revisit symmetry reduction...

**2020-03-17 Han** *PrimeTiles.nb* generates all prime tiles that can tile a larger tile. It gives some not obvious results. For example, let the large tile be  $[3 \times 2]_1$ , and consider the full-shift 9-symbol  $[3 \times 2]_1$  blocks. The number  $[3 \times 2]_0$  blocks is given by (??). The program shows that the  $[3 \times 2]_0$  tile can only be tiled by  $[1 \times 1]_0$ ,  $[1 \times 2]_0$  and  $[3 \times 1]_0$  tiles. So we get the result in (??):

$$N_{[3 \times 2]_0} = 9^{3 \times 2} = 88440 [3 \times 2]_0 + 240 [3 \times 1]_0 + 36 [1 \times 2]_0 + 9 [1 \times 1]_0 .$$

For the full-shift the number of periodic blocks is given by the area of the larger



tile, and number of  $[3 \times 2]_S$  blocks is the same for all  $S$ . But now  $[3 \times 1]_0$  tile cannot tile the  $[3 \times 2]_1$  tile. Instead, the  $[3 \times 2]_1$  can be tiled by  $[1 \times 1]_0$ ,  $[3 \times 1]_2$  and  $[1 \times 2]_0$  tiles,

$$N_{[3 \times 2]_1} = 9^{3 \times 2} = 88440 [3 \times 2]_1 + 240 [3 \times 1]_2 + 36 [1 \times 2]_0 + 9 [1 \times 1]_0 .$$

*A priori* is not obvious that  $[3 \times 1]_2$  tile can tile a  $[3 \times 2]_1$  tile. But if you stack  $[3 \times 1]_2$  tile in the shifted temporal direction by 2 then the left edge of the tile is shifted by 4 in the spatial direction. With the spatial period being 3, shifted by 4 in the spatial direction is same as shifted by 1. So the bc's of  $[3 \times 2]_1$  tile are satisfied by the  $[3 \times 1]_2$  tiles.

## 5. Hill determinant: stability of an orbit vs. its time-evolution stability

The  $d = 2$  lattice spatiotemporal cat equations can be recast in a matrix form, by rewriting the defining equations in terms of *block matrices* [35, 37, 70, 110], constructed by the **Kronecker product**  $\mathbf{A} \otimes \mathbf{B}$ , an operation (introduced by Zehfuss in 1858) that replaces the  $a_{ij}$  element of an  $[n \times n]$  matrix  $\mathbf{A}$  by  $[m \times m]$  matrix block  $a_{ij}\mathbf{B}$ , resulting in an  $[mn \times mn]$  block matrix [7, 218]

$$\mathbf{A} \otimes \mathbf{B} = \begin{bmatrix} a_{11}\mathbf{B} & \cdots & a_{1n}\mathbf{B} \\ \vdots & \ddots & \vdots \\ a_{n1}\mathbf{B} & \cdots & a_{nn}\mathbf{B} \end{bmatrix}. \quad (113)$$

Consider  $\mathbf{A}, \mathbf{A}'$  square matrices of size  $[n \times n]$ , and  $\mathbf{B}, \mathbf{B}'$  square matrices of size  $[m \times m]$ . The matrix product of two block matrices is a block matrix [7, 217],

$$(\mathbf{A} \otimes \mathbf{B})(\mathbf{A}' \otimes \mathbf{B}') = (\mathbf{A}\mathbf{A}') \otimes (\mathbf{B}\mathbf{B}'). \quad (114)$$

The trace and the determinant of a block matrix are given by

$$\begin{aligned} \text{tr}(\mathbf{A} \otimes \mathbf{B}) &= \text{tr} \mathbf{A} \text{tr} \mathbf{B} \\ \det(\mathbf{A} \otimes \mathbf{B}) &= \det(\mathbf{A}^m) \det(\mathbf{B}^n). \end{aligned} \quad (115)$$

The two  $[mn \times mn]$  block matrices  $\mathbf{A} \otimes \mathbf{B}$  and  $\mathbf{B} \otimes \mathbf{A}$  are equivalent by a similarity transformation

$$\mathbf{B} \otimes \mathbf{A} = \mathbf{P}^\top (\mathbf{A} \otimes \mathbf{B}) \mathbf{P}, \quad (116)$$

where  $\mathbf{P}$  is permutation matrix. As  $\det \mathbf{P} = 1$ , the block matrix determinant  $\det(\mathbf{A} \otimes \mathbf{B}) = \det(\mathbf{B} \otimes \mathbf{A})$  is independent of the order in which blocks are constructed.

Consider a rectangular  $d = 2$  lattice  $[L \times T]_0$  Bravais cell. The orbit Jacobian matrix (75) written as a  $[LT \times LT]$  Kronecker product block matrix is

$$\mathcal{J} = \mathbf{1}_1 \otimes (\sigma_2 + \sigma_2^{-1}) - 2s \mathbf{1}_1 \otimes \mathbf{1}_2 + (\sigma_1 + \sigma_1^{-1}) \otimes \mathbf{1}_2, \quad (117)$$

where the (113) matrix  $\mathbf{A}$  and identity  $\mathbf{1}_1$  matrix are ‘spatial’  $[L \times L]$  matrices, with blocks  $\mathbf{B}$  and identity  $\mathbf{1}_2$  ‘temporal’  $[T \times T]$  matrix blocks. Indices ‘1’, ‘2’ referring to ‘spatial’, ‘temporal’ lattice directions, respectively.

Our task is to compute the Hill determinant  $|\det \mathcal{J}|$ . We first show how to do that directly, by computing the volume of the fundamental parallelepiped.

### 5.1. Hill determinant: fundamental parallelepiped evaluation

As a concrete example consider the Bravais lattice (82) with basis vectors  $\mathbf{a}_1 = (3, 0)$  and  $\mathbf{a}_2 = (0, 2)$ . A periodic orbit over this Bravais cell has 6 field values, one for each lattice site  $z = (n, t)$  on a  $[3 \times 2]_0$  rectangle:

$$\begin{bmatrix} \phi_{01} & \phi_{11} & \phi_{21} \\ \phi_{00} & \phi_{10} & \phi_{20} \end{bmatrix}.$$

Stack up the columns of this lattice state and the corresponding sources into 6-dimensional vectors,

$$\Phi_{[3 \times 2]_0} = \begin{pmatrix} \phi_{01} \\ \phi_{00} \\ \phi_{11} \\ \phi_{10} \\ \phi_{21} \\ \phi_{20} \end{pmatrix}, \quad \mathbf{M}_{[3 \times 2]_0} = \begin{pmatrix} m_{01} \\ m_{00} \\ m_{11} \\ m_{10} \\ m_{21} \\ m_{20} \end{pmatrix}. \quad (118)$$

The corresponding orbit Jacobian matrix (79) is the block-matrix (117), a block circulant matrix with circulant blocks [37],

$$\mathcal{J}_{[3 \times 2]_0} = \left( \begin{array}{cc|cc|cc} -2s & 2 & 1 & 0 & 1 & 0 \\ 2 & -2s & 0 & 1 & 0 & 1 \\ \hline 1 & 0 & -2s & 2 & 1 & 0 \\ 0 & 1 & 2 & -2s & 0 & 1 \\ \hline 1 & 0 & 1 & 0 & -2s & 2 \\ 0 & 1 & 0 & 1 & 2 & -2s \end{array} \right). \quad (119)$$

of  $[L \times L]$  block form,  $L = 3$ , with  $[T \times T]$  blocks,  $T = 2$ .

The fundamental parallelepiped generated by the action of orbit Jacobian matrix  $\mathcal{J}_{[3 \times 2]_0}$  is spanned by  $LT = 6$  basis vectors, the columns (18) of the orbit Jacobian matrix (119):

$$\mathcal{J}_{[3 \times 2]_0} = \left( \begin{array}{c|c|c|c|c|c} -2s & 2 & 1 & 0 & 1 & 0 \\ 2 & -2s & 0 & 1 & 0 & 1 \\ 1 & 0 & -2s & 2 & 1 & 0 \\ 0 & 1 & 2 & -2s & 0 & 1 \\ 1 & 0 & 1 & 0 & -2s & 2 \\ 0 & 1 & 0 & 1 & 2 & -2s \end{array} \right). \quad (120)$$

The ‘fundamental fact’ (16) now yields the Hill determinant as the number of doubly-periodic lattice states,

$$N_{[3 \times 2]_0} = |\text{Det } \mathcal{J}_{[3 \times 2]_0}| = 4(s-2)s(2s-1)^2(2s+3)^2. \quad (121)$$

## 5.2. Hill determinant: time-evolution evaluation

In practice, one often computes the Hill determinant using a Hamiltonian, or ‘transfer matrix’ formulation. An example is the temporal cat 3-term recurrence (47),

$$\begin{aligned} \phi_t &= \phi_t \\ \phi_{t+1} &= -\phi_{t-1} + s\phi_t - m_t, \end{aligned}$$

in the Percival-Vivaldi [176] ‘two-configuration’ cat map representation (45)

$$\hat{\phi}_{t+1} = \hat{\mathbf{J}}_1 \hat{\phi}_t - \hat{\mathbf{m}}_t, \quad (122)$$

with the one-time step temporal evolution  $[2 \times 2]$  Jacobian matrix  $\hat{\mathbf{J}}_1$  generating a time orbit by acting on the 2-dimensional ‘phase space’ of states on successive lattice sites

$$\hat{\mathbf{J}}_1 = \begin{bmatrix} 0 & 1 \\ -1 & s \end{bmatrix}, \quad \hat{\boldsymbol{\phi}}_t = \begin{bmatrix} \phi_{t-1} \\ \phi_t \end{bmatrix}, \quad \hat{\mathbf{m}}_t = \begin{bmatrix} 0 \\ m_t \end{bmatrix}, \quad (123)$$

Similarly, for the  $d = 2$  spatiotemporal cat lattice at hand, one can recast the 5-term recurrence (74)

$$\begin{aligned} \phi_{nt} &= \phi_{nt} \\ \phi_{n,t+1} &= -\phi_{n,t-1} + (-\phi_{n-1,t} + 2s\phi_{nt} - \phi_{n+1,t}) - m_{nt} \end{aligned} \quad (124)$$

in the ‘two-configuration’ matrix form (122) by picking the vertical direction (indexed ‘2’) as the ‘time’, with temporal 1-time step Jacobian  $[2L \times 2L]$  block matrix

$$\hat{\mathbf{J}}_1 = \left[ \begin{array}{c|c} \mathbf{0} & \mathbf{1}_1 \\ \hline -\mathbf{1}_1 & -\mathcal{J}_1 \end{array} \right], \quad (125)$$

(known as a transfer matrix in statistical mechanics [166, 174]) generating a ‘time’ orbit by acting on a  $2L$ -dimensional ‘phase space’ lattice strip  $\hat{\boldsymbol{\phi}}_t$  along the ‘spatial’ direction (indexed ‘1’),

$$\hat{\boldsymbol{\phi}}_t = \begin{bmatrix} \phi_{t-1} \\ \phi_t \end{bmatrix}, \quad \hat{\mathbf{m}}_t = \begin{bmatrix} \mathbf{0} \\ \mathbf{m}_t \end{bmatrix}, \quad \boldsymbol{\phi}_t = \begin{bmatrix} \phi_{1t} \\ \vdots \\ \phi_{Lt} \end{bmatrix}, \quad \mathbf{m}_t = \begin{bmatrix} m_{1t} \\ \vdots \\ m_{Lt} \end{bmatrix},$$

where the hat  $\hat{\phantom{x}}$  indicates a  $2L$ -dimensional ‘two-configuration’ state, and  $\mathcal{J}_1$  is the spatial  $[L \times L]$  orbit Jacobian matrix of  $d = 1$  temporal cat form (50),

$$\mathcal{J}_1 = \sigma_1^{-1} - 2s\mathbf{1}_1 + \sigma_1 \quad (126)$$

The ‘two-configuration’ coupled cat maps system (122) is a generalization of the Bernoulli map time evolution formulation (10) to a high-dimensional spatially-coupled lattice. Just as in the temporal Bernoulli condition (13), the first order in time difference equation (122) can be viewed as a lattice state fixed point condition (13), a zero of the function  $F[\hat{\boldsymbol{\phi}}] = \hat{\mathcal{J}}\hat{\boldsymbol{\phi}} + \hat{\mathbf{M}} = 0$ , with the entire periodic *lattice state*  $\hat{\boldsymbol{\phi}}_{\mathbf{M}}$  treated as a single fixed *point* in the  $2LT$ -dimensional state space unit hyper-cube, and the  $[2LT \times 2LT]$  block matrix orbit Jacobian matrix given either by

$$\hat{\mathcal{J}} = \hat{\mathbf{1}} - \hat{\mathbf{J}}_1 \otimes \sigma_2^{-1}, \quad (127)$$

or by

$$\hat{\mathcal{J}}' = \hat{\mathbf{1}} - \sigma_2^{-1} \otimes \hat{\mathbf{J}}_1. \quad (128)$$

Here the unity  $\hat{\mathbf{1}} = \hat{\mathbf{1}}_1 \otimes \mathbf{1}_2$  is a  $[2LT \times 2LT]$  block matrix, and the time-evolution Jacobian matrix  $\hat{\mathbf{J}}_1$  (125) is a  $[2L \times 2L]$  matrix.

The order in which the block matrix blocks are composed does not matter, yielding the same the Hill determinant  $\det \hat{\mathcal{J}} = \det \hat{\mathcal{J}}'$  by (116). However, written out explicitly, the two orbit Jacobian matrices (129) and (132) are of a very different form.

For example, for the  $[L \times T]_0$  rectangular Bravais cell, the spatiotemporal cat orbit Jacobian matrix (127) involves the  $[T \times T]$  time shift operator block matrix  $\sigma_2$  (11) with the one-time-step  $[2L \times 2L]$  time-evolution Jacobian matrix  $\hat{\mathbf{J}}_1$  (125)

$$\hat{\mathcal{J}} = \left[ \begin{array}{c|c} \mathbf{1}_1 \otimes \mathbf{1}_2 & -\mathbf{1}_1 \otimes \sigma_2^{-1} \\ \hline \mathbf{1}_1 \otimes \sigma_2^{-1} & \mathbf{1}_1 \otimes \mathbf{1}_2 + \mathcal{J}_1 \otimes \sigma_2^{-1} \end{array} \right], \quad (129)$$

and for spatiotemporal cat (124) this is a time-periodic  $[T \times T]$  shift operator block matrix  $\sigma_2$  (11), each block now a space-periodic  $[2L \times 2L]$  matrix  $\hat{\mathbf{J}}_1$  (125).

If a block matrix is composed of four blocks, its determinant can be evaluated using Schur's 1917 formula [194, 217]

$$\det \left[ \begin{array}{c|c} \mathbf{A} & \mathbf{B} \\ \hline \mathbf{C} & \mathbf{D} \end{array} \right] = \det(\mathbf{A}) \det(\mathbf{D} - \mathbf{C}\mathbf{A}^{-1}\mathbf{B}). \quad (130)$$

so, noting (114), (117) and (126), we find that

$$\begin{aligned} \det \hat{\mathcal{J}} &= \det \left[ \begin{array}{c|c} \mathbf{1}_1 \otimes \mathbf{1}_2 & -\mathbf{1}_1 \otimes \sigma_2^{-1} \\ \hline \mathbf{1}_1 \otimes \sigma_2^{-1} & \mathbf{1}_1 \otimes \mathbf{1}_2 + \mathcal{J}_1 \otimes \sigma_2^{-1} \end{array} \right] \\ &= \det [\mathbf{1}_1 \otimes \mathbf{1}_2 + \mathcal{J}_1 \otimes \sigma_2^{-1} + (\mathbf{1}_1 \otimes \sigma_2^{-1})(\mathbf{1}_1 \otimes \mathbf{1}_2)(\mathbf{1}_1 \otimes \sigma_2^{-1})] \\ &= \det [\mathbf{1}_1 \otimes \mathbf{1}_2 + \mathcal{J}_1 \otimes \sigma_2^{-1} + \mathbf{1}_1 \otimes \sigma_2^{-2}] \\ &= \det(\mathbf{1}_1 \otimes \sigma_2^{-1}) \det [\mathbf{1}_1 \otimes \sigma_2^{-1} + (\sigma_1^{-1} - 2s\mathbf{1}_1 + \sigma_1) \otimes \mathbf{1}_2 + \mathbf{1}_1 \otimes \sigma_2] \\ &= \det \mathcal{J}, \end{aligned} \quad (131)$$

where we have used  $\det \mathbf{1}_1 = \det \mathbf{1}_2 = \det \sigma_1 = \det \sigma_2 = 1$ .

This proves that  $\det \hat{\mathcal{J}}$  of the ‘Hamiltonian’ or ‘two-configuration’  $[2LT \times 2LT]$  ‘phase space’ orbit Jacobian matrix  $\hat{\mathcal{J}}$  defined by (129) equals the ‘Lagrangian’ Hill determinant of the  $[LT \times LT]$  orbit Jacobian matrix  $\mathcal{J}$ .

### 5.3. Hill's formula

Consider next (128), the equivalent way of forming of the block matrix for the  $[L \times T]_0$  rectangular Bravais cell, with temporal period taken for definitiveness  $T = 4$ . The spatiotemporal cat orbit Jacobian matrix (128) is now constructed as the  $[4 \times 4]$  time shift operator block matrix  $\sigma_2$  (11), with the one-time-step  $[2L \times 2L]$  time-evolution Jacobian matrix  $\hat{\mathbf{J}}_1$  (125) and unit matrix  $\hat{\mathbf{1}}_1$  as blocks

$$\hat{\mathcal{J}}' = \mathbf{1}_2 \otimes \hat{\mathbf{1}}_1 - \sigma_2^{-1} \otimes \hat{\mathbf{J}}_1 = \left[ \begin{array}{c|c|c|c} \hat{\mathbf{1}}_1 & \mathbf{0} & \mathbf{0} & -\hat{\mathbf{J}}_1 \\ \hline -\hat{\mathbf{J}}_1 & \hat{\mathbf{1}}_1 & \mathbf{0} & \mathbf{0} \\ \hline \mathbf{0} & -\hat{\mathbf{J}}_1 & \hat{\mathbf{1}}_1 & \mathbf{0} \\ \hline \mathbf{0} & \mathbf{0} & -\hat{\mathbf{J}}_1 & \hat{\mathbf{1}}_1 \end{array} \right]. \quad (132)$$

The Hill determinant  $\det \hat{\mathcal{J}}'$  evaluation follows essentially the same path as the Bernoulli Hill determinant evaluation of section 1.5, generalized to block matrices. From the block-matrix multiplication rule (114) and the determinant rule (115) it follows that

$$(\sigma_2^{-1} \otimes \hat{\mathbf{J}}_1)(\sigma_2^{-1} \otimes \hat{\mathbf{J}}_1) = \sigma_2^{-2} \otimes \hat{\mathbf{J}}_1^2, \quad \text{so } (\sigma_2^{-1} \otimes \hat{\mathbf{J}}_1)^k = \sigma_2^{-k} \otimes \hat{\mathbf{J}}_1^k, \quad (133)$$

and

$$\det(\sigma_2^{-1} \otimes \hat{\mathbf{J}}_1) = (\det \sigma_2)^{-L} (\det \hat{\mathbf{J}}_1)^T = \det \hat{\mathbf{J}}_p, \quad \hat{\mathbf{J}}_p = \hat{\mathbf{J}}_1^T, \quad (134)$$

where  $\hat{\mathbf{J}}_p$  is the Jacobian matrix of a temporal periodic orbit  $p$ . Expand  $\ln \det \hat{\mathcal{J}}' = \text{tr} \ln \hat{\mathcal{J}}'$  as a series using (115) and (133),

$$\text{tr} \ln \hat{\mathcal{J}}' = \text{tr} \ln(1 - \sigma_2^{-1} \otimes \hat{\mathbf{J}}_1) = - \sum_{k=1}^{\infty} \frac{1}{k} \text{tr}(\sigma_2^{-k}) \text{tr} \hat{\mathbf{J}}_1^k, \quad (135)$$

and use  $\text{tr} \sigma_2^k = T$  if  $k$  is a multiple of  $T$ , 0 otherwise (follows from  $\sigma_2^T = 1$ ):

$$\ln \det(1 - \sigma_2^{-1} \otimes \hat{\mathbf{J}}_1) = - \sum_{r=1}^{\infty} \frac{1}{r} \text{tr} \hat{\mathbf{J}}_p^r = \ln \det(\hat{\mathbf{1}}_1 - \hat{\mathbf{J}}_p).$$

So for the spatiotemporal cat the orbit Jacobian matrix and the temporal evolution (122) stability  $\hat{\mathbf{J}}_p$  are related by the remarkable (discrete time) Hill's formula [28, 154]

$$|\det \mathcal{J}| = |\det(\hat{\mathbf{1}}_1 - \hat{\mathbf{J}}_p)|. \quad (136)$$

which expresses the Hill determinant of the arbitrarily large orbit Jacobian matrix  $\mathcal{J}$  in terms of a determinant of a small  $[2L \times 2L]$  time-evolution Jacobian matrix  $\hat{\mathbf{J}}_p$ .

Two remarks. First, the reformulation of the spatiotemporal cat 5-term recurrence (124) as the ‘two-configuration’ form (122) is a passage from the Lagrangian to the Hamiltonian formulation, also known as ‘transfer matrix’ formulation of lattice field theories [166, 171] and Ising models [127, 174]. We chose to prove it here using only elementary linear algebra, not only because the Lagrangian formalism [28] is not needed for the problem at hand, but because it actually obscures the generality of Hill's formula, which works equally well for dissipative systems (see Bernoulli Hill's formula (67)), systems with no Lagrangian formulation.

Second, for Hamiltonian evolution (42), the  $[2 \times 2]$  Jacobian matrix  $J^T$  (the monodromy matrix of a periodic orbit) describes the growth of an initial state perturbation in  $T$  steps. For the corresponding Lagrangian system with action  $W$ , the first variation of the action  $\delta W = 0$  yields the temporal cat condition (48), while the second variation, the  $[T \times T]$  orbit Jacobian matrix (50), describes the stability of the *entire* given periodic orbit. In this, classical mechanics context, Bolotin and Treschev [28] refer to  $\mathcal{J}$  as the ‘Hessian operator’, but, as it is clear from our Bernoulli discussion of section 1.3, and applications to Kuramoto-Sivashinsky and Navier-Stokes systems [94], this notion of global stability of orbits is general, and applies to all dynamical systems, not only the Hamiltonian ones.

Accordingly, by the discrete time Hill's formula (136), just as for the Bernoulli example (24) these two expressions are equivalent,

$$|\text{Det } \mathcal{J}_M| = |\det(1 - J_M)|. \quad (137)$$

As the cat map hyperbolicity is the same everywhere and does not depend on a particular solution  $\Phi_p$ , counting periodic orbits is all that is needed to solve a cat-map dynamical system completely; once periodic orbits are counted, all cycle averaging formulas [54] follow.

## 6. Summary and discussion

In this paper we have analyzed the spatiotemporal cat (80) linear symbolic dynamics. We now summarize our main findings.

[2016-11-08 Predrag] Say: THE BIG DEAL is for  $d$ -dimensional field theory, symbolic dynamics is not one temporal sequence with a huge alphabet, but  $d$ -dimensional spatiotemporal tiling by a finite alphabet corresponding dynamical zeta functions should be sums over  $d$ -dimensional periodic orbits, rather than 1-dimensional periodic orbits

[2016-11-10 Predrag] Curb your enthusiasm **How to think about matters spatiotemporal?** text currently purged from the introduction:

Laws of motion drive a spatially extended system (clouds, say) through a repertoire of unstable patterns, each defined over a finite spatiotemporal region.

But in dynamics, we have no fear of the infinite extent in time. That is periodic orbit theory's [59] *raison d'être*; the dynamics itself describes the infinite time strange sets by a hierarchical succession of periodic orbits, of longer and longer, but always finite periods (with no artificial external periodicity imposed along the time axis). And, since 1996 we know how to deal with both spatially and temporally infinite regions by tiling them with finite spatiotemporally periodic tiles [42, 85]. More precisely: a time periodic orbit is computed in a finite time, with period  $T$ , but it repeats "tile" the time axis for all times. Similarly, a spatiotemporally periodic "tile" or "periodic orbit" is computed on a finite spatial region  $L$ , for a finite period  $T$ , but it repeats in both time and space directions tile the infinite spacetime.

Taken together, these open a path to determining exact solutions on *spatially infinite* regions. This is important, as many turbulent flows of physical interest come equipped with  $D$  continuous spatial symmetries. For example, in a pipe flow at transitional Reynolds number, the azimuthal and radial directions (measured in viscosity length units) are compact, while the pipe length is infinite. If the theory is recast as a  $d$ -dimensional space-time theory,  $d = D + 1$ , spatiotemporally translational invariant recurrent solutions are invariant  $d$ -tori (and *not* the 1-dimensional periodic orbits of the traditional periodic orbit theory), and the symbolic dynamics is likewise  $d$ -dimensional (rather than what is today taken for given, a single 1-dimensional temporal string of symbols).

This changes everything. Instead of studying time evolution of a chaotic system, one now studies the repertoire of spatiotemporal patterns allowed by a given PDE. To put it more provocatively: junk your old equations and look for guidance in clouds' repeating patterns. There is no more *time* in this vision of nonlinear *dynamics*! Instead, there is the space of all spatiotemporal patterns, and the likelihood that a given finite spatiotemporally pattern can appear, like the mischievous grin of Cheshire cat, anywhere in the turbulent evolution of a flow. A bold proposal, but how does it work?

and thus a  $d$ -dimensional spatiotemporal pattern is mapped one-to-one onto a  $d$ -dimensional discrete lattice state, symbolic dynamics labelled configuration - a configuration very much like that of an Ising model of statistical mechanics.

### 6.1. Discussion.

[2020-05-31 Predrag] Politi and Torcini [183] note that a problem in reconstructing the statistical properties of an spatiotemporal Hénon attractor is ensuring that all periodic orbits used are embedded into the inertial manifold. For instance, in the single Hénon map, one of the two fixed points is isolated and it does not belong to the strange attractor.

[2019-06-26 Predrag] Mramor and Rink [169]  **$d$ -dimensional Frenkel-Kontorova lattice:** Here, the goal is to find a  $d$ -dimensional “lattice configuration”  $x : \mathbb{Z}^d \rightarrow \mathbb{R}$  that satisfies

$$V'(\phi_i) - (\Delta\phi)_i = 0 \text{ for all } i \in \mathbb{Z}^d. \quad (138)$$

The smooth function  $V : \mathbb{R} \rightarrow \mathbb{R}$  satisfies  $V(\xi + 1) = V(\xi)$  for all  $\xi \in \mathbb{R}$ . It has the interpretation of a periodic onsite potential.

I like their definition of the discrete Laplace operator  $\Delta : \mathbb{R}^{\mathbb{Z}^d} \rightarrow \mathbb{R}^{\mathbb{Z}^d}$ , defined as

$$(\Delta x)_i := \frac{1}{2d} \sum_{\|j-i\|=1} (\phi_j - \phi_i) \text{ for all } i \in \mathbb{Z}^d. \quad (139)$$

where  $\|i\| := \sum_{k=1}^d |i_k|$ . Thus,  $(\Delta x)_i$  is the average of the quantity  $\phi_j - \phi_i$  computed over the lattice points that are nearest to that with index  $i$ , i.e., the graph Laplacian [44, 186] (??) for the case of hypercubic lattice, or the “central difference operator” [176].

[2019-06-26 Predrag] Mramor and Rink [169]: “Eq. (138) is relevant for statistical mechanics, because it is related to the Frenkel-Kontorova Hamiltonian lattice differential equation

$$\frac{d^2\phi_i}{dt^2} + V'(\phi_i) - (\Delta\phi)_i = 0 \text{ for all } i \in \mathbb{Z}^d. \quad (140)$$

This differential equation describes the motion of particles under the competing influence of an onsite periodic potential field and nearest neighbor attraction. Eq. (138) describes its stationary solutions.

While the setting is classical, such classical field-theory advances offer new semi-classical approaches to quantum field theory and many-body problems.

## Acknowledgments

Work of P. C. was in part supported by the family of late G. Robinson, Jr.. We are grateful to Sara A. Solla’s many perspicacious comments on this manuscript. No actual cats, graduate or undergraduate were harmed during this research. This paper sets up the necessary underpinnings for the quantum field theory of spatiotemporal cat, the details of which we leave to our friends Jon Keating and Marcos Saraceno.



## Appendix A. Discrete Fourier transforms

[2020-07-11 Predrag] As  $n, t$  are integers, the 2-dimensional Fourier transform is periodic with rectangular period  $2\pi \times 2\pi$ , and only needs be calculated for one period, usually taken to be  $[-\pi, \pi] \times [-\pi, \pi]$ .

In this appendix we show how compute the orbit Jacobian matrix or Hill determinants  $|\text{Det } \mathcal{J}|$  using crystallographer's favorite tool, the discrete Fourier transform.

### Appendix A.1. Temporal Bernoulli

Due to the time-translation invariance of Bernoulli time evolution law (9), the orbit Jacobian matrix  $\mathcal{J} = \mathbf{1} - s\sigma^{-1}$  is an  $[n \times n]$  is a circulant matrix. A circulant matrix is constant along each diagonal,

$$C = \begin{pmatrix} c_0 & c_{n-1} & \dots & c_2 & c_1 \\ c_1 & c_0 & c_{n-1} & & c_2 \\ \vdots & c_1 & c_0 & \ddots & \vdots \\ c_{n-2} & & \ddots & \ddots & c_{n-1} \\ c_{n-1} & c_{n-2} & \dots & c_1 & c_0 \end{pmatrix}, \quad C_{jk} = c_{j-k}, \quad (\text{A.1})$$

diagonalizable by a discrete Fourier transform,

$$U^\dagger C U = \text{diag}(\lambda), \quad U_{jk} = \frac{1}{\sqrt{n}} \epsilon^{(j-1)(k-1)}, \quad (\text{A.2})$$

with discrete Fourier mode eigenvectors

$$\tilde{e}_k = \frac{1}{\sqrt{n}} (1, \epsilon^k, \epsilon^{2k}, \dots, \epsilon^{k(n-1)})^\text{T}, \quad k = 0, 1, \dots, n-1, \quad (\text{A.3})$$

and eigenvalues  $C\tilde{e}_k = \lambda_k \tilde{e}_k$ ,

$$\lambda_k = c_0 + c_{n-1}\epsilon^k + c_{n-2}\epsilon^{2k} + \dots + c_1\epsilon^{k(n-1)}, \quad (\text{A.4})$$

where

$$\epsilon = e^{2\pi i/n} \quad (\text{A.5})$$

is an  $n$ th root of unity. The eigenvalues of the Bernoulli orbit Jacobian matrix  $(\mathbf{1} - s\sigma^{-1})$  are given by the nonzero coefficients  $c_0 = 1, c_1 = -s$ ,

$$\lambda_k = 1 - s\epsilon^{-k}, \quad (\text{A.6})$$

with discrete Fourier transform diagonalizing the Bernoulli equation (10),

$$(1 - s\sigma^{-1}) \tilde{\Phi}_k = (1 - s\epsilon^{-k}) \tilde{\Phi}_k = -\tilde{\mathbf{M}}_k, \quad (\text{A.7})$$

where the  $\tilde{\Phi}_k$  and  $\tilde{\mathbf{M}}_k$  are the  $k$ th Fourier modes of the lattice state  $\Phi$  and symbol block  $\mathbf{M}$ :

$$\tilde{\Phi}_k = (\tilde{e}_k^\text{T} \Phi) \tilde{e}_k, \quad \tilde{\mathbf{M}}_k = (\tilde{e}_k^\text{T} \mathbf{M}) \tilde{e}_k. \quad (\text{A.8})$$

The total number of the solutions of the fixed point condition (13) is given by (16), the ‘fundamental fact’ Hill determinant  $|\text{Det } \mathcal{J}|$ , i.e., the product of the orbit Jacobian matrix eigenvalues,

$$N_n = |\text{Det } \mathcal{J}| = \prod_{k=0}^{n-1} |1 - s \epsilon^{-k}| = \prod_{k=0}^{n-1} |s - \epsilon^k| = s^n - 1, \quad (\text{A.9})$$

where the last equality follows from  $\epsilon^k$  being the  $k$ th root of equation  $s^n - 1 = 0$ , so

$$s^n - 1 = \prod_{k=0}^{n-1} (s - \epsilon^k).$$

This verifies the ‘fundamental fact’ count of Bernoulli solutions (21).

### Appendix A.2. Temporal cat

The temporal cat orbit Jacobian matrix  $\mathcal{J} = \sigma - s \mathbf{1} + \sigma^{-1}$  is an  $[n \times n]$  circulant matrix (51), with eigenvalues (A.4)

$$\lambda_k = \epsilon^{-k} - s + \epsilon^k = -s + 2 \cos(2\pi k/n), \quad (\text{A.10})$$

and the Hill determinant

$$N_n = |\text{Det } \mathcal{J}| = \prod_{k=0}^{n-1} |s - 2 \cos(2\pi k/n)|. \quad (\text{A.11})$$

It is not immediately obvious that such products of trigonometric functions should be integer-valued [73], and establishing that usually requires some work [222].

In case at hand we observe that as the Chebyshev polynomials of the first kind [31] satisfy  $T_n(\cos(x)) = \cos(nx)$ , for  $x = 2\pi k/n$ ,  $k = 0, 1, \dots, n-1$ ,  $\cos(2\pi k/n)$  is the  $k$ th root of equation

$$T_n(x) - 1 = 0.$$

This equation, in analogy with the Bernoulli eigenvalue product (A.9), can be written as a product over the eigenvalues (A.10)

$$T_n(x) - 1 = 2^{n-1} \prod_{k=0}^{n-1} [x - \cos(2\pi k/n)]. \quad (\text{A.12})$$

Here the coefficient  $2^{n-1}$  comes from matching the coefficient of  $x^n$  term in the definition of  $T_n(x) = \dots + 2^{n-1}x^n$ . For  $x = s/2$ , this is the Hill determinant formula (56)

$$N_n = \prod_{k=0}^{n-1} [s - 2 \cos(2\pi k/n)] = 2T_n(s/2) - 2. \quad (\text{A.13})$$

## Appendix A.3. Spatiotemporal cat

In order to count the periodic lattice states as we did for the temporal cat (A.11), we need to compute the eigenvalues and eigenvectors of the orbit Jacobian matrix (79). The eigenvalues determine the Hill determinant of the orbit Jacobian matrix, and thus count the number of the periodic lattice states. The eigenvectors enable us to diagonalize the orbit Jacobian matrix.

In the spatiotemporal cat equation (80) the operators, fields and sources are defined on the spatiotemporally infinite 2-dimensional cubic lattice. This equation is also satisfied on a single tile, provided the translation operators satisfy the periodic bc's on the tile. Thus, in order to count the periodic orbits, it suffices to determine the eigenvalues of the orbit Jacobian matrix on finite tiles.

Now consider 2-dimensional spatiotemporal cat. The periodicity is described by 2-dimensional Bravais lattice (82).

Periodic fields with the periodicity described by Bravais lattice  $\Lambda$  satisfy:

$$f(z + R) = f(z), \quad R \in \Lambda. \quad (\text{A.14})$$

The orbit Jacobian matrix (79) is constructed from 2 commuting translation operators  $\{\sigma_1, \sigma_2\}$ . The eigenvectors of these translation operators are plane waves:

$$f_k(z) = e^{ik \cdot z}, \quad (\text{A.15})$$

where  $\mathbf{k}$  is a 2-dimensional wave vector. A general plane wave does not satisfy the periodicity (A.14), unless

$$e^{ik \cdot R} = 1. \quad (\text{A.16})$$

Since  $R$  is a vector from the Bravais lattice  $\Lambda$ , the wave vector  $\mathbf{k}$  must lie in the reciprocal lattice of  $\Lambda$ :

$$\mathbf{k} \in \Lambda^*, \quad \Lambda^* = \left\{ \sum_{i=1}^2 m_i \mathbf{b}_i \mid m_i \in \mathbb{Z} \right\}, \quad (\text{A.17})$$

where the primitive reciprocal lattice vectors  $\mathbf{b}_i$  satisfy:

$$\mathbf{b}_i \cdot \mathbf{a}_j = 2\pi \delta_{ij}. \quad (\text{A.18})$$

To get the eigenvectors and the corresponding eigenvalues of the orbit Jacobian matrix, note that

$$(\sigma_j + \sigma_j^{-1})e^{ik \cdot z} = e^{i(k \cdot z - k_j)} + e^{i(k \cdot z + k_j)} = (2 \cos k_j) e^{ik \cdot z}, \quad (\text{A.19})$$

where the  $\mathbf{k} = (k_1, k_2)$ . Hence the eigenvalue of the orbit Jacobian matrix (79) corresponding to the eigenvector with the wave vector  $\mathbf{k}$  is

$$\lambda_k = -2s + 2 \cos k_1 + 2 \cos k_2. \quad (\text{A.20})$$

Choosing primitive vectors with Hermite normal form (84), the reciprocal lattice is:

$$\Lambda^* = \{n_1 \mathbf{b}_1 + n_2 \mathbf{b}_2 \mid n_i \in \mathbb{Z}\}, \quad (\text{A.21})$$

where the primitive reciprocal lattice vectors  $\mathbf{b}_1$  and  $\mathbf{b}_2$  are:

$$\begin{bmatrix} \mathbf{b}_1 & \mathbf{b}_2 \end{bmatrix} = \frac{2\pi}{LT} \begin{bmatrix} T & 0 \\ -S & L \end{bmatrix}, \quad (\text{A.22})$$

so (A.18) is satisfied. The eigenvectors of the translation operator have the form of a plane wave

$$f_k(z) = e^{ik \cdot z}, \quad k \in \Lambda^*, \quad (\text{A.23})$$

and, in addition, satisfy the Bravais lattice (82) periodicity. The eigenvalues are:

$$\lambda_k = 2 \cos k_1 + 2 \cos k_2 - 2s, \quad (\text{A.24})$$

where  $\mathbf{k} = (k_1, k_2)$ . If  $\mathbf{k} = n_1 \mathbf{b}_1 + n_2 \mathbf{b}_2$ , then  $k_1$  and  $k_2$  are:

$$\mathbf{k} = \begin{bmatrix} k_1 \\ k_2 \end{bmatrix} = \begin{bmatrix} \mathbf{b}_1 & \mathbf{b}_2 \end{bmatrix} \begin{bmatrix} n_1 \\ n_2 \end{bmatrix} = \frac{2\pi}{LT} \begin{bmatrix} n_1 T \\ -n_1 S + n_2 L \end{bmatrix}. \quad (\text{A.25})$$

As the field has support only on the integer lattice sites, it suffices to use the wave vectors  $\mathbf{k} = n_1 \mathbf{b}_1 + n_2 \mathbf{b}_2$  with  $n_1$  from 0 to  $L - 1$  and  $n_2$  from 0 to  $T - 1$  to get all of the eigenvectors.

This range contains all the wave vectors in one primitive cell of reciprocal lattice of the square lattice, as shown in figure A1, where the wave vectors with  $n_1$  from 0 to  $L - 1$ , and  $n_2$  from 0 to  $T - 1$  are enclosed by the green dashed square. Any wave vector on the reciprocal lattice  $\Lambda^*$  outside of this range will give an eigenvector which is equivalent to an eigenvector with the wave vector within this range. So the number of eigenvectors is  $LT$ , which is equal to the number of integer lattice sites in the Bravais cell of the Bravais lattice  $\Lambda$ .

The number of periodic lattice states is then given by the Hill determinant of the orbit Jacobian matrix, which is the product of the eigenvalues:

$$\begin{aligned} N_{[L \times T]_S} &= \left| \prod_k \lambda_k \right| \\ &= \prod_{n_1=0}^{L-1} \prod_{n_2=0}^{T-1} \left[ 2s - 2 \cos\left(\frac{2\pi n_1}{L}\right) - 2 \cos\left(-\frac{2\pi n_1 S}{LT} + \frac{2\pi n_2}{T}\right) \right]. \end{aligned} \quad (\text{A.26})$$

#### Appendix A.4. Backup from s previous version of spatiotemporal cat

The set of all wave vectors  $\mathbf{K}_m$  that yield plane waves with the periodicity of a given Bravais lattice defines its reciprocal lattice. The  $\mathbf{K}_m$  are called reciprocal lattice vectors.

Let  $\langle \cdot, \cdot \rangle$  be the scalar product on  $\mathbb{R}^d$ . Let  $\Lambda \subset \mathbb{R}^d$  be a lattice, and let  $\Lambda^* \subset \mathbb{R}^d$  be its *reciprocal* lattice

$$\Lambda^* = \left\{ x \in \mathbb{R}^d : \langle x, y \rangle \in \mathbb{Z} \text{ for all } y \in \Lambda \right\}. \quad (\text{A.27})$$

The reciprocal lattice of the Bravais lattice (82) is spanned by reciprocal basis (A.18)

$$\Lambda^* = \{ n_1 \mathbf{b}_1 + n_2 \mathbf{b}_2 \mid n_i \in \mathbb{Z} \}. \quad (\text{A.28})$$

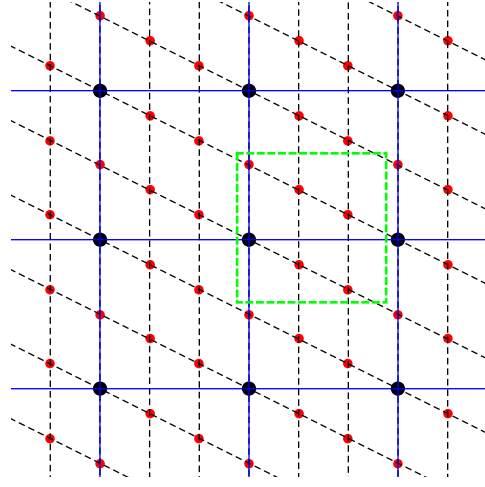


**Figure A1.** (Color online) The reciprocal lattices of both the Bravais lattice  $\Lambda$  and the integer square lattice. The red points are the reciprocal lattice  $\Lambda^*$  of the Bravais lattice  $\Lambda$  in figure 4. The black points are the reciprocal lattice of the square lattice. Each of these squares enclosed by the blue lines has edge length  $2\pi$ . Two wave vectors are equivalent if they are different by a reciprocal lattice vector of the square lattice.

The eigenvectors of the translation operator have the form of a plane wave

$$f_k(z) = e^{ik \cdot z}, \quad k \in \Lambda^*, \quad (\text{A.29})$$

and, in addition, satisfy the Bravais lattice (82) periodicity.

Then the basis vectors of the reciprocal lattice are:

$$\begin{bmatrix} \mathbf{b}_1 & \mathbf{b}_2 \end{bmatrix} = \frac{2\pi}{LT} \begin{bmatrix} T & 0 \\ -S & L \end{bmatrix}. \quad (\text{A.30})$$

A plane wave with wave vector  $\mathbf{k}$  in the reciprocal lattice  $\Lambda^*$  is an eigenvector of the orbit Jacobian matrix (80) that satisfies the periodic condition of Bravais lattice  $\Lambda$ . The eigenvector with wave vector  $\mathbf{k} = n_1 \mathbf{b}_1 + n_2 \mathbf{b}_2$  is

$$f_k(z) = e^{ik \cdot z} = \exp \left( i \frac{2\pi}{LT} (n_1 T z_1 - n_1 S z_2 + n_2 L z_2) \right), \quad (\text{A.31})$$

where the  $z = (z_1, z_2)$ , with the orbit Jacobian matrix eigenvalue

$$\lambda_k = \sum_{j=1}^2 (s - 2 \cos k_j) = 2s - 2 \cos 2\pi \left( \frac{n_1}{L} \right) - 2 \cos 2\pi \left( \frac{n_1 S}{LT} - \frac{n_2}{T} \right). \quad (\text{A.32})$$

As the field has support on the square lattice sites, it suffices to use the wave vectors  $\mathbf{k} = n_1 \mathbf{b}_1 + n_2 \mathbf{b}_2$  with  $n_1$  from 0 to  $L - 1$  and  $n_2$  from 0 to  $T - 1$  to get all the reciprocal lattice eigenvectors.

[2020-05-28 Predrag] Perhaps use

$$\cos(a - b) = \cos(a) \cos(b) + \sin(a) \sin(b) ?$$

$$\cos(2a) = \cos(a)^2 - \sin(a)^2 = 1 - 2 \sin(a)^2 ?$$

$$s - 2 \cos k_1 = (s - 2) + 4(\sin(k_1/2))^2$$

$$s - 2 \cos k_2 = (s - 2) + 4(\sin(k_1/2))^2$$

$$\text{Set } q_1 = 2\pi k_1/L, \quad q_2 = 2\pi k_2/T, \quad C = L/T,$$

$$2 \cos(q_2 - Cq_1) = 2 \cos(q_2) \cos(Cq_1) + 2 \sin(q_2) \sin(Cq_1)$$

or

$$\lambda_m = 2 - 2 \cos \alpha_m = 4 \sin^2(\alpha_m/2), \quad \alpha_m = \pi m/n$$

we should state the  $\sin^2(\alpha_m/2)$  version of the eigenvalues at least once.

This range contains all of the wave vectors in one lattice cell of reciprocal lattice of the square lattice, as shown in figure A1, where wave vectors with  $n_1$  from 0 to  $L - 1$ , and  $n_2$  from 0 to  $T - 1$  are enclosed by the green dashed square. Any wave vector on the reciprocal lattice  $\Lambda^*$  outside of this range will give an eigenvector which is equivalent to an eigenvector with the wave vector within this range. So the number of eigenvectors is  $LT$ , which is the number of square lattice sites within the minimal repeating tile.

The 4-index orbit Jacobian matrix (80) is a matrix with indices in a finite range. The orbit Jacobian matrix has  $LT$  eigenmodes. We know that the number of periodic orbits is equal to the Hill determinant of the orbit Jacobian matrix, which is the product of all the eigenvalues,

$$N_{[L \times T]_S} = 2^{LT} \prod_{k_1=0}^{L-1} \prod_{k_2=0}^{T-1} \left[ s - \cos\left(\frac{2\pi k_1}{L}\right) - \cos\left(\frac{2\pi k_2}{T} - \frac{2\pi k_1}{L} \frac{S}{T}\right) \right] \quad (\text{A.33})$$

Given the eigenmodes with a given periodic condition, one can reduce the 2-dimensional square lattice to a finite repeating tile. The screened Poisson equation in this tile is still (80). But now the fields and sources are defined over an  $[L \times T]_S$  lattice.

$$N_{[1 \times 1]_0} = 2s - 4 = 1. \quad (\text{A.34})$$

$$N_{[L \times 1]_0} = \prod_{k_1=0}^{L-1} \left[ 2s_2 - 2 - 2 \cos\left(\frac{2\pi k_1}{L}\right) \right]. \quad (\text{A.35})$$

Comparing with the temporal cat count (A.13) we see that the count is the same, provided we replace  $s_1 \rightarrow 2(s_2 - 1)$ , in agreement with the 3-term recurrence (92).

*Appendix A.4.1.  $[2 \times 1]_1$  periodic orbits.* For  $s = 5/2$  spatiotemporal cat.

$$N_{[2 \times 1]_1} = \prod_{l=0}^1 \left[ 2s - 4 \cos 2\pi \left( \frac{l}{2} \right) \right] = 9. \quad (\text{A.36})$$

*Appendix A.4.2.  $[2 \times 2]_0$  periodic orbits.* For  $s = 5/2$  spatiotemporal cat.

$$N_{[2 \times 2]} = 2^4 (s - 2)(s - \cos \pi - 1)(s - 1 - \cos \pi)(s - \cos \pi - \cos \pi) = 225.$$

*Appendix A.4.3.  $[3 \times 2]_0$  periodic orbits.* For  $s = 5/2$  only 850 prime  $[3 \times 2]_0$  blocks are admissible. The integer points count (??) is in agreement with the counting formula (A.33) for the  $[3 \times 2]_0$  periodic orbits:

$$N_{[3 \times 2]_0} = \prod_{l=0}^2 \prod_{t=0}^1 \left[ 2s - 2 \cos \left( \frac{2\pi l}{3} \right) - 2 \cos \left( \frac{2\pi t}{2} \right) \right] = 5120.$$

## Appendix B. Temporal Bernuolli

Applied to a temporal lattice state  $\Phi$  of period  $n$ , the shift operator (11) acts as a cyclic permutation that translates the lattice state  $\Phi$  by one site,  $(\sigma\Phi)^\top = (\phi_2, \phi_3, \dots, \phi_n, \phi_1)$ , with ‘1’ in the lower left corner assuring periodicity.

After  $n$  shifts, the lattice state  $\Phi$  returns to the initial state,  $\sigma^n = 1$ . This relation leads to the explicit expression for the orbit Jacobian matrix (28),

$$\mathbf{g} = \frac{\sigma}{s \mathbf{1} - \sigma} = \frac{1}{1 - \frac{\sigma}{s}} \frac{\sigma}{s} = \sum_{k=1}^{\infty} \frac{\sigma^k}{s^k} = \frac{s^n}{s^n - 1} \sum_{k=1}^n \frac{\sigma^k}{s^k}. \quad (\text{B.1})$$

From (28) it then follows that the last field in  $\Phi$  is the field at lattice site  $n$

$$\phi_n = \frac{s^n}{s^n - 1} \cdot m_1 m_2 m_3 \cdots m_n = \frac{1}{s - 1} \frac{s^{n-1} m_1 + \cdots + s m_{n-1} + m_n}{s^{n-1} + \cdots + s + 1}, \quad (\text{B.2})$$

and the rest are obtained by cyclic permutations of  $\mathbf{M}$ .

For example, for  $s = 2$ , the lattice fields are rational-valued,

$$\begin{aligned} \phi_{m_1 m_2 \cdots m_n} &= \sum_{k=1}^n \frac{m_k}{2^k} \sum_{m=0}^{\infty} \frac{1}{2^{nm}} = \frac{2^n}{2^n - 1} \cdot m_1 m_2 \cdots m_n \\ &= \frac{1}{2^n - 1} \sum_{k=1}^n m_k 2^{n-k}, \end{aligned} \quad (\text{B.3})$$

where  $p = \overline{m_1 m_2 \cdots m_n}$  is a prime cycle of period  $n$ , with stability multiplier  $\Lambda_p = 2^n$ .

For a Bernoulli map, the rational  $\phi_0$  are either periodic or land eventually on a periodic orbit (the base- $s$  version of the familiar fact that the decimal expansion of a rational number is eventually periodic), while the orbit of a normal irrational  $\phi_0$  is ergodic.

[2019-07-30 Predrag] Since all coefficients in (71) are integers, the lattice states  $\phi_t$  are always rational. This allows for their exact evaluation by integer arithmetic.



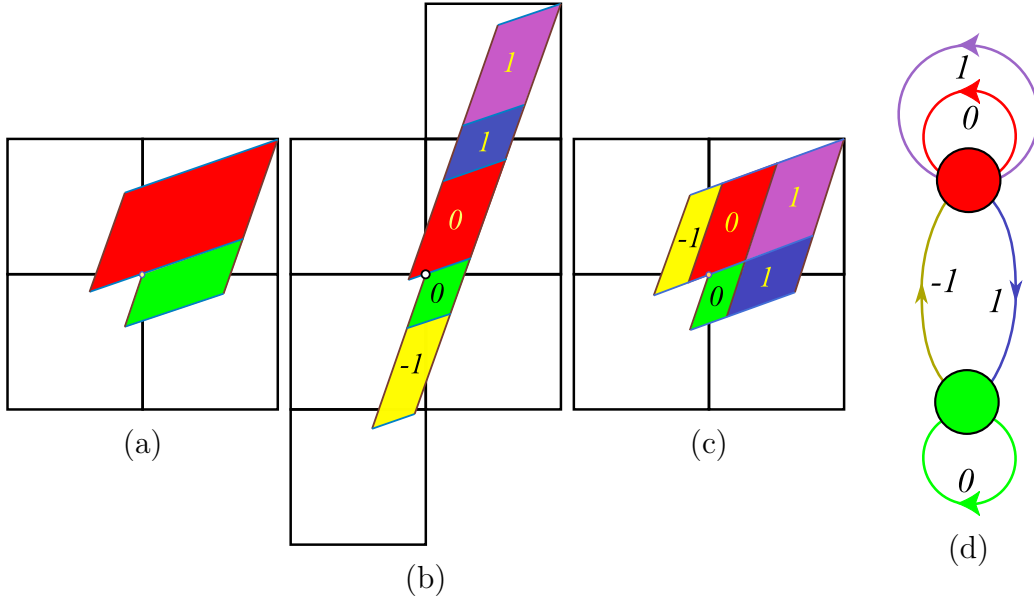


**Figure C1.** (Color online) (a) An Adler-Weiss generating partition of the unit torus for the  $s = 3$  Percival-Vivaldi cat map (45), with rectangle  $\mathcal{M}_A$  (red) and  $\mathcal{M}_B$  (green) borders given by the cat map stable (blue) and unstable (dark red) manifolds, i.e., along the two eigenvectors corresponding to the eigenvalues (43). (b) Mapped one step forward in time, the rectangles are stretched along the unstable direction and shrunk along the stable direction. Sub-rectangles  $\mathcal{M}_j$  that have to be translated back into the partition are indicated by color and labeled by their lattice translation  $m_j \in \mathcal{A} = \{\underline{1}, 0, 1\}$ , which also doubles as the 3-letter alphabet  $\mathcal{A}$ . (c) The sub-rectangles  $\mathcal{M}_j$  translated back into the initial partition yield a generating partition, with the finite grammar given by the transition graph (d). The nodes refer to the rectangles  $A$  and  $B$ , and the five links correspond to the five sub-rectangles induced by one step forward-time dynamics. For details, see ChaosBook [59].

## Appendix C. Cat map: Hamiltonian formulation

### Appendix C.1. Adler-Weiss partition of the cat map state space

Cat maps, also known as Thom-Anosov diffeomorphisms, or Thom-Anosov-Arnol'd-Sinai cat maps [8, 65, 203], have been extensively studied as the simplest examples of chaotic Hamiltonian systems.

Percival-Vivaldi cat map (45) is a discrete time non-autonomous Hamiltonian system, time-forced by ‘pulses’  $m_t$ . The  $m_t$  translations reshuffle the state space, as in figure C1, thus partitioning it into regions  $\mathcal{M}_m$ , labeled with letters  $m$  of the  $|\mathcal{A}|$ -letter alphabet  $\mathcal{A}$ , and associating a symbol sequence  $\{m_t\}$  to the dynamical trajectory  $\{\phi_t\}$ . As the relation (45) between the trajectory  $\phi_t$  and its symbolic dynamics encoding  $m_t$  is linear, Percival and Vivaldi refer to  $m_t$  as a ‘linear code’.

As explained in the companion paper [96], the deep problem with the Percival-Vivaldi code prescription is that it does not yield a generating partition; the borders (i.e.,  $\phi_0, \phi_1$  axes) of their unit-square partition  $(\phi_{t-1}, \phi_t) \in (0, 1] \times (0, 1]$  do not map onto

themselves, resulting in the infinity of, to us unknown, grammar rules for inadmissible symbol sequences.

This problem was resolved in 1967 by Adler and Weiss [1, 2, 8] who utilized the stable/unstable manifolds of the fixed point at the origin to cover a unit area torus by a two-rectangles generating partition; for the Percival-Vivaldi cat map (45), such partition [59] is drawn in figure C1. Following Bowen [29], one refers to parallelograms in figure C1 as ‘rectangles’; for details see Devaney [65], Robinson [191], or ChaosBook [59]. Siemaszko and Wojtkowski [198] refer to such partitions as the ‘Berg partitions’, and Creagh [49] studies their generalization to weakly nonlinear mappings. Symbolic dynamics on this partition is a subshift of finite type, with the 3-letter alphabet

$$\mathcal{A} = \{\underline{1}, 0, 1\} \quad (\text{C.1})$$

that indicates the translation needed to return the given sub-rectangle  $\mathcal{M}_j$  back into the two-rectangle partition  $\mathcal{M} = \mathcal{M}_A \cup \mathcal{M}_B$ .

While Percival and Vivaldi were well aware of Adler-Weiss partitions, they felt that their “coding is less efficient in requiring more symbols, but it has the advantage of linearity.” Our construction demonstrates that one can have both: an Adler-Weiss generating cat map partition, and a linear code. The only difference from the Percival-Vivaldi formulation [176] is that one trades the single unit-square cover of the torus of (45) for the dynamically intrinsic, two-rectangles cover of figure C1, but the effect is magic - now every infinite walk on the transition graph of figure C1 (d) corresponds to a unique admissible orbit  $\{\phi_t\}$ , and the transition graph generates all admissible itineraries  $\{m_t\}$ .

To summarize: an explicit Adler-Weiss generating partition, such as figure C1, completely solves the Hamiltonian cat map problem, in the sense that it generates all admissible orbits. Rational and irrational initial states generate periodic and ergodic orbits, respectively [131, 177], with every state space orbit uniquely labeled by an admissible bi-infinite itinerary of symbols from alphabet  $\mathcal{A}$ .

### Appendix C.2. Counting Hamiltonian cat map periodic orbits

2CB

The five sub-rectangles  $\mathcal{M}_j$  of the two-rectangle Adler-Weiss partition of figure C1 (c) motivate introduction of a 5-letter alphabet

$$\bar{\mathcal{A}} = \{1, 2, 3, 4, 5\} = \{A^0A, B^1A, A^1A, B^0B, A^1B\}, \quad (\text{C.2})$$

see figure C2 (b), which encodes the links of the transition graph of figure C1 (d). The loop expansion of the determinant [55] of the transition graph  $T$  of figure C2 (b) is given by all non-intersecting walks on the graph

$$\det(1 - zT) = 1 - z(t_1 + t_3 + t_4) - z^2(t_{25} - (t_1 + t_3)t_4), \quad (\text{C.3})$$

where  $t_p$  are traces over fundamental cycles, the three fixed points  $t_1 = T_{A^0A}$ ,  $t_3 = T_{A^1A}$ ,  $t_4 = T_{B^0B}$ , and the 2-cycle  $t_{25} = T_{B^1A}T_{A^1B}$ .

As the simplest application, consider counting all admissible cat map periodic orbits. This is accomplished by setting the non-vanishing links of the transition graph to  $T_{ji} = 1$ , resulting in the  $s = 3$  cat map topological zeta function [59, 115],

$$1/\zeta_{\text{top}}(z) = \frac{1 - 3z + z^2}{(1 - z)^2}, \quad (\text{C.4})$$

where the numerator  $(1 - z)^2$  corrects the overcounting of the fixed point at the origin due to assigning it to both  $\mathcal{M}_A$  (twice) and  $\mathcal{M}_B$  rectangles [156].

[2020-02-08 Predrag] Note:  $N_2 = \text{Det } \mathcal{J} = (s - 2)(s + 2)$ ,  $N_3 = (s - 2)(s + 1)^2$ ,  $N_4 = (s - 2)(s + 1)s^2$ ,  $N_5 = (s - 2)(s^2 + s - 1)^2$ . I think the factorization is true for all  $n$ , as the  $s = 2$  Laplacian has a zero mode (constant  $\phi_i$ , I think).

an sequence of non-negative integers counting the orbits of a map; the sequence of periodic points for that map.

2CB

The number of *periodic points* of period  $n$  is given by (33), the logarithmic derivative of the topological zeta function. Substituting the cat map topological zeta function (C.4) we obtain

$$\begin{aligned} \sum_{n=1} N_n z^n &= z + 5z^2 + 16z^3 + 45z^4 + 121z^5 + 320z^6 + 841z^7 \\ &\quad + 2205z^8 + 5776z^9 + 15125z^{10} + 39601z^{11} + \dots \end{aligned} \quad (\text{C.5})$$

WolframAlpha says, compare with (69):

$$\sum_{n=1} N_n z^n = \frac{s - 2z}{1 - sz + z^2} - \frac{2}{1 - z} \quad (\text{C.6})$$

The number of *prime* cycles is given by (36),

$$\begin{aligned} \sum_{n=1} M_n z^n &= z + 2z^2 + 5z^3 + 10z^4 + 24z^5 + 50z^6 + 120z^7 \\ &\quad + 270z^8 + 640z^9 + 1500z^{10} + 3600z^{11} + \dots, \end{aligned} \quad (\text{C.7})$$

in agreement with the Bird and Vivaldi [26] census.

This derivation was based on the Adler-Weiss generating partition, a clever explicit visualization of the cat map dynamics, whose generalization to several coupled maps (let alone spatially infinite coupled cat maps lattice) is far from obvious: one would have to construct covers of high-dimensional fundamental parallelepipeds by sets of sub-volumes. However, as Keating [131] explains, no such explicit generating partition is needed to count cat map periodic orbits. Cat map (45) lattice states are the fixed points of

$$\begin{bmatrix} q_t \\ p_t \end{bmatrix} = \begin{bmatrix} q_{t+n} \\ p_{t+n} \end{bmatrix} = J^n \begin{bmatrix} q_t \\ p_t \end{bmatrix} \pmod{1},$$

so on the unwrapped phase space lattice, tiled by repeats of the unit square of the cat map torus,

$$(J^n - \mathbf{1}) \begin{bmatrix} q_t \\ p_t \end{bmatrix} = \begin{bmatrix} m_t^q \\ m_t^p \end{bmatrix}, \quad (m_t^q, m_t^p) \in \mathbb{Z}^2, \quad (\text{C.8})$$

matrix  $(J^n - \mathbf{1})$  stretches the unit square into the ‘fundamental parallelepiped’.

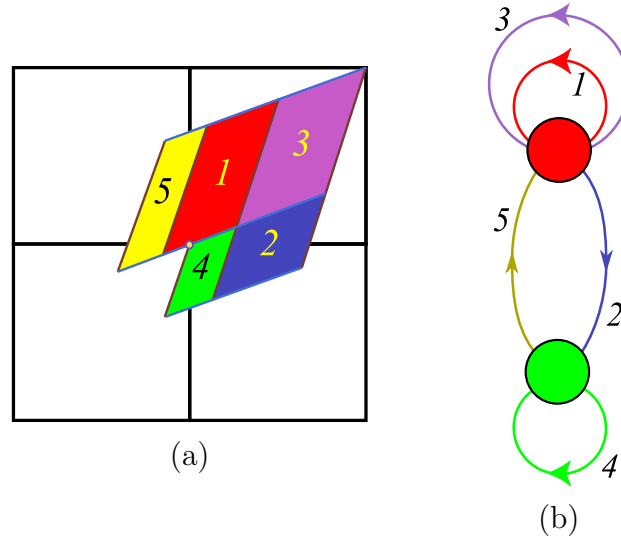


**Figure C2.** (Color online) (a) The sub-rectangles  $\mathcal{M}_j$  of figure C1 (c). (b) Admissible orbits correspond to walks on the transition graph of figure C1 (d), with rectangles  $\mathcal{M}_A$  (red) and  $\mathcal{M}_B$  (green) as nodes, and the links labeled by 5-letter alphabet (C.2), see the loop expansion (C.3).

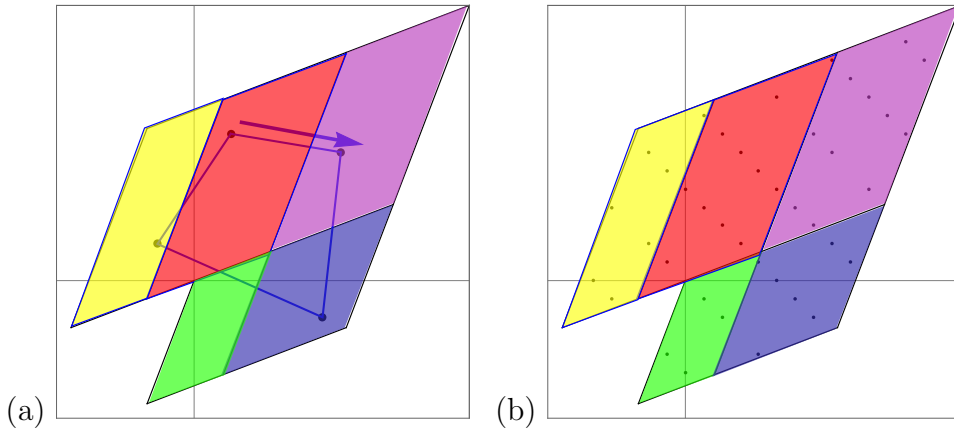


**Figure C3.** (a) An example of a 4-cycle:  $\Phi_{011\bar{1}}$ . (b) All prime period-4 lattice states land in the partition of figure C2 (a).

### Appendix C.3. An example: period-4 prime cycles

As a hands-on example, let us count the  $M_4 = 10$  admissible prime 4-cycles, as stated in (??). The admissible blocks  $M_p$  can be read off as walks on either the 5-letter alphabet (C.2) graph, see figure C2 (b), or the 3-letter alphabet (C.1) graph, see figure C1 (d). They are, in 5-letter (top), and 3-letter (bottom) alphabets

[2019-12-20 Predrag] For covering symbolic dynamics, use/refer to ChaosBook.  
Order (C.9) lexically.

$\overline{1113}$	$\overline{1125}$	$\overline{1245}$	$\overline{1253}$	$\overline{1325}$
0001	001 $\underline{1}$	010 $\underline{1}$	011 $\underline{1}$	011 $\underline{1}$

$$\begin{array}{ccccc} \overline{1133} & \overline{3325} & \overline{3331} & \overline{3245} & \overline{4452} \\ 0011 & 111\bar{1} & 1110 & 110\bar{1} & 00\bar{1}1 \end{array} . \quad (\text{C.9})$$

The corresponding periodic orbits  $\Phi_p$  are computed using Green's function (66) (the inverse of the  $[4 \times 4]$  orbit Jacobian matrix (51), easiest to evaluate by discrete Fourier transforms, see Appendix A):

$$\mathbf{M}_{0001} \Rightarrow \Phi_{0001} = g \begin{bmatrix} 0 \\ 0 \\ 0 \\ 1 \end{bmatrix} = \frac{1}{15} \begin{bmatrix} 3 \\ 2 \\ 3 \\ 7 \end{bmatrix} .$$

Likewise,

[2019-12-20 Predrag] To Han: order lexically.

$$\begin{aligned} \Phi_{001\bar{1}}^\top &= \frac{1}{15} \begin{bmatrix} -1 & 1 & 4 & -4 \end{bmatrix}, & \Phi_{010\bar{1}}^\top &= \frac{1}{15} \begin{bmatrix} 0 & 5 & 0 & -5 \end{bmatrix} \\ \Phi_{01\bar{1}1}^\top &= \frac{1}{15} \begin{bmatrix} 4 & 6 & -1 & 6 \end{bmatrix}, & \Phi_{011\bar{1}}^\top &= \frac{1}{15} \begin{bmatrix} 2 & 8 & 7 & -2 \end{bmatrix} \\ \Phi_{0011}^\top &= \frac{1}{15} \begin{bmatrix} 5 & 5 & 10 & 10 \end{bmatrix}, & \Phi_{111\bar{1}}^\top &= \frac{1}{15} \begin{bmatrix} 9 & 11 & 9 & 1 \end{bmatrix} \\ \Phi_{1110}^\top &= \frac{1}{15} \begin{bmatrix} 12 & 13 & 12 & 8 \end{bmatrix}, & \Phi_{110\bar{1}}^\top &= \frac{1}{15} \begin{bmatrix} 7 & 8 & 2 & -2 \end{bmatrix} \\ \Phi_{00\bar{1}1}^\top &= \frac{1}{15} \begin{bmatrix} 1 & -1 & -4 & 4 \end{bmatrix}. \end{aligned} \quad (\text{C.10})$$

One can verify that for each of these 10 prime 4-cycles the lattice states  $(\phi_t, \phi_{t+1})$  visit the rectangles  $\mathcal{M}_A$  or  $\mathcal{M}_B$  of figure C1(b) in the temporal order dictated by the transition graph, and thus they are all admissible cycles.

[2020-01-28 Predrag] Perhaps summarize here our failed efforts to make an time-reversal invariant Adler-Weiss partition; Ihara zeta functions, ...

## Appendix D. Spatiotemporal stability

Here we address two questions: (i) how is the high-dimensional orbit Jacobian matrix  $\mathcal{J}$  related to the temporal  $[d \times d]$  Jacobian matrix  $J$ ? and (ii) how does one evaluate the orbit Jacobian matrix  $\mathcal{J}$ ?

### Appendix D.1. Temporal lattice

$$\mathcal{J}_M = 1 - J \otimes \sigma^{-1}, \quad (\text{D.1})$$

the temporal Bernoulli condition (10) is the zero of function

$$F[\Phi; M] = \mathcal{J}\Phi + M = 0, \quad \mathcal{J} = 1 - s\sigma^{-1}, \quad (\text{D.2})$$

For a  $d$ -dimensional discrete time map  $f$ , with the lattice state  $\Phi$  of discrete period  $n$ , every temporal lattice site satisfies

$$\phi_{t+1} = f(\phi_t), \quad (\text{D.3})$$

where  $\phi_t$  is a  $d$ -dimensional field at lattice site  $t$ . Consider an approximate lattice state, known only to a finite precision

$$\hat{\Phi} = (\hat{\phi}_1, \hat{\phi}_2, \dots, \hat{\phi}_n), \quad \hat{\phi}_t = \phi_t + \Delta\phi_t, \quad (\text{D.4})$$

where  $\phi_t$  is the exact field at lattice site  $t$ . Define the error field by  $F[\hat{\Phi}] = f(\hat{\Phi}) - \sigma^{-1} \otimes \hat{\Phi}$ , an operator which compares the forward map of every point in  $\hat{\Phi}$  with the next point  $\hat{\Phi} \otimes \sigma$ .

$F[\hat{\Phi}]$  is a  $(n \times d)$ -dimensional temporal lattice field obtained by stacking a  $d$ -dimensional field  $\hat{\phi}_t$  at each of the  $n$  lattice sites,

$$F[\hat{\Phi}] = F \begin{pmatrix} \hat{\phi}_1 \\ \hat{\phi}_2 \\ \dots \\ \hat{\phi}_n \end{pmatrix} = \begin{pmatrix} \hat{\phi}_1 - \hat{f}_n \\ \hat{\phi}_2 - \hat{f}_1 \\ \dots \\ \hat{\phi}_n - \hat{f}_{n-1} \end{pmatrix}, \quad \hat{f}_t = f(\hat{\phi}_t), \quad (\text{D.5})$$

which measures the misalignment of every finite forward-in-time segment  $f(\hat{\phi})_t$  with the next site  $\hat{\phi}_{t+1}$  on the lattice state  $\hat{\Phi}$ .

By (D.3), the exact lattice state  $\Phi$  is a zero of this vector field,  $F[\Phi] = 0$ . Assuming that the  $d$ -dimensional error vectors  $\Delta\phi_t$  are small in magnitude, and Taylor expanding the one discrete time-step map  $f$  to linear order around the exact solution,

$$f(\phi_t + \Delta\phi_t) = \phi_{t+1} + J_t \Delta\phi_t + (\dots),$$

where

$$[J_t]_{ij} = \frac{\partial f_i(\phi_t)}{\partial \phi_j}, \quad t = (1, 2, \dots, n), \quad i, j = (1, 2, \dots, d) \quad (\text{D.6})$$

one finds that the neighborhood of entire cycle  $p$  is linearly deformed by the  $[nd \times nd]$  orbit Jacobian matrix

$$\Delta\phi' = \mathcal{J}(\phi) \Delta\phi, \quad \mathcal{J}_{ij}(\phi) = \frac{\delta F[\phi]_i}{\delta \phi_j}, \quad (\text{D.7})$$

with

$$\mathcal{J} = 1 - \sigma J,$$

the one discrete time-step temporal  $[d \times d]$  Jacobian matrix  $J$  evaluated on the entire cycle  $p$ , and  $\sigma$  the shift operator

$$\sigma = \begin{pmatrix} 0 & & & & 1 \\ 1 & 0 & & & \\ & 1 & 0 & & \\ & & 1 & & \\ & & & \ddots & 0 \\ & & & & 1 & 0 \end{pmatrix}, \quad J = \begin{pmatrix} J_1 & & & & \\ & J_2 & & & \\ & & J_3 & & \\ & & & \ddots & \\ & & & & J_{n-1} \\ & & & & & J_n \end{pmatrix}, \quad (\text{D.8})$$

with 1 in the upper right corner assuring periodicity,  $\sigma^n = 1$ .

Consider a  $d$ -dimensional map  $\phi_{t+1} = f(\phi_t)$ , where  $\phi_t = \{\phi_{t,1}, \phi_{t,2}, \dots, \phi_{t,d}\}$  is the state of the system at time  $t$ . In case at hand, the one time step Jacobian matrix

$$J(\phi_t)_{ij} = \left. \frac{\partial f(\phi)_i}{\partial \phi_j} \right|_{\phi_i = \phi_{i,t}} \quad (\text{D.9})$$

stretches uniformly, so the Jacobian matrix does not depend on the field value  $\phi_t$  or time  $t$ ,  $J(\phi_t) = J$ .

For a lattice state  $\Phi_p$  with period  $n$ , the orbit Jacobian matrix is a  $[nd \times nd]$  block matrix

$$\mathcal{J} = \begin{pmatrix} \mathbf{1} & & & -J \\ -J & \mathbf{1} & & \\ & \cdots & \mathbf{1} & \\ & & \cdots & \mathbf{1} \\ & & & -J & \mathbf{1} \end{pmatrix} = 1 - J \otimes \sigma^{-1}, \quad (\text{D.10})$$

where  $\mathbf{1}$  is a  $d$ -dimensional identity matrix,  $J$  is the one time step  $[d \times d]$  Jacobian matrix (D.9), and  $\sigma$  is the  $[n \times n]$  shift operator matrix with period  $n$ .

To evaluate the Hill determinant of the orbit Jacobian matrix, expand  $\ln \text{Det } \mathcal{J}_p = \text{Tr} \ln \mathcal{J}_p$ :

$$\begin{aligned} \ln \text{Det } \mathcal{J}_p &= \text{Tr} \ln(1 - J \otimes \sigma^{-1}) \\ &= - \sum_{k=1}^{\infty} \frac{\text{Tr}(J \otimes \sigma^{-1})^k}{k}. \end{aligned} \quad (\text{D.11})$$

Note that  $(J \otimes \sigma^{-1})^k = J^k \otimes \sigma^{-k}$  and  $\text{Tr}(J^k \otimes \sigma^{-k}) = \text{Tr}(J^{nr} \otimes \mathbf{1}_{[n \times n]}) \delta_{k,nr} = n \text{tr}(J^{nr}) \delta_{k,nr}$  which is not 0 only when  $k$  is a multiple of  $n$ .

$$\begin{aligned} \ln \text{Det } \mathcal{J}_p &= - \sum_{r=1}^{\infty} \frac{n \text{tr}(J^{nr})}{rn} = \text{tr} \left[ - \sum_{r=1}^{\infty} \frac{(J^n)^r}{r} \right] \\ &= \text{tr} \ln(1 - J^n) = \ln \det(1 - J^n). \end{aligned} \quad (\text{D.12})$$

So the Hill determinant of the orbit Jacobian matrix is  $\text{Det } \mathcal{J} = \det(1 - J^{n_p})$ .

[2020-01-21 Han] A possible problem is  $\mathcal{J}_p$  could be negative. And here we have the one time step Jacobian matrix instead of a scalar  $s$  so I'm not sure if we can expand  $\ln(1 - J \otimes \sigma^{-1})$  as a series in  $J \otimes \sigma^{-1} \dots$

### Appendix D.2. Temporal stability

To summarize, a discretized, temporal lattice periodic orbit linear stability can be computed in two ways - either by computing the  $[nd \times nd]$  orbit Jacobian matrix  $jMorb$ , or by computing  $J_p$

$$\text{Det } \mathcal{J}_M = \det(1 - J_M), \quad (\text{D.13})$$

where  $J_M$  is the  $n$  time-steps  $[d \times d]$  forward-time Jacobian matrix. In the limit of discretization  $n \rightarrow \infty$  the left hand side is a *functional* Hill determinant of an  $\infty$ -dimensional *operator*. Nevertheless, thanks to the discrete Fourier diagonalization of  $\mathcal{J}(x)$ , [Appendix A](#), the Hill determinant  $\text{Det } \mathcal{J}_M$  is easier to compute than the ill-posed  $J_M$ .

[2019-10-10 Predrag]  $\mathcal{J}(x)$  is block-diagonalized by the discrete Fourier transform on a periodic lattice of three sites. Write up next the discrete Fourier evaluation of  $\text{Det } \mathcal{J}_p$ .

[2019-10-10 Predrag] Rewrite the derivation of the Hill-Poincaré -Van Vleck stability matrix (??) for symplectic / Lagrangian orbit Jacobian matrix using the shift operator (??).

The projection operator on the  $k$ th Fourier mode is

$$P_k = \prod_{j \neq k} \frac{\sigma - \omega_j}{\omega_k - \omega_j}. \quad (\text{D.14})$$

The set of the projection operators is complete,

$$\sum_k P_k = 1, \quad (\text{D.15})$$

and orthonormal

$$P_k P_j = \delta_{kj} P_k \quad (\text{no sum on } k). \quad (\text{D.16})$$

[TO BE CONTINUED]

## Appendix E. Spatiotemporal lattice

In spatiotemporal settings,  $J_p$  can be defined only for finite numbers of spatial sites, and it gets funkier and funkier as the spatial direction increases (that is why we are able to work only with very small spatial domain Kuramoto-Sivashinsky discretizations). But, as shown for the spatiotemporal cat in [\[61\]](#),  $\text{Det } \mathcal{J}_p$  works just fine on any spatiotemporal torus. In particular, for any periodic orbit Kuramoto-Sivashinsky discretization.



[2020-05-31 Predrag] Politi and Torcini [183] numerical method for finding periodic orbits of *spatiotemporal Hénon* is an extension of Biham and Wenzel [25] for a single Hénon map. Any fixed point in Biham-Wenzel fictitious time corresponds to a doubly-periodic spatiotemporal cycle  $[L \times T]_S$ .

## Appendix F. Symbolic dynamics: a glossary

Analysis of a low-dimensional chaotic dynamical system typically starts [59] with establishing that a flow is locally stretching, globally folding. The flow is then reduced to a discrete time return map by appropriate Poincaré sections. Its state space is partitioned, the partitions labeled by an alphabet, and the qualitatively distinct solutions classified by their temporal symbol sequences. Thus our analysis of the cat map and the spatiotemporal cat requires recalling and generalising a few standard symbolic dynamics notions.

**Partitions, alphabets.** A division of state space  $\mathcal{M}$  into a disjoint union of distinct regions  $\mathcal{M}_A, \mathcal{M}_B, \dots, \mathcal{M}_Z$  constitutes a *partition*. Label each region by a symbol  $m$  from an  $N$ -letter *alphabet*  $\mathcal{A} = \{A, B, C, \dots, Z\}$ , where  $N = n_{\mathcal{A}}$  is the number of such regions. Alternatively, one can distinguish different regions by coloring them, with colors serving as the “letters” of the alphabet. For notational convenience, in alphabets we sometimes denote negative integer  $m$  by underlining it, as in  $\mathcal{A} = \{-2, -1, 0, 1\} = \{2, \underline{1}, 0, 1\}$ .

**Itineraries.** For a dynamical system evolving in time, every state space point  $\phi_0 \in \mathcal{M}$  has the *future itinerary*, an infinite sequence of symbols  $S^+(\phi_0) = m_1 m_2 m_3 \dots$  which indicates the temporal order in which the regions shall be visited. Given a trajectory  $\phi_1, \phi_2, \phi_3, \dots$  of the initial point  $\phi_0$  generated by a time-evolution law  $\phi_{n+1} = f(\phi_n)$ , the itinerary is given by the symbol sequence

$$m_n = m \quad \text{if} \quad \phi_n \in \mathcal{M}_m. \quad (\text{F.1})$$

The *past itinerary*  $S^-(\phi_0) = \dots m_{-2} m_{-1} m_0$  describes the order in which the regions were visited up to arriving to the point  $\phi_0$ . Each point  $\phi_0$  thus has associated with it the bi-infinite itinerary

$$S(\phi_0) = S^- . S^+ = \dots m_{-2} m_{-1} m_0 . m_1 m_2 m_3 \dots, \quad (\text{F.2})$$

or simply ‘itinerary’, if we chose not to use the decimal point to indicate the present,

$$\{m_t\} = \dots m_{-2} m_{-1} m_0 m_1 m_2 m_3 \dots \quad (\text{F.3})$$

**Shifts.** A forward iteration of temporal dynamics  $x \rightarrow x' = f(x)$  shifts the entire itinerary to the left through the ‘decimal point’. This operation, denoted by the shift operator  $\sigma$ ,

$$\sigma(\dots m_{-2} m_{-1} m_0 . m_1 m_2 m_3 \dots) = \dots m_{-2} m_{-1} m_0 m_1 . m_2 m_3 \dots, \quad (\text{F.4})$$

demotes the current partition label  $m_1$  from the future  $S^+$  to the past  $S^-$ . The inverse shift  $\sigma^{-1}$  shifts the entire itinerary one step to the right.

The set of all itineraries that can be formed from the letters of the alphabet  $\mathcal{A}$  is called the *full shift*

$$\hat{\Sigma} = \{(m_k) : m_k \in \mathcal{A} \text{ for all } k \in \mathbb{Z}\}. \quad (\text{F.5})$$

The itinerary is infinite for any trapped (non-escaping or non-wandering set orbit) orbit (such as an orbit that stays on a chaotic repeller), and infinitely repeating for a

periodic orbit  $p$  of period  $n_p$ . A map  $f$  is said to be a *horseshoe* if its restriction to the non-wandering set is hyperbolic and topologically conjugate to the full  $\mathcal{A}$ -shift.

**Lattices.** Consider a  $d$ -dimensional hypercubic lattice infinite in extent, with each site labeled by  $d$  integers  $z \in \mathbb{Z}^d$ . Assign to each site  $z$  a letter  $m_z$  from a finite alphabet  $\mathcal{A}$ . A particular fixed set of letters  $m_z$  corresponds to a particular lattice state  $\mathbf{M} = \{m_z\}$ . In other words, a  $d$ -dimensional lattice requires a  $d$ -dimensional code  $\mathbf{M} = \{m_{n_1 n_2 \dots n_d}\}$  for a complete specification of the corresponding state  $\Phi$ . In the lattice case, the *full shift* is the set of all  $d$ -dimensional symbol blocks that can be formed from the letters of the alphabet  $\mathcal{A}$

$$\hat{\Sigma} = \{\{m_z\} : m_z \in \mathcal{A} \text{ for all } z \in \mathbb{Z}^d\}. \quad (\text{F.6})$$

**Commuting discrete translations.** For an autonomous dynamical system, the evolution law  $f$  is of the same form for all times. If  $f$  is also of the same form at every lattice site, the group of lattice translations (sometimes called multidimensional shifts), acting along  $j$ th lattice direction by shift  $\sigma_j$ , is a spatial symmetry that commutes with the temporal evolution. A temporal mapping  $f$  that satisfies  $f \circ \sigma_j = \sigma_j \circ f$  along the  $d-1$  spatial lattice directions is said to be *shift invariant*, with the associated symmetry of dynamics given by the  $d$ -dimensional group of discrete spatiotemporal translations.

Assign to each site  $z$  a letter  $m_z$  from the alphabet  $\mathcal{A}$ . A particular fixed set of letters  $m_z$  corresponds to a particular lattice symbol array  $\mathbf{M} = \{m_z\} = \{m_{n_1 n_2 \dots n_d}\}$ , which yields a complete specification of the corresponding state  $\Phi$ . In the lattice case, the *full shift* is the set of all  $d$ -dimensional symbol arrays that can be formed from the letters of the alphabet  $\mathcal{A}$

as in (F.6)

A  $d$ -dimensional spatiotemporal field  $\Phi = \{\phi_z\}$  is determined by the corresponding  $d$ -dimensional spatiotemporal symbol array  $\mathbf{M} = \{m_z\}$ . Consider next a finite block of symbols  $\mathbf{M}_{\mathcal{R}} \subset \mathbf{M}$ , over a finite rectangular  $[L_1 \times L_2 \times \dots \times L_d]$  lattice region  $\mathcal{R} \subset \mathbb{Z}^d$ . In particular, let  $\mathbf{M}_p$  over a finite rectangular  $[L_1 \times L_2 \times \dots \times L_d]$  lattice region be the  $[L_1 \times L_2 \times \dots \times L_d]$   $d$ -periodic block of  $\mathbf{M}$  whose repeats tile  $\mathbb{Z}^d$ .

**Blocks.** In the case of temporal dynamics, a finite itinerary  $\mathbf{M}_{\mathcal{R}} = m_{k+1} m_{k+2} \dots m_{k+L}$  of symbols from  $\mathcal{A}$  is called a *block* of length  $L = n_{\mathcal{R}}$ . More generally, let  $\mathcal{R} \subset \mathbb{Z}^d$  be a  $[L_1 \times L_2 \times \dots \times L_d]$  rectangular lattice region,  $L_k \geq 1$ , whose lower left corner is the  $n = (n_1 n_2 \dots n_d)$  lattice site

$$\mathcal{R} = \mathcal{R}_n^{[L_1 \times L_2 \times \dots \times L_d]} = \{(n_1 + j_1, \dots, n_d + j_d) \mid 0 \leq j_k \leq L_k - 1\}. \quad (\text{F.7})$$

The associated finite block of symbols  $m_z \in \mathcal{A}$  restricted to  $\mathcal{R}$ ,  $\mathbf{M}_{\mathcal{R}} = \{m_z \mid z \in \mathcal{R}\} \subset \mathbf{M}$  is called the block  $\mathbf{M}_{\mathcal{R}}$  of volume  $n_{\mathcal{R}} = L_1 L_2 \dots L_d$ . For example, for a 2-dimensional lattice a  $\mathcal{R} = [3 \times 2]$  block is of form

$$\mathbf{M}_{\mathcal{R}} = \begin{bmatrix} m_{12} & m_{22} & m_{32} \\ m_{11} & m_{21} & m_{31} \end{bmatrix} \quad (\text{F.8})$$

and volume (in this case, an area) equals  $3 \times 2 = 6$ . In our convention, the first index is ‘space’, increasing from left to right, and the second index is ‘time’, increasing from bottom up.

**Cylinder sets.** While a particular admissible infinite symbol array  $\mathbf{M} = \{m_z\}$  defines a point  $\Phi$  (a unique lattice state) in the state space, the *cylinder set*  $\mathcal{M}_{\mathbf{M}_{\mathcal{R}}}$ , corresponds to the totality of state space points  $\Phi$  that share the same given finite block  $\mathbf{M}_{\mathcal{R}}$  symbolic representation over the region  $\mathcal{R}$ . For example, in  $d = 1$  case

$$\mathcal{M}_{\mathbf{M}_{\mathcal{R}}} = \{\cdots a_{-2}a_{-1} \cdot m_1m_2 \cdots m_L a_{L+1}a_{L+2} \cdots\}, \quad (\text{F.9})$$

with the symbols  $a_j$  outside of the block  $\mathbf{M}_{\mathcal{R}} = [m_1m_2 \cdots m_L]$  unspecified.

**Periodic orbits, invariant  $d$ -tori.** A state space point  $\phi_z \in \Phi$  is spatiotemporally *periodic*,  $\phi_z = \phi_{z+L}$ , if its spacetime orbit returns to it after a finite lattice shift  $L = (L_1, L_2, \cdots, L_d)$  over region  $\mathcal{R}$  defined in (F.7). The infinity of repeats of the corresponding block  $\mathbf{M}_{\mathcal{R}}$  then tiles the lattice. For a spatiotemporally periodic state  $\Phi$ , a *prime* block  $\mathbf{M}_p$  (or  $p$ ) is a smallest such block  $L_p = (L_1, L_2, \cdots, L_d)$  that cannot itself be tiled by repeats of a shorter block.

The periodic tiling of the lattice by the infinitely many repeats of a prime block is denoted by a bar:  $\overline{\mathbf{M}}_p$ . We shall omit the bar whenever it is clear from the context that the state is periodic.

[2019-01-19 Predrag] eliminate  $\_m_{-m+1} \cdots m_0$ - and  $[m_{-m+1} \cdots m_0,]$  notation in favor a single convention

[2018-11-07 Predrag] Generalize to invariant  $d$ -tori.

In  $d = 1$  dimensions, prime block is called a *prime cycle*  $p$ , or a single traversal of the orbit; its label is a block of  $n_p$  symbols that cannot be written as a repeat of a shorter block. Each *periodic point*  $\phi_{m_1m_2 \cdots m_{n_p}}$  is then labeled by the starting symbol  $m_1$ , followed by the next  $(n_p - 1)$  steps of its future itinerary. The set of periodic points  $\mathcal{M}_p$  that belong to a given periodic orbit form a *cycle*

$$p = \overline{m_1m_2 \cdots m_{n_p}} = \{\phi_{m_1m_2 \cdots m_{n_p}}, \phi_{m_2 \cdots m_{n_p}m_1}, \cdots, \phi_{m_{n_p}m_1 \cdots m_{n_p-1}}\}. \quad (\text{F.10})$$

More generally, a state space point is *spatiotemporally periodic* if it belongs to an invariant  $d$ -torus, i.e., its symbolic representation is a block over region  $\mathcal{R}$  defined by (F.7),

$$\mathbf{M}_p = \mathbf{M}_{\mathcal{R}}, \quad \mathcal{R} = \mathcal{R}_0^{[L_1 \times L_2 \times \cdots \times L_d]}, \quad (\text{F.11})$$

that tiles the lattice state  $\mathbf{M}$  periodically, with period  $L_j$  in the  $j$ th lattice direction.

**Generating partitions.** A temporal partition is called *generating* if every bi-infinite itinerary corresponds to a distinct point in state space. In practice almost any generating partition of interest is infinite. Even when the dynamics assigns a unique infinite itinerary  $\cdots m_{-2}m_{-1}m_0.m_1m_2m_3 \cdots$  to each distinct orbit, there generically exist full shift itineraries (F.5) which are not realized as orbits; such sequences are called *inadmissible*, and we say that the symbolic dynamics is *pruned*.

**Dynamical partitions.** If the symbols outside of given temporal block  $b$  remain unspecified, the set of all admissible blocks of length  $n_b$  yield a dynamically generated partition of the state space,  $\mathcal{M} = \cup_b \mathcal{M}_b$ .

**Subshifts.** A dynamical system  $(\mathcal{M}, f)$  given by a mapping  $f : \mathcal{M} \rightarrow \mathcal{M}$  together with a partition  $\mathcal{A}$  induces *topological dynamics*  $(\Sigma, \sigma)$ , where the *subshift*

$$\Sigma = \{(m_k)_{k \in \mathbb{Z}}\}, \quad (\text{F.12})$$

is the set of all *admissible* itineraries, and  $\sigma : \Sigma \rightarrow \Sigma$  is the shift operator (F.4). The designation ‘subshift’ comes from the fact that  $\Sigma$  is a subset of the full shift.

Let  $\hat{\Sigma}$  be the full lattice shift (F.5), i.e., the set of all possible lattice state  $\mathbf{M}$  labelings by the alphabet  $\mathcal{A}$ , and  $\hat{\Sigma}(\mathbf{M}_{\mathcal{R}})$  is the set of such blocks over a region  $\mathcal{R}$ . The principal task in developing the symbolic dynamics of a dynamical system is to determine  $\Sigma$ , the set of all *admissible* itineraries/lattice states, i.e., all states that can be realized by the given system.

**Pruning, grammars, recoding.** If certain states are inadmissible, the alphabet must be supplemented by a *grammar*, a set of pruning rules. Suppose that the grammar can be stated as a finite number of pruning rules, each forbidding a block of finite size,

$$\mathcal{G} = \{b_1, b_2, \dots, b_k\}, \quad (\text{F.13})$$

where a *pruned block*  $b$  is an array of symbols defined over a finite  $\mathcal{R}$  lattice region of size  $[L_1 \times L_2 \times \dots \times L_d]$ . In this case we can construct a finite Markov partition by replacing finite size blocks of the original partition by letters of a new alphabet. In the case of a 1-dimensional, the temporal lattice, if the longest forbidden block is of length  $L + 1$ , we say that the symbolic dynamics is Markov, a shift of finite type with  $L$ -step memory.

**Subshifts of finite type.** A topological dynamical system  $(\Sigma, \sigma)$  for which all admissible states  $\mathbf{M}$  are generated by recursive application of the finite set of pruning rules (F.13) is called a subshift of *finite type*. 2CB

If a map can be topologically conjugated to a linear map, the symbolic dynamics of the linear map offers a dramatically simplified description of all admissible solutions of the original flow, with the temporal symbolic dynamics and the state space dynamics related by linear recoding formulas. For example, if a map of an interval, such as a parabola, can be conjugated to a piecewise linear map, the kneading theory [165] classifies *all* of its admissible orbits.

## References

- [1] R. L. Adler and B. Weiss, “Entropy, a complete metric invariant for automorphisms of the torus”, *Proc. Natl. Acad. Sci. USA* **57**, 1573–1576 (1967).
- [2] R. L. Adler and B. Weiss, *Similarity of automorphisms of the torus*, Vol. 98, *Memoirs Amer. Math. Soc.* (Amer. Math. Soc., Providence RI, 1970).
- [3] E. Allroth, “Ground state of one-dimensional systems and fixed points of 2n-dimensional map”, *J. Phys. A* **16**, L497 (1983).

- [4] A. M. Ozorio de Almeida and J. H. Hannay, “Periodic orbits and a correlation function for the semiclassical density of states”, *J. Phys. A* **17**, 3429 (1984).
- [5] R. E. Amritkar, P. M. Gade, A. D. Gangal, and V. M. Nandkumaran, “Stability of periodic orbits of coupled-map lattices”, *Phys. Rev. A* **44**, R3407–R3410 (1991).
- [6] W. N. Anderson and T. D. Morley, “Eigenvalues of the Laplacian of a graph”, *Lin. Multilin. Algebra* **18**, 141–145 (1985).
- [7] G. B. Arfken, H. J. Weber, and F. E. Harris, *Mathematical Methods for Physicists: A Comprehensive Guide*, 7th ed. (Academic, New York, 2013).
- [8] V. I. Arnol’d and A. Avez, *Ergodic Problems of Classical Mechanics* (Addison-Wesley, Redwood City, 1989).
- [9] F. Arrigo, P. Grindrod, D. J. Higham, and V. Noferini, “On the exponential generating function for non-backtracking walks”, *Linear Algebra Appl.* **556**, 381–399 (2018).
- [10] M. Artin and B. Mazur, “On periodic points”, *Ann. Math.* **81**, 82–99 (1965).
- [11] R. Artuso, E. Aurell, and P. Cvitanović, “Recycling of strange sets: I. Cycle expansions”, *Nonlinearity* **3**, 325–359 (1990).
- [12] J. H. Asad, “Differential equation approach for one- and two-dimensional lattice green’s function”, *Mod. Phys. Lett. B* **21**, 139–154 (2007).
- [13] D. Atkinson and F. J. van Steenwijk, “Infinite resistive lattices”, *Am. J. Phys* **67**, 486–492 (1999).
- [14] M. Baake, J. Hermisson, and A. B. Pleasants, “The torus parametrization of quasiperiodic LI-classes”, *J. Phys. A* **30**, 3029–3056 (1997).
- [15] J.-C. Ban, W.-G. Hu, S.-S. Lin, and Y.-H. Lin, *Zeta Functions for Two-dimensional Shifts of Finite Type*, Vol. 221, *Memoirs Amer. Math. Soc.* (Amer. Math. Soc., Providence RI, 2013).
- [16] R. Band, J. M. Harrison, and C. H. Joyner, “Finite pseudo orbit expansions for spectral quantities of quantum graphs”, *J. Phys. A* **45**, 325204 (2012).
- [17] A. Barvinok, *A Course in Convexity* (Amer. Math. Soc., New York, 2002).
- [18] A. Barvinok, *Lattice Points, Polyhedra, and Complexity*, tech. rep. (Univ. of Michigan, Ann Arbor MI, 2004).
- [19] A. Barvinok, *Integer Points in Polyhedra* (European Math. Soc. Pub., Berlin, 2008).
- [20] A. I. Barvinok, “A polynomial time algorithm for counting integral points in polyhedra when the dimension is fixed”, *Math. Oper. Res.* **19**, 769–779 (1994).
- [21] H. Bass, “The Ihara-Selberg zeta function of a tree lattice”, *Int. J. Math.* **3**, 717–797 (1992).
- [22] R. J. Baxter, “The bulk, surface and corner free energies of the square lattice Ising model”, *J. Phys. A* **50**, 014001 (2016).

- [23] M. Beck and S. Robins, *Computing the Continuous Discretely* (Springer, New York, 2007).
- [24] H. S. Bhat and B. Osting, “Diffraction on the two-dimensional square lattice”, *SIAM J. Appl. Math.* **70**, 1389–1406 (2010).
- [25] O. Biham and W. Wenzel, “Characterization of unstable periodic orbits in chaotic attractors and repellers”, *Phys. Rev. Lett.* **63**, 819 (1989).
- [26] N. Bird and F. Vivaldi, “Periodic orbits of the sawtooth maps”, *Physica D* **30**, 164–176 (1988).
- [27] P. Blanchard and D. Volchenkov, *Random Walks and Diffusions on Graphs and Databases* (Springer, Berlin, 2011).
- [28] S. V. Bolotin and D. V. Treschev, “Hill’s formula”, *Russ. Math. Surv.* **65**, 191 (2010).
- [29] R. Bowen, “Markov partitions for Axiom A diffeomorphisms”, *Amer. J. Math.* **92**, 725–747 (1970).
- [30] R. Bowen and O. Lanford, Zeta functions of restrictions of the shift transformation, in *Global Analysis (Proc. Sympos. Pure Math., Berkeley, CA, 1968)*, Vol. 1, edited by S.-S. Chern and S. Smale (1970), pp. 43–50.
- [31] J. P. Boyd, *Chebyshev and Fourier Spectral Methods*, 2nd ed. (Dover, New York, 2000).
- [32] L. Boyle and P. J. Steinhardt, *Self-similar one-dimensional quasilattices*, 2016.
- [33] R. B. S. Brooks, R. F. Brown, J. Pak, and D. H. Taylor, “Nielsen numbers of maps of tori”, *Proc. Amer. Math. Soc.* **52**, 398–398 (1975).
- [34] L. A. Bunimovich and Y. G. Sinai, “Spacetime chaos in coupled map lattices”, *Nonlinearity* **1**, 491 (1988).
- [35] B. L. Buzbee, G. H. Golub, and C. W. Nielson, “On direct methods for solving Poisson’s equations”, *SIAM J. Numer. Anal.* **7**, 627–656 (1970).
- [36] J. L. Cardy, “Operator content of two-dimensional conformally invariant theories”, *Nucl. Phys. B* **270**, 186–204 (1986).
- [37] M. Chen, “On the solution of circulant linear systems”, *SIAM J. Numer. Anal.* **24**, 668–683 (1987).
- [38] G. Chinta, J. Jorgenson, and A. Karlsson, “Zeta functions, heat kernels, and spectral asymptotics on degenerating families of discrete tori”, *Nagoya Math. J.* **198**, 121–172 (2010).
- [39] G. Chinta, J. Jorgenson, and A. Karlsson, “Heat kernels on regular graphs and generalized Ihara zeta function formulas”, *Monatsh. Math.* **178**, 171–190 (2014).
- [40] B. V. Chirikov, “A universal instability of many-dimensional oscillator system”, *Phys. Rep.* **52**, 263–379 (1979).
- [41] W. G. Choe and J. Guckenheimer, “Computing periodic orbits with high accuracy”, *Computer Meth. Appl. Mech. and Engin.* **170**, 331–341 (1999).



- [42] F. Christiansen, P. Cvitanović, and V. Putkaradze, “Spatiotemporal chaos in terms of unstable recurrent patterns”, *Nonlinearity* **10**, 55–70 (1997).
- [43] F. Chung and S.-T. Yau, “Discrete Green’s functions”, *J. Combin. Theory A* **91**, 19–214 (2000).
- [44] D. Cimasoni, “The critical Ising model via Kac-Ward matrices”, *Commun. Math. Phys.* **316**, 99–126 (2012).
- [45] B. Clair, “The Ihara zeta function of the infinite grid”, *Electron. J. Combin.* **21**, P2–16 (2014).
- [46] B. Clair and S. Mokhtari-Sharghi, “Zeta functions of discrete groups acting on trees”, *J. Algebra* **237**, 591–620 (2001).
- [47] B. Clair and S. Mokhtari-Sharghi, “Convergence of zeta functions of graphs”, *Proc. Amer. Math. Soc.* **130**, 1881–1887 (2002).
- [48] H. Cohen, *A Course in Computational Algebraic Number Theory* (Springer, Berlin, 1993).
- [49] S. C. Creagh, “Quantum zeta function for perturbed cat maps”, *Chaos* **5**, 477–493 (1995).
- [50] J. Cserti, “Application of the lattice Green’s function for calculating the resistance of an infinite network of resistors”, *Amer. J. Physics* **68**, 896–906 (2000).
- [51] J. Cserti, G. Széchenyi, and G. Dávid, “Uniform tiling with electrical resistors”, *J. Phys. A* **44**, 215201 (2011).
- [52] P. Cvitanović, “Invariant measurement of strange sets in terms of cycles”, *Phys. Rev. Lett.* **61**, 2729–2732 (1988).
- [53] P. Cvitanović, “Recurrent flows: The clockwork behind turbulence”, *J. Fluid Mech. Focus Fluids* **726**, 1–4 (2013).
- [54] P. Cvitanović, “Trace formulas”, in *Chaos: classical and quantum*, edited by P. Cvitanović, R. Artuso, R. Mainieri, G. Tanner, and G. Vattay (Niels Bohr Inst., Copenhagen, 2017).
- [55] P. Cvitanović, “Counting”, in *Chaos: Classical and Quantum* (Niels Bohr Inst., Copenhagen, 2020).
- [56] P. Cvitanović, “Why cycle?”, in *Chaos: Classical and Quantum*, edited by P. Cvitanović, R. Artuso, R. Mainieri, G. Tanner, and G. Vattay (Niels Bohr Inst., Copenhagen, 2020).
- [57] P. Cvitanović, “World in a mirror”, in *Chaos: Classical and Quantum* (Niels Bohr Inst., Copenhagen, 2020).
- [58] P. Cvitanović, R. Artuso, R. Mainieri, G. Tanner, and G. Vattay, *Chaos: Classical and Quantum* (Niels Bohr Inst., Copenhagen, 2020).
- [59] P. Cvitanović, R. Artuso, R. Mainieri, G. Tanner, and G. Vattay, *Chaos: Classical and Quantum* (Niels Bohr Inst., Copenhagen, 2020).



- [60] P. Cvitanović and Y. Lan, Turbulent fields and their recurrences, in *Correlations and Fluctuations in QCD : Proceedings of 10. International Workshop on Multiparticle Production*, edited by N. Antoniou (2003), pp. 313–325.
- [61] P. Cvitanović and H. Liang, *Spatiotemporal cat: a chaotic field theory*, in preparation, 2020.
- [62] F. Dannan, S. Elaydi, and P. Liu, “Periodic solutions of difference equations”, *J. Difference Equations and Applications* **6**, 203–232 (2000).
- [63] J. A. De Loera, R. Hemmecke, J. Tauzer, and R. Yoshida, “Effective lattice point counting in rational convex polytopes”, *J. Symbolic Comp.* **38**, 1273–1302 (2004).
- [64] A. Deitmar, “Thara zeta functions of infinite weighted graphs”, *SIAM J. Discrete Math.* **29**, 2100–2116 (2015).
- [65] R. L. Devaney, *An Introduction to Chaotic Dynamical systems*, 2nd ed. (Westview Press, 2008).
- [66] A. Dienstfrey, F. Hang, and J. Huang, “Lattice sums and the two-dimensional, periodic Green’s function for the Helmholtz equation”, *Proc. Roy. Soc. Ser A* **457**, 67–85 (2001).
- [67] X. Ding, H. Chaté, P. Cvitanović, E. Siminos, and K. A. Takeuchi, “Estimating the dimension of the inertial manifold from unstable periodic orbits”, *Phys. Rev. Lett.* **117**, 024101 (2016).
- [68] X. Ding and P. Cvitanović, “Periodic eigendecomposition and its application in Kuramoto-Sivashinsky system”, *SIAM J. Appl. Dyn. Syst.* **15**, 1434–1454 (2016).
- [69] E. J. Doedel, A. R. Champneys, T. F. Fairgrieve, Y. A. Kuznetsov, B. Sandstede, and X. Wang, *AUTO: Continuation and Bifurcation Software for Ordinary Differential Equations* (2007).
- [70] F. W. Dorr, “The direct solution of the discrete Poisson equation on a rectangle”, *SIAM Rev.* **12**, 248–263 (1970).
- [71] P. G. Doyle and J. L. Snell, “Random walks and electric networks”, in *Intelligent Systems, Control and Automation: Science and Engineering* (Springer, 2012), pp. 259–265.
- [72] M. S. Dresselhaus, G. Dresselhaus, and A. Jorio, *Group Theory: Application to the Physics of Condensed Matter* (Springer, New York, 2007).
- [73] J. Dubout, *Zeta functions of graphs, their symmetries and extended Catalan numbers*.
- [74] D. Dudgeon and R. M. Mersereau, *Multidimensional Digital Signal Processing* (Prentice-Hall, Englewood Cliffs, NJ, 1984).
- [75] H. R. Dullin and J. D. Meiss, “Stability of minimal periodic orbits”, *Phys. Lett. A* **247**, 227–234 (1998).
- [76] E. N. Economou, *Green’s Functions in Quantum Physics* (Springer, Berlin, 2006).
- [77] S. Elaydi, *An Introduction to Difference Equations* (Springer, Berlin, 2005).

- [78] A. L. Fetter and J. D. Walecka, *Theoretical Mechanics of Particles and Continua* (Dover, New York, 2003).
- [79] M. Fiedler, “Algebraic connectivity of graphs”, *Czech. Math. J* **23**, 298–305 (1973).
- [80] D. Fischer, G. Golub, O. Hald, C. Leiva, and O. Widlund, “On Fourier-Toeplitz methods for separable elliptic problems”, *Math. Comput.* **28**, 349–349 (1974).
- [81] F. Flicker, “Time quasilattices in dissipative dynamical systems”, *SciPost Phys.* **5**, 001 (2018).
- [82] E. Fradkin, *Field Theories of Condensed Matter Physics* (Cambridge Univ. Press, Cambridge UK, 2013).
- [83] P. M. Gade and R. E. Amritkar, “Spatially periodic orbits in coupled-map lattices”, *Phys. Rev. E* **47**, 143–154 (1993).
- [84] G. Giacomelli, S. Lepri, and A. Politi, “Statistical properties of bidimensional patterns generated from delayed and extended maps”, *Phys. Rev. E* **51**, 3939–3944 (1995).
- [85] J. F. Gibson, J. Halcrow, and P. Cvitanović, “Visualizing the geometry of state-space in plane Couette flow”, *J. Fluid Mech.* **611**, 107–130 (2008).
- [86] R. Giles and C. B. Thorn, “Lattice approach to string theory”, *Phys. Rev. D* **16**, 366–386 (1977).
- [87] F. Ginelli, P. Poggi, A. Turchi, H. Chaté, R. Livi, and A. Politi, “Characterizing dynamics with covariant Lyapunov vectors”, *Phys. Rev. Lett.* **99**, 130601 (2007).
- [88] J. I. Glaser, “Numerical solution of waveguide scattering problems by finite-difference Green’s functions”, *IEEE Trans. Microwave Theory Tech.* **18**, 436–443 (1970).
- [89] C. Godsil and G. F. Royle, *Algebraic Graph Theory* (Springer, New York, 2013).
- [90] J. W. von Goethe, *Faust I, Studierzimmer 2*. M. Greenberg, transl. (Yale Univ. Press, 1806).
- [91] G. H. Golub and C. F. Van Loan, *Matrix Computations*, 4th ed. (J. Hopkins Univ. Press, Baltimore, MD, 2013).
- [92] G. Grimmett, *Probability on Graphs: : Random Processes on Graphs and Lattices* (Cambridge Univ. Press, 2009).
- [93] J. Guckenheimer and B. Meloon, “Computing periodic orbits and their bifurcations with automatic differentiation”, *SIAM J. Sci. Comput.* **22**, 951–985 (2000).
- [94] M. N. Guderof and P. Cvitanović, *Spatiotemporal tiling of the Kuramoto-Sivashinsky flow*, in preparation, 2020.
- [95] D. Guido, T. Isola, and M. L. Lapidus, “A trace on fractal graphs and the Ihara zeta function”, *Trans. Amer. Math. Soc.* **361**, 3041–3041 (2009).

- [96] B. Gutkin, L. Han, R. Jafari, A. K. Saremi, and P. Cvitanović, [Linear encoding of the spatiotemporal cat map](#), *Nonlinearity*, to appear, 2020.
- [97] B. Gutkin and V. Osipov, [“Clustering of periodic orbits and ensembles of truncated unitary matrices”](#), *J. Stat. Phys.* **153**, 1049–1064 (2013).
- [98] B. Gutkin and V. Osipov, [“Clustering of periodic orbits in chaotic systems”](#), *Nonlinearity* **26**, 177 (2013).
- [99] B. Gutkin and V. Osipov, [“Classical foundations of many-particle quantum chaos”](#), *Nonlinearity* **29**, 325–356 (2016).
- [100] A. J. Guttmann, [“Lattice Green’s functions in all dimensions”](#), *J. Phys. A* **43**, 305205 (2010).
- [101] K. Hashimoto, [“Zeta functions of finite graphs and representations of p-adic groups”](#), *Adv. Stud. Pure Math.* **15**, 211–280 (1989).
- [102] G. W. Hill, [“On the part of the motion of the lunar perigee which is a function of the mean motions of the sun and moon”](#), *Acta Math.* **8**, 1–36 (1886).
- [103] H. Hobrecht and F. Hucht, [“Anisotropic scaling of the two-dimensional Ising model I: the torus”](#), *SciPost Phys.* **7**, 026 (2019).
- [104] H. Hobrecht and F. Hucht, [“Anisotropic scaling of the two-dimensional Ising model II: surfaces and boundary fields”](#), *SciPost Physics* **8**, 032 (2020).
- [105] W. G. Hoover and K. Aoki, [“Order and chaos in the one-dimensional  \$\phi^4\$  model : N-dependence and the Second Law of Thermodynamics”](#), *Commun. Nonlinear Sci. Numer. Simul.* **49**, 192–201 (2017).
- [106] T. Horiguchi, [“Lattice Green’s function for the simple cubic lattice”](#), *J. Phys. Soc. Jpn.* **30**, 1261–1272 (1971).
- [107] T. Horiguchi and T. Morita, [“Note on the lattice Green’s function for the simple cubic lattice”](#), *J. Phys. C* **8**, L232 (1975).
- [108] M. D. Horton, [“Ihara zeta functions of digraphs”](#), *Linear Algebra Appl.* **425**, 130–142 (2007).
- [109] G. Y. Hu and R. F. O’Connell, [“Analytical inversion of symmetric tridiagonal matrices”](#), *J. Phys. A* **29**, 1511 (1996).
- [110] G. Y. Hu, J. Y. Ryu, and R. F. O’Connell, [“Analytical solution of the generalized discrete Poisson equation”](#), *J. Phys. A* **31**, 9279 (1998).
- [111] A. Hucht, [“The square lattice Ising model on the rectangle I: finite systems”](#), *J. Phys. A* **50**, 065201 (2017).
- [112] B. D. Hughes, *Random Walks and Random Environments: Vol. I, Random Walks* (Clarendon Press, Oxford, 1995).
- [113] C. A. Hurst and H. S. Green, [“New solution of the Ising problem for a rectangular lattice”](#), *J. Chem. Phys.* **33**, 1059–1062 (1960).
- [114] Y. Ihara, [“On discrete subgroups of the two by two projective linear group over p-adic fields”](#), *J. Math. Soc. Japan* **18**, 219–235 (1966).

- [115] S. Isola, “ $\zeta$ -functions and distribution of periodic orbits of toral automorphisms”, *Europhys. Lett.* **11**, 517–522 (1990).
- [116] E. V. Ivashkevich, N. S. Izmailian, and C.-K. Hu, “Kronecker’s double series and exact asymptotic expansions for free models of statistical mechanics on torus”, *J. Phys. A* **35**, 5543–5561 (2002).
- [117] N. S. Izmailian, “Finite-size effects for anisotropic 2D Ising model with various boundary conditions”, *J. Phys. A* **45**, 494009 (2012).
- [118] N. S. Izmailian and C.-K. Hu, “Finite-size effects for the Ising model on helical tori”, *Phys. Rev. E* **76**, 041118 (2007).
- [119] N. S. Izmailian, K. B. Oganessian, and C.-K. Hu, “Exact finite-size corrections for the square-lattice Ising model with Brascamp-Kunz boundary conditions”, *Phys. Rev. E* **65**, 056132 (2002).
- [120] K. Jansen, “Lattice field theory”, *Int. J. Mod. Phys. E* **16**, 2638–2679 (2007).
- [121] J. Jorgenson and S. Lang, “The ubiquitous heat kernel”, in *Mathematics Unlimited - 2001 and Beyond* (Springer, Berlin, 2001), pp. 655–683.
- [122] L. P. Kadanoff, *Statistical Physics: Statics, Dynamics and Renormalization* (World Scientific, Singapore, 2000).
- [123] K. Kaneko, “Transition from torus to chaos accompanied by frequency lockings with symmetry breaking: In connection with the coupled-logistic map”, *Prog. Theor. Phys.* **69**, 1427–1442 (1983).
- [124] K. Kaneko, “Period-doubling of kink-antikink patterns, quasiperiodicity in antiferro-like structures and spatial intermittency in coupled logistic lattice: Towards a prelude of a “field theory of chaos””, *Prog. Theor. Phys.* **72**, 480–486 (1984).
- [125] H. Kantz and P. Grassberger, “Chaos in low-dimensional Hamiltonian maps”, *Phys. Let. A* **123**, 437–443 (1987).
- [126] A. Karlsson and M. Neuhauser, “Heat kernels, theta identities, and zeta functions on cyclic groups”, *Contemp. Math.* **394**, 177–190 (2006).
- [127] B. Kastening, “Simplified transfer matrix approach in the two-dimensional Ising model with various boundary conditions”, *Phys. Rev. E* **66**, 057103 (2002).
- [128] S. Katsura and S. Inawashiro, “Lattice Green’s functions for the rectangular and the square lattices at arbitrary points”, *J. Math. Phys.* **12**, 1622–1630 (1971).
- [129] S. Katsura, S. Inawashiro, and Y. Abe, “Lattice Green’s function for the simple cubic lattice in terms of a Mellin-Barnes type integral”, *J. Math. Phys.* **12**, 895–899 (1971).
- [130] S. Katsura, T. Morita, S. Inawashiro, T. Horiguchi, and Y. Abe, “Lattice Green’s function. Introduction”, *J. Math. Phys.* **12**, 892–895 (1971).
- [131] J. P. Keating, “The cat maps: quantum mechanics and classical motion”, *Nonlinearity* **4**, 309–341 (1991).

- [132] V. Khoromskaia and B. N. Khoromskij, “Block circulant and Toeplitz structures in the linearized Hartree-Fock equation on finite lattices: Tensor approach”, *Comput. Methods Appl. Math.* **17**, 43–455 (2017).
- [133] G. Kirchhoff, “Üeber die Auflösung der Gleichungen, auf welche man bei der Untersuchung der linearen Vertheilung galvanischer Ströme geführt wird”, *Ann. Phys. Chem.* **148**, 497–508 (1847).
- [134] H.-T. Kook and J. D. Meiss, “Application of Newton’s method to Lagrangian mappings”, *Physica D* **36**, 317–326 (1989).
- [135] M. Kotani and T. Sunada, “Zeta functions of finite graphs”, *J. Math. Sci. Univ. Tokyo* **7**, 7–25 (2000).
- [136] Y. Lan and P. Cvitanović, “Variational method for finding periodic orbits in a general flow”, *Phys. Rev. E* **69**, 016217 (2004).
- [137] S. Lang, *Linear Algebra* (Addison-Wesley, Reading, MA, 1987).
- [138] D. Lenz, F. Pogorzelski, and M. Schmidt, “The Ihara zeta function for infinite graphs”, *Trans. Amer. Math. Soc.* **371**, 5687–5729 (2018).
- [139] S. Lepri, A. Politi, and A. Torcini, “Chronotopic Lyapunov analysis. I. A detailed characterization of 1D systems”, *J. Stat. Phys.* **82**, 1429–1452 (1996).
- [140] S. Lepri, A. Politi, and A. Torcini, “Chronotopic Lyapunov analysis. II. Towards a unified approach”, *J. Stat. Phys.* **88**, 31–45 (1997).
- [141] S. Levit and U. Smilansky, “A new approach to Gaussian path integrals and the evaluation of the semiclassical propagator”, *Ann. Phys.* **103**, 198–207 (1977).
- [142] S. Levit and U. Smilansky, “A theorem on infinite products of eigenvalues of Sturm-Liouville type operators”, *Proc. Amer. Math. Soc.* **65**, 299–299 (1977).
- [143] J. Li and S. Tomsovic, “Exact relations between homoclinic and periodic orbit actions in chaotic systems”, *Phys. Rev. E* **97**, 022216 (2017).
- [144] T. M. Liaw, M. C. Huang, Y. L. Chou, S. C. Lin, and F. Y. Li, “Partition functions and finite-size scalings of Ising model on helical tori”, *Phys. Rev. E* **73**, 041118 (2006).
- [145] A. J. Lichtenberg and M. A. Lieberman, *Regular and Chaotic Dynamics*, 2nd ed. (Springer, New York, 2013).
- [146] W. J. Lick, *Difference Equations from Differential Equations* (Springer, Berlin, 1989).
- [147] J. S. Lim, *Two-dimensional Signal and Image Processing* (Prentice Hall, Englewood Cliffs, N.J, 1990).
- [148] D. Lind and K. Schmidt, “Symbolic and algebraic dynamical systems”, in *Handbook of Dynamical Systems*, Vol. 1, edited by B. Hasselblatt and A. Katok (Elsevier, New York, 2002), pp. 765–812.
- [149] D. A. Lind, “A zeta function for  $Z^d$ -actions”, in *Ergodic Theory of  $Z^d$  Actions*, edited by M. Pollicott and K. Schmidt (Cambridge Univ. Press, 1996), pp. 433–450.

- [150] D. A. Lind and B. Marcus, *An Introduction to Symbolic Dynamics and Coding* (Cambridge Univ. Press, Cambridge, 1995).
- [151] R. de la Llave, Variational methods for quasiperiodic solutions of partial differential equations, in *Hamiltonian Systems and Celestial Mechanics (HAMSYS-98)*, edited by J. Delgado, E. A. Lacomba, E. Pérez-Chavela, and J. Llibre (2000).
- [152] E. N. Lorenz, “Deterministic nonperiodic flow”, *J. Atmos. Sci.* **20**, 130–141 (1963).
- [153] I. Lyberg, “Free energy of the anisotropic Ising lattice with Brascamp-Kunz boundary conditions”, *Phys. Rev. E* **87**, 062141 (2013).
- [154] R. S. Mackay and J. D. Meiss, “Linear stability of periodic orbits in Lagrangian systems”, *Phys. Lett. A* **98**, 92–94 (1983).
- [155] S. MacKay, J. D. Meiss, and I. C. Percival, “Transport in Hamiltonian systems”, *Physica D* **13**, 55–81 (1984).
- [156] A. Manning, “Axiom A diffeomorphisms have rational zeta function”, *Bull. London Math. Soc.* **3**, 215–220 (1971).
- [157] E. C. Marino, *Quantum Field Theory Approach to Condensed Matter Physics* (Cambridge Univ. Press, Cambridge UK, 2017).
- [158] P. A. Martin, “Discrete scattering theory: Green’s function for a square lattice”, *Wave Motion* **43**, 619–629 (2006).
- [159] B. M. McCoy and T. T. Wu, *The Two-Dimensional Ising Model*, 2nd ed. (Dover, 1973).
- [160] J. D. Meiss, “Symplectic maps, variational principles, and transport”, *Rev. Mod. Phys.* **64**, 795–848 (1992).
- [161] B. D. Mestel and I. Percival, “Newton method for highly unstable orbits”, *Physica D* **24**, 172 (1987).
- [162] H. B. Meyer, “Lattice QCD: A brief introduction”, in *Lattice QCD for Nuclear Physics*, edited by H.-W. Lin and H. B. Meyer (Springer, York New, 2015), pp. 1–34.
- [163] M. Michałek and B. Sturmfels, *Invitation to Nonlinear Algebra* (MPI Leipzig, 2020).
- [164] R. Miles, “A dynamical zeta function for group actions”, *Monatsh. Math.* **182**, 683–708 (2016).
- [165] J. Milnor and W. Thurston, “Iterated maps of the interval”, in *Dynamical Systems (Maryland 1986-87)*, edited by A. Dold and B. Eckmann (Springer, New York, 1988), pp. 465–563.
- [166] I. Montvay and G. Münster, *Quantum Fields on a Lattice* (Cambridge Univ. Press, Cambridge, 1994).



- [167] T. Morita, “Useful procedure for computing the lattice Green’s function - square, tetragonal, and bcc lattices”, *J. Math. Phys.* **12**, 1744–1747 (1971).
- [168] T. Morita and T. Horiguchi, “Calculation of the lattice Green’s function for the bcc, fcc, and rectangular lattices”, *J. Math. Phys.* **12**, 986–992 (1971).
- [169] B. Mramor and B. Rink, “Ghost circles in lattice Aubry-Mather theory”, *J. Diff. Equ.* **252**, 3163–3208 (2012).
- [170] S. Müller, S. Heusler, P. Braun, F. Haake, and A. Altland, “Semiclassical foundation of universality in quantum chaos”, *Phys. Rev. Lett.* **93**, 014103 (2004).
- [171] G. Münster and M. Walzl, *Lattice gauge theory - A short primer*, 2000.
- [172] J. Nielsen, “Über die Minimalzahl der Fixpunkte bei den Abbildungstypen der Ringflächen”, *Math. Ann.* **82**, 83–93 (1920).
- [173] Y. Okabe, K. Kaneda, M. Kikuchi, and C.-K. Hu, “Universal finite-size scaling functions for critical systems with tilted boundary conditions”, *Phys. Rev. E* **59**, 1585–1588 (1999).
- [174] L. Onsager, “Crystal statistics. I. A Two-dimensional model with an order-disorder transition”, *Phys. Rev.* **65**, 117–149 (1944).
- [175] G. Papathanasiou and C. B. Thorn, “Worldsheet propagator on the lightcone worldsheet lattice”, *Phys. Rev. D* **87**, 066005 (2013).
- [176] I. Percival and F. Vivaldi, “A linear code for the sawtooth and cat maps”, *Physica D* **27**, 373–386 (1987).
- [177] I. Percival and F. Vivaldi, “Arithmetical properties of strongly chaotic motions”, *Physica D* **25**, 105–130 (1987).
- [178] Y. B. Pesin and Y. G. Sinai, “Space-time chaos in the system of weakly interacting hyperbolic systems”, *J. Geom. Phys.* **5**, 483–492 (1988).
- [179] S. D. Pethel, N. J. Corron, and E. Boltt, “Symbolic dynamics of coupled map lattices”, *Phys. Rev. Lett.* **96**, 034105 (2006).
- [180] S. D. Pethel, N. J. Corron, and E. Boltt, “Deconstructing spatiotemporal chaos using local symbolic dynamics”, *Phys. Rev. Lett.* **99**, 214101 (2007).
- [181] A. Poghosyan, N. Izmailian, and R. Kenna, “Exact solution of the critical Ising model with special toroidal boundary conditions”, *Phys. Rev. E* **96**, 062127 (2017).
- [182] H. Poincaré, “Sur les déterminants d’ordre infini”, *Bull. Soc. Math. France* **14**, 77–90 (1886).
- [183] A. Politi and A. Torcini, “Periodic orbits in coupled Hénon maps: Lyapunov and multifractal analysis”, *Chaos* **2**, 293–300 (1992).
- [184] A. Politi and A. Torcini, “Towards a statistical mechanics of spatiotemporal chaos”, *Phys. Rev. Lett.* **69**, 3421–3424 (1992).
- [185] A. Politi, A. Torcini, and S. Lepri, “Lyapunov exponents from node-counting arguments”, *J. Phys. IV* **8**, 263 (1998).

- [186] M. Pollicott, *Dynamical zeta functions*, in *Smooth Ergodic Theory and Its Applications*, Vol. 69, edited by A. Katok, R. de la Llave, Y. Pesin, and H. Weiss (2001), pp. 409–428.
- [187] C. Pozrikidis, *An Introduction to Grids, Graphs, and Networks* (Oxford Univ. Press, Oxford, UK, 2014).
- [188] L. Qi, H. Chen, and Y. Chen, *Tensor Eigenvalues and Their Applications* (Springer, Singapore, 2018).
- [189] P. Ren, T. Aleksić, D. Emms, R. C. Wilson, and E. R. Hancock, “Quantum walks, Ihara zeta functions and cospectrality in regular graphs”, *Quantum Inf. Process.* **10**, 405–417 (2010).
- [190] M. Rezaghi and L. Eldén, “Diagonalization of tensors with circulant structure”, *Linear Algebra Appl.* **435**, 422–447 (2011).
- [191] R. C. Robinson, *An Introduction to Dynamical Systems: Continuous and Discrete* (Amer. Math. Soc., New York, 2012).
- [192] H. J. Rothe, *Lattice Gauge Theories - An Introduction* (World Scientific, Singapore, 2005).
- [193] I. Sato, “Bartholdi zeta functions of group coverings of digraphs”, *Far East J. Math. Sci.* **18**, 321–339 (2005).
- [194] I. Schur, “Über Potenzreihen, die im Innern des Einheitskreises beschränkt sind”, *J. reine angewandte Math.* **147**, 205–232 (1917).
- [195] J.-P. Serre, *Trees* (Springer, Berlin, 1980).
- [196] R. Shankar, *Quantum Field Theory and Condensed Matter* (Cambridge Univ. Press, Cambridge UK, 2017).
- [197] M. Sieber and K. Richter, “Correlations between periodic orbits and their role in spectral statistics”, *Phys. Scr.* **2001**, 128 (2001).
- [198] A. Siemaszko and M. P. Wojtkowski, “Counting Berg partitions”, *Nonlinearity* **24**, 2383–2403 (2011).
- [199] J. Smit, *Introduction to Quantum Fields on a Lattice* (Cambridge Univ. Press, Cambridge, 2002).
- [200] R. Sommer, *Introduction to Lattice Gauge Theories*, tech. rep. (Humboldt Univ., 2015).
- [201] H. M. Stark and A. A. Terras, “Zeta functions of finite graphs and coverings”, *Adv. Math.* **121**, 124–165 (1996).
- [202] I. Stewart and D. Gökyaydin, “Symmetries of quotient networks for doubly periodic patterns on the square lattice”, *Int. J. Bifur. Chaos* **29**, 1930026 (2019).
- [203] R. Sturman, J. M. Ottino, and S. Wiggins, *The Mathematical Foundations of Mixing* (Cambridge Univ. Press, 2006).
- [204] R. Suarez, “Difference equations and a principle of double induction”, *Math. Mag.* **62**, 334–339 (1989).



- [205] T. Sunada, *Topological Crystallography* (Springer, Tokyo, 2013).
- [206] A. Tarfulea and R. Perlis, “An Ihara formula for partially directed graphs”, *Linear Algebra Appl.* **431**, 73–85 (2009).
- [207] A. Terras, *Zeta Functions of Graphs: A Stroll through the Garden* (Cambridge Univ. Press, 2010).
- [208] M. Toda, *Theory of Nonlinear Lattices* (Springer, Berlin, 1989).
- [209] J. H. Van Vleck, “The correspondence principle in the statistical interpretation of quantum mechanics”, *Proc. Natl. Acad. Sci.* **14**, 178–188 (1928).
- [210] G. Venezian, “On the resistance between two points on a grid”, *Am. J. Phys* **62**, 1000–1004 (1994).
- [211] Y. Colin de Verdière, “Spectrum of the Laplace operator and periodic geodesics: thirty years after”, *Ann. Inst. Fourier* **57**, 2429–2463 (2007).
- [212] D. Viswanath, “The Lindstedt-Poincaré technique as an algorithm for finding periodic orbits”, *SIAM Rev.* **43**, 478–496 (2001).
- [213] D. Viswanath, “Symbolic dynamics and periodic orbits of the Lorenz attractor”, *Nonlinearity* **16**, 1035–1056 (2003).
- [214] D. Viswanath, “The fractal property of the Lorenz attractor”, *Physica D* **190**, 115–128 (2004).
- [215] U.-J. Wiese, *An Introduction to Lattice Field Theory*, tech. rep. (Univ. Bern, 2009).
- [216] I. Wigman, “Counting singular matrices with primitive row vectors”, *Monatsh. Math.* **144**, 71–84 (2005).
- [217] Wikipedia contributors, *Block matrix — Wikipedia, The Free Encyclopedia*, 2020.
- [218] Wikipedia contributors, *Kronecker product — Wikipedia, The Free Encyclopedia*, 2020.
- [219] H. S. Wilf, *Generatingfunctionology* (Academic Press, New York, 1994).
- [220] W. L. Wood, “Periodicity effects on the iterative solution of elliptic difference equations”, *SIAM J. Numer. Anal.* **8**, 439–464 (1971).
- [221] J. Woods, *Multidimensional Signal, Image, and Video Processing and Coding* (Academic Press, Amsterdam, 2012).
- [222] F. Y. Wu, “Theory of resistor networks: the two-point resistance”, *J. Phys. A* **37**, 6653–6673 (2004).
- [223] M.-C. Wu and C.-K. Hu, “Exact partition functions of the Ising model on  $M \times N$  planar lattices with periodic-aperiodic boundary conditions”, *J. Phys. A* **35**, 5189–5206 (2002).
- [224] Z.-J. Xie, X.-Q. Jin, and Y.-M. Wei, “A fast algorithm for solving circulant tensor systems”, *Lin. Multilin. Algebra* **65**, 1894–1904 (2016).

- [225] Y. Yamasaki, “An explicit prime geodesic theorem for discrete tori and the hypergeometric functions”, *Math. Z.* **289**, 361–376 (2017).
- [226] A. Zee, *Quantum Field Theory in a Nutshell*, 2nd ed. (Princeton Univ. Press, Princeton NJ, 2010).
- [227] Q. Zhilin, A. Gangal, M. Benkun, and T. Gang, “Spatiotemporally periodic patterns in symmetrically coupled map lattices”, *Phys. Rev. E* **50**, 163–170 (1994).
- [228] D. Zhou, Y. Xiao, and Y.-H. He, “Seiberg duality, quiver gauge theories, and Ihara’s zeta function”, *Int. J. Mod. Phys. A* **30**, 1550118 (2015).
- [229] R. M. Ziff, C. D. Lorenz, and P. Kleban, “Shape-dependent universality in percolation”, *Physica A* **266**, 17–26 (1999).

## Appendix G. Nonlinearity journal tips

### *Appendix G.1. Naming your files*

Please name all your files, both figures and text, as follows:

- Use only characters from the set a to z, A to Z, 0 to 9 and underscore (`_`).
- Do not use spaces or punctuation characters in file names.
- Do not use any accented characters such as á, ê, ñ, ö.
- Include an extension to indicate the file type (e.g., `.tex`, `.eps`, `.txt`, etc).
- Use consistent upper and lower case in filenames and in your  $\text{\LaTeX}$  file. If your  $\text{\LaTeX}$  file contains the line `\includegraphics{fig1.eps}` the figure file must be called `fig1.eps` and not `Fig1.eps` or `fig1.EPS`. If you are on a Unix system, please ensure that there are no pairs of figures whose names differ only in capitalization, such as `fig_2a.eps` and `fig_2A.eps`, as Windows systems will be unable to keep the two files in the same directory.

### *Appendix G.2. Preparing your article*

Footnotes should be avoided whenever possible and can often be included in the text as phrases or sentences in parentheses. If required, they should be used only for brief notes that do not fit conveniently into the text. The use of displayed mathematics in footnotes should be avoided wherever possible and no equations within a footnote should be numbered. The standard  $\text{\LaTeX}$  macro `\footnote` should be used. Note that in `iopart.cls` the `\footnote` command produces footnotes indexed by a variety of different symbols, whereas in published articles we use numbered footnotes. This is not a problem: we will convert symbol-indexed footnotes to numbered ones during the production process.

### *Appendix G.3. The abstract*

The abstract should be self-contained—there should be no references to figures, tables, equations, bibliographic references etc.

### *Appendix G.4. Some matters of style*

It will help the readers if your article is written in a clear, consistent and concise manner. During the production process we will try to make sure that your work is presented to its readers in the best possible way without sacrificing the individuality of your writing.

- (i) We recommend using ‘-ize’ spellings (diagonalize, renormalization, minimization, etc) but there are some common exceptions to this, for example: devise, promise and advise.

Do not include ‘eq.’, ‘equation’ etc before an equation number or ‘ref.’ ‘reference’ etc before a reference number.

*Appendix G.5. Two-line constructions*

For simple fractions in the text the solidus /, as in  $\lambda/2\pi$ , should be used instead of `\frac` or `\over`, using parentheses where necessary to avoid ambiguity, for example to distinguish between  $1/(n-1)$  and  $1/n-1$ . Exceptions to this are the proper fractions  $\frac{1}{2}$ ,  $\frac{1}{3}$ ,  $\frac{3}{4}$ , etc, which are better left in this form. In displayed equations horizontal lines are preferable to solidi provided the equation is kept within a height of two lines. A two-line solidus should be avoided where possible; the construction  $(\dots)^{-1}$  should be used instead. For example use:

$$\frac{1}{M_a} \left( \int_0^\infty d\omega \frac{|S_o|^2}{N} \right)^{-1} \quad \text{instead of} \quad \frac{1}{M_a} / \int_0^\infty d\omega \frac{|S_o|^2}{N}.$$

*Appendix G.6. Roman and italic in mathematics*

In mathematics mode there are some cases where it is preferable to use a Roman font; for instance, a Roman d for a differential d, a Roman e for an exponential e and a Roman i for the square root of  $-1$ . To accommodate this and to simplify the typing of equations, `iopart.cls` provides some extra definitions. `\rmd`, `\rme` and `\rmi` now give Roman d, e and i respectively for use in equations, e.g.  $i x e^{2x} dx/dy$  is obtained by typing `\$ \rmi x \rme^{2x} \rmd x / \rmd y \$`.

Certain other common mathematical functions, such as cos, sin, det and ker, should appear in Roman type. Standard L<sup>A</sup>T<sub>E</sub>X provides macros for most of these functions (in the cases above, `\cos`, `\sin`, `\det` and `\ker` respectively); `iopart.cls` also provides additional definitions for Tr, tr and O (`\Tr`, `\tr` and `\Or`, respectively).

Subscripts and superscripts should be in Roman type if they are labels rather than variables or characters that take values. For example in the equation

$$\epsilon_m = -g\mu_n Bm$$

$m$ , the  $z$  component of the nuclear spin, is italic because it can have different values whereas  $n$  is Roman because it is a label meaning nuclear ( $\mu_n$  is the nuclear magneton).

*Appendix G.7. Special characters for mathematics*

Bold italic characters can be used in our journals to signify vectors (rather than using an upright bold or an over arrow). To obtain this effect when using `iopart.cls`, use `\bi{#1}` within maths mode, e.g. ***ABCdef***. Similarly, in `iopart.cls`, if upright bold characters are required in maths, use `\mathbf{#1}` within maths mode, e.g. **XYZabc**. The calligraphic (script) uppercase alphabet is obtained with `\mathcal{AB}` or `\cal{CD}` (*ABCD*).

The package `iopams.sty` uses the definition `\boldsymbol` in `amsbsy.sty` which allows individual non-alphabetical symbols and Greek letters to be made bold within equations. The bold Greek lowercase letters  $\alpha \dots \omega$ , are obtained with the commands `\balpha \dots \bomega` (but note that bold eta,  $\boldsymbol{\eta}$ , is `\bfeta` rather than `\betaeta`) and the capitals,  $\Gamma \dots \Omega$ , with commands `\bGamma \dots \bOmega`. Bold versions of the

**Table G1.** Other macros defined in `iopart.cls` for use in maths.

Macro	Result	Description
<code>\fl</code>		Start line of equation full left
<code>\case{#1}{#2}</code>	$\frac{\#1}{\#2}$	Text style fraction in display
<code>\Tr</code>	Tr	Roman Tr (Trace)
<code>\tr</code>	tr	Roman tr (trace)
<code>\Or</code>	O	Roman O (of order of)
<code>\lshad</code>	$\ll$	Text size left shadow bracket
<code>\rshad</code>	$\rr$	Text size right shadow bracket

following symbols are predefined in `iopams.sty`: bold partial,  $\partial$ , `\bpartial`, bold ‘ell’,  $\ell$ , `\bell`, bold imath,  $\imath$ , `\bimath`, bold jmath,  $\jmath$ , `\bjmath`, bold infinity,  $\infty$ , `\binfty`, bold nabla,  $\nabla$ , `\bnabla`, bold centred dot,  $\cdot$ , `\bdot`. Other characters are made bold using `\boldsymbol{\symbolname}`.

#### Appendix G.8. Alignment of displayed equations

The `iopart.cls` class file aligns left and indents each line of a display. To make any line start at the left margin of the page, add `\fl` at start of the line (to indicate full left).

Using the `eqnarray` environment equations will naturally be aligned left and indented without the use of any ampersands for alignment, see equations (G.1) and (G.2)

$$\alpha + \beta = \gamma^2, \quad (\text{G.1})$$

$$\alpha^2 + 2\gamma + \cos \theta = \delta. \quad (\text{G.2})$$

Where some secondary alignment is needed, for instance a second part of an equation on a second line, a single ampersand is added at the point of alignment in each line (see (G.3) and (G.4)).

$$\alpha = 2\gamma^2 + \cos \theta + \frac{XY \sin \theta}{X + Y \cos \theta} \quad (\text{G.3})$$

$$= \delta \theta PQ \cos \gamma. \quad (\text{G.4})$$

Two points of alignment are possible using two ampersands for alignment (see (G.5) and (G.6)). Note in this case extra space `\qqquad` is added before the second ampersand in the longest line (the top one) to separate the condition from the equation.

$$\alpha = 2\gamma^2 + \cos \theta + \frac{XY \sin \theta}{X + Y \cos \theta} \quad \theta > 1 \quad (\text{G.5})$$

$$= \delta \theta PQ \cos \gamma \quad \theta \leq 1. \quad (\text{G.6})$$

For a long equation which has to be split over more than one line the first line should start at the left margin, this is achieved by inserting `\fl` (full left) at the start of

the line. The use of the alignment parameter `&` is not necessary unless some secondary alignment is needed.

$$\alpha + 2\gamma^2 = \cos \theta + \frac{XY \sin \theta}{X + Y \cos \theta} + \frac{XY \sin \theta}{X - Y \cos \theta} + \left( \frac{XY \sin \theta}{X + Y \cos \theta} \right)^2 + \left( \frac{XY \sin \theta}{X - Y \cos \theta} \right)^2. \quad (\text{G.7})$$

The plain `TeX` command `\eqalign` can be used within an `equation` environment to obtain a multiline equation with a single centred number, for example

$$\begin{aligned} \alpha + \beta &= \gamma^2 \\ \alpha^2 + 2\gamma + \cos \theta &= \delta. \end{aligned} \quad (\text{G.8})$$

### Appendix G.9. Miscellaneous

Exponential expressions, especially those containing subscripts or superscripts, are clearer if the notation `exp(...)` is used, except for simple examples. For instance `exp[i(kx - \omega t)]` and `exp(z^2)` are preferred to `e^{i(kx - \omega t)}` and `e^{z^2}`, but `e^x` is acceptable.

The square root sign  $\sqrt{\phantom{x}}$  should only be used with relatively simple expressions, e.g.  $\sqrt{2}$  and  $\sqrt{a^2 + b^2}$ ; in other cases the power  $1/2$  should be used; for example,  $[(x^2 + y^2)/xy(x - y)]^{1/2}$ .

It is important to distinguish between  $\ln = \log_e$  and  $\lg = \log_{10}$ . Braces, brackets and parentheses should be used in the following order: `{[( )]}`.

Decimal fractions should always be preceded by a zero: for example `0.123` **not** `.123`. For long numbers use thin spaces after every third character away from the position of the decimal point, unless this leaves a single separated character: e.g. `60 000`, `0.123 456 78` but `4321` and `0.7325`.

Equations should be followed by a full stop (periods) when at the end of a sentence.

### Appendix G.10. Equation numbering and layout in `iopart.cls`

If the command `\eqnobysec` is included in the preamble, equation numbering by section is obtained, e.g. (2.1), (2.2), etc. Refer to equations in the text using the equation number in parentheses. It is not normally necessary to include the word `equation` before the number; and abbreviations such as `eqn` or `eq` should not be used. In `iopart.cls`, there are alternatives to the standard `\ref` command that you might find useful—see table G2.

Sometimes it is useful to number equations as parts of the same basic equation. This can be accomplished in `iopart.cls` by inserting the commands `\numparts` before the equations concerned and `\endnumparts` when reverting to the normal sequential numbering. For example using `\numparts \begin{eqnarray} ... \end{eqnarray} \endnumparts`:

$$T_{11} = (1 + P_e)I_{\uparrow\uparrow} - (1 - P_e)I_{\uparrow\downarrow}, \quad (7.9a)$$

$$T_{-1-1} = (1 + P_e)I_{\downarrow\downarrow} - (1 - P_e)I_{\uparrow\downarrow}, \quad (7.9b)$$

$$S_{11} = (3 + P_e)I_{\downarrow\uparrow} - (3 - P_e)I_{\uparrow\uparrow}, \quad (7.9c)$$

$$S_{-1-1} = (3 + P_e)I_{\uparrow\downarrow} - (3 - P_e)I_{\downarrow\downarrow}. \quad (7.9d)$$

Equation labels within the `\eqnarray` environment will be referenced as subequations, e.g. (7.9a).

#### *Appendix G.11. Miscellaneous extra commands for displayed equations*

The `\cases` command has been amended slightly in `iopart.cls` to increase the space between the equation and the condition. Equation (7.10) demonstrates simply the output from the `\cases` command

$$X = \begin{cases} 1 & \text{for } x \geq 0 \\ -1 & \text{for } x < 0 \end{cases} \quad (7.10)$$

To obtain text style fractions within displayed maths the command `\case{#1}{#2}` can be used instead of the usual `\frac{#1}{#2}` command or `{#1 \over #2}`.

When two or more short equations are on the same line they should be separated by a ‘qquad space’ (`\qquad`), rather than `\quad` or any combination of `\,`, `\>`, `\;` and `\ .`

#### *Appendix G.12. Preprint references*

Preprints may be referenced but if the article concerned has been published in a peer-reviewed journal, that reference should take precedence. If only a preprint reference can be given, it is helpful to include the article title. Examples are:

- [1] Neilson D and Choptuik M 2000 *Class. Quantum Grav.* **17** 761 (arXiv:gr-qc/9812053)
- [2] Sundu H, Azizi K, Süngü J Y and Yinelek N 2013 Properties of  $D_{s2}^*(2573)$  charmed-strange tensor meson arXiv:1307.6058

#### *Appendix G.13. Cross-referencing*

`label` may contain letters, numbers or punctuation characters but must not contain spaces or commas. It is also recommended that the underscore character `_` is not used in cross referencing.

Thus labels of the form `eq:partial`, `fig:run1`, `eq:dy`, etc, may be used. When several references occur together in the text `\cite` may be used with multiple labels with commas but no spaces separating them; the output will be the numbers within a single pair of square brackets with a comma and a thin space separating the numbers. Thus `\cite{label1,label2,label4}` would give [1,2,4]. Note that no attempt is made by the style file to sort the labels and no shortening of groups of consecutive numbers is done. Authors should therefore either try to use multiple labels in the correct order, or use a package such as `cite.sty` that reorders labels correctly.

**Table G2.** Alternatives to the normal references command `\ref` available in `iopart.cls`, and the text generated by them. Note it is not normally necessary to include the word equation before an equation number except where the number starts a sentence. The versions producing an initial capital should only be used at the start of sentences.

Reference	Text produced
<code>\eref{&lt;label&gt;}</code>	(<num>)
<code>\Eref{&lt;label&gt;}</code>	Equation (<num>)
<code>\fref{&lt;label&gt;}</code>	figure <num>
<code>\Fref{&lt;label&gt;}</code>	Figure <num>
<code>\sref{&lt;label&gt;}</code>	section <num>
<code>\Sref{&lt;label&gt;}</code>	Section <num>
<code>\tref{&lt;label&gt;}</code>	table <num>
<code>\Tref{&lt;label&gt;}</code>	Table <num>

#### *Appendix G.14. Tables and table captions*

Tables are numbered serially and referred to in the text by number (table 1, etc, **not** tab. 1). Each table should have an explanatory caption which should be as concise as possible. If a table is divided into parts these should be labelled (*a*), (*b*), (*c*), etc but there should be only one caption for the whole table, not separate ones for each part.

The standard form for a table in `iopart.cls` is:

```
\begin{table}
\caption{\label{label}Table caption.}
\begin{indented}
\item[]\begin{tabular}{@{}llll}
\br
Head 1&Head 2&Head 3&Head 4\\
\mr
1.1&1.2&1.3&1.4\\
2.1&2.2&2.3&2.4\\
\br
\end{tabular}
\end{indented}
\end{table}
```

- (i) The caption comes before the table. It should have a period at the end.
- (ii) Tables are normally set in a smaller type than the text. The normal style is for tables to be indented. This is accomplished by using `\begin{indented}` ... `\end{indented}` and putting `\item[]` before the start of the tabular environment. Omit these commands for any tables which will not fit on the page when indented.
- (iii) The default is for columns to be aligned left and adding `@{}` omits the extra space before the first column.
- (iv) Tables have only horizontal rules and no vertical ones. The rules at the top and bottom are thicker than internal rules and are set with `\br` (bold rule). The rule



**Table G3.** A simple example produced using the standard table commands and `\lineup` to assist in aligning columns on the decimal point. The width of the table and rules is set automatically by the preamble.

<i>A</i>	<i>B</i>	<i>C</i>	<i>D</i>	<i>E</i>	<i>F</i>	<i>G</i>
23.5	60	0.53	-20.2	-0.22	1.7	14.5
39.7	-60	0.74	-51.9	-0.208	47.2	146
123.7	0	0.75	-57.2	—	—	—
3241.56	60	0.60	-48.1	-0.29	41	15

separating the headings from the entries is set with `\mr` (medium rule). These are special `iopart.cls` commands.

- (v) Numbers in columns should be aligned on the decimal point; to help do this a control sequence `\lineup` has been defined in `iopart.cls` which sets `\0` equal to a space the size of a digit, `\m` to be a space the width of a minus sign, and `\-` to be a left overlapping minus sign. `\-` is for use in text mode while the other two commands may be used in maths or text. (`\lineup` should only be used within a table environment after the caption so that `\-` has its normal meaning elsewhere.) See table G3 for an example of a table where `\lineup` has been used.

#### Appendix G.15. Simplified coding and extra features for tables

The basic coding format can be simplified using extra commands provided in the `iopart` class file. The commands up to and including the start of the tabular environment can be replaced by

```
\Table{\label{label}Table caption}
```

and this also activates the definitions within `\lineup`. The final three lines can also be reduced to `\endTable` or `\endtab`. Similarly for a table which does not fit on the page when indented `\fulltable{\label{label}caption} ... \endfulltable` can be used. L<sup>A</sup>T<sub>E</sub>X optional positional parameters can, if desired, be added after `\Table{\label{label}caption}` and `\fulltable{\label{label}caption}`.

`\centre{#1}{#2}` can be used to centre a heading `#2` over `#1` columns and `\crule{#1}` puts a rule across `#1` columns. A negative space `\ns` is usually useful to reduce the space between a centred heading and a centred rule. `\ns` should occur immediately after the `\\` of the row containing the centred heading (see code for table G4). A small space can be inserted between rows of the table with `\ms` and a half line space with `\bs` (both must follow a `\\` but should not have a `\\` following them).

Units should not normally be given within the body of a table but given in brackets following the column heading; however, they can be included in the caption for long column headings or complicated units. Where possible tables should not be broken over pages. If a table has related notes these should appear directly below

**Table G4.** A table with headings spanning two columns and containing notes. To improve the visual effect a negative skip (`\ns`) has been put in between the lines of the headings. Commands set-up by `\lineup` are used to aid alignment in columns. `\lineup` is defined within the `\Table` definition.

Nucleus	Thickness (mg cm <sup>-2</sup> )	Composition	Separation energies	
			$\gamma$ , n (MeV)	$\gamma$ , 2n (MeV)
<sup>181</sup> Ta	19.3 ± 0.1 <sup>a</sup>	Natural	7.6	14.2
<sup>208</sup> Pb	3.8 ± 0.8 <sup>b</sup>	99% enriched	7.4	14.1
<sup>209</sup> Bi	2.86 ± 0.01 <sup>b</sup>	Natural	7.5	14.4

<sup>a</sup> Self-supporting.

<sup>b</sup> Deposited over Al backing.

the table rather than at the bottom of the page. Notes can be designated with footnote symbols (preferable when there are only a few notes) or superscripted small roman letters. The notes are set to the same width as the table and in normal tables follow after `\end{tabular}`, each note preceded by `\item[]`. For a full width table `\noindent` should precede the note rather than `\item[]`. To simplify the coding `\tabnotes` can, if desired, replace `\end{tabular}` and `\endtabnotes` replaces `\end{indented}\end{table}`.

#### *Appendix G.16. Inclusion of graphics files*

Below each figure should be a brief caption describing it and, if necessary, interpreting the various lines and symbols on the figure. As much lettering as possible should be removed from the figure itself and included in the caption. If a figure has parts, these should be labelled (a), (b), (c), etc and all parts should be described within a single caption. Table G5 gives the definitions for describing symbols and lines often used within figure captions (more symbols are available when using the optional packages loading the AMS extension fonts).

#### *Appendix G.17. Supplementary Data*

Supplementary data enhancements typically consist of video clips, animations or data files, tables of extra information or extra figures. See guidelines on supplementary data file formats, ‘Author Guidelines’ link at <http://authors.iop.org>.

Software, in the form of input scripts for mathematical packages (such as Mathematica notebook files), or source code that can be interpreted or compiled (such as Python scripts or Fortran or C programs), or executable files, can sometimes be accepted as supplementary data, but the journal may ask you for assurances about the software and distribute them from the article web page only subject to a disclaimer. Contact the journal in the first instance if you want to submit software.

**Table G5.** Control sequences to describe lines and symbols in figure captions.

Control sequence	Output	Control sequence	Output
<code>\dotted</code>	.....	<code>\opencircle</code>	○
<code>\dashed</code>	----	<code>\opentriangle</code>	△
<code>\broken</code>	---	<code>\opentriangledown</code>	▽
<code>\longbroken</code>	— — —	<code>\fullsquare</code>	■
<code>\chain</code>	— . —	<code>\opensquare</code>	□
<code>\dashddot</code>	— . . —	<code>\fullcircle</code>	●
<code>\full</code>	——	<code>\opendiamond</code>	◇

**Table G6.** Macros defined within `iopart.cls` for use with figures and tables.

Macro name	Purpose
<code>\Figures</code>	Heading for list of figure captions
<code>\Figure{#1}</code>	Figure caption
<code>\Tables</code>	Heading for tables and table captions
<code>\Table{#1}</code>	Table caption
<code>\fulltable{#1}</code>	Table caption for full width table
<code>\endTable</code>	End of table created with <code>\Table</code>
<code>\endfulltab</code>	End of table created with <code>\fulltable</code>
<code>\endtab</code>	End of table
<code>\br</code>	Bold rule for tables
<code>\mr</code>	Medium rule for tables
<code>\ns</code>	Small negative space for use in table
<code>\centre{#1}{#2}</code>	Centre heading over columns
<code>\crule{#1}</code>	Centre rule over columns
<code>\lineup</code>	Set macros for alignment in columns
<code>\m</code>	Space equal to width of minus sign
<code>\-</code>	Left overhanging minus sign
<code>\0</code>	Space equal to width of a digit

## Appendix H. Integer lattices literature

There are many reasons why one needs to compute an “orbit Jacobian matrix” Hill determinant  $|\text{Det } \mathcal{J}|$ , in fields ranging from number theory to engineering, and many methods to accomplish that:

- discretizations of Helmholtz [66, 78, 146] and screened Poisson (also known as Klein–Gordon or Yukawa) [70, 91, 109, 110] equations

- Green’s functions on integer lattices [6, 12, 24, 35, 37, 43, 79, 88, 106, 107, 128–130, 151, 158, 161, 167, 168, 176, 202, 220]

- Gaussian model [82, 122, 157, 196]

- linearized Hartree-Fock equation on finite lattices [132]

- random walks, resistor networks [13, 27, 50, 51, 71, 92, 100, 112, 133, 187, 205, 210, 222]

- tight-binding Hamiltonians [50, 51, 76]

- quasilattices [32, 81]

- circulant tensor systems [35, 37, 163, 188, 190, 224]

- Ising model [22, 103, 104, 111, 113, 116–118, 144, 153, 159, 173, 181, 223],

- Ising model transfer matrices [174, 223]

- lattice field theory [120, 162, 166, 171, 192, 199, 200, 215]

- modular transformations [36, 229]

- lattice string theory [86, 175]

- spatiotemporal stability in coupled map lattices [5, 83, 227]

- Van Vleck determinant, Laplace operator spectrum, semiclassical Gaussian path integrals [141, 142, 209, 211]

- Hill determinant [28, 154, 211]; discrete Hill’s formula and the Hill discriminant [208]

- Lindstedt-Poincaré technique [212–214]

- heat kernel [38, 73, 77, 121, 126, 161, 176, 225]

- chronotopic models [185]

- lattice points enumeration [17, 19, 23, 63]

- primitive parallelogram [14, 33, 172, 216]

- difference equations [62, 80, 204]

- digital signal processing [74, 147, 221]

- generating functions, Z-transforms [77, 219]

- integer-point transform [23]

- graph Laplacians [44, 89, 150, 186]

- graph zeta functions [9, 16, 21, 30, 45–47, 64, 73, 95, 101, 108, 114, 135, 138, 186, 189, 193, 195, 201, 206, 207, 228]

- zeta functions for multi-dimensional shifts [15, 148, 149, 164]

- zeta functions on discrete tori [38, 39, 225]

## Appendix I. Sidney exercises

### (i) Hénon temporal lattice.

1-dimensional temporal Hénon lattice (see ChaosBook [Example 3.5](#)) is given by a 3-term recurrence

$$\phi_{n+1} + a\phi_n^2 - b\phi_{n-1} = 1. \quad (9.1)$$

The parameter  $a$  quantifies the “stretching” and  $b$  quantifies the “contraction”.

The single Hénon map is nice because the system is nonlinear, but has binary dynamics.

Implement the variational searches for periodic states in Matt’s [OrbitHunter](#), find all periodic lattice states up to  $n = 6$ .

(a)  $a = 1.4$   $b = 0.3$ , compare with ChaosBook [Table 34.3](#).

(b) For  $b = -1$  the system is time-reversible or ‘Hamiltonian’, see ChaosBook [Example 8.5](#).

Note also [sect A10.3](#) *Hénon map symmetries* and [Exer. 7.2](#) *Inverse iteration method*.

The deviation of an approximate trajectory from the 3-term recurrence is

$$v_n = \phi_{n+1} - (1 - a\phi_n^2 + b\phi_{n-1}) \quad (9.2)$$

In classical mechanics force is the gradient of potential, which Biham-Wenzel [\[25\]](#) construct as a cubic potential

$$V_n = \phi_n(\phi_{n+1} - b\phi_{n-1} - 1) + a\phi_n^3 \quad (9.3)$$

With the cubic potential of a single Hénon map we can start to look for orbits with initial conditions of two points (two point recurrence relation requires this) and make the guess as we iterate in time. A particular guess is to choose a sequence of maxima/minima of the potential.

Compare with XXX

### Solution ?? - Hénon temporal lattice.

(a) *It’s just the roots of a quadratic equation, with blah blah* (Sidney Williams)

## Appendix J. Sidney blog on matters spatiotemporal

**2020-05-20 Predrag** to

Sidney V. Williams

swilliams425@gatech.edu and sidneywilliams1231@gmail.com

cell 208 310 3866

You can write up your narrative in this file. Can clip & paste anything from above sections you want to discuss, that saves you LaTeXing time.

**2020-08-22 Predrag** First task:

Start reading section 1.1 *Bernoulli map*. Everything up to section 1.2 *Temporal Bernuolli* you know from the ChaosBook course.

New stuff starts here. See how much you understand. Write your study notes up here, ask questions - this is your personal blog.

You refer to an equation like this: (10);

to figure like this: figure 2;

to table like this: table 1;

to a reference like this: Gutkin and Osipov [99] (*GutOsi15* refers to an article listed in *../bibtex/siminos.bib*).

and to external link like this: “For great wallpapers, see overheads in Engel’s course.”

**2020-08-22 Predrag** An example of referring to the main text: Why do you write *orbit Jacobian matrix* (15) as a partial derivative, when you already know  $\mathcal{J}$ , see (13)?

**2020-08-24 Sidney** Started reading from the beginning as that only adds an additional 4 pages, and it would be beneficial to review.

General Notes: Showing what modern chaos calculations look like. The spatiotemporal cat is the arbitrary dimension generalization of the 1-D Bernoulli map.

(mod 1) subtracts the integer part of  $s\phi_t$ , this keeps  $\phi_{t+1}$  within the unit interval (group theoretic analogue?). Also partitions the state-space into  $s$  sub-intervals.

**2020-08-24 Predrag** The group theory here compatifying translations on (infinite) line  $\phi \in (-\infty, \infty)$  to translations on (compact) circle  $\phi \in [0, 2\pi)$ .

**2020-08-24 Sidney** Reminder to self: review the symbolic dynamics, and binary operations from chapter 14 of Chaosbook The unit interval is partitioned into  $s^n$  subintervals, each with one unstable period- $n$  point, except the rightmost fixed point is the same as the fixed point at the origin. So there are  $s^n - 1$  total period- $n$  periodic points.  $\sigma$  in (10) is a cyclic permutation that translates forward in time the lattice state by one site. Inverse  $\sigma$  because the second term is always one step behind the first term and an inverse  $\sigma$  moves the state back one.

Questions 1. I’ve pretty much never done modular arithmetic before, I understand

(2) in the idea that the circle map wraps in on itself and contributes the value of its slope after one go around, but I am unsure on how to use the modular arithmetic to do that, should I look into that?

**2020-08-24 Predrag** As I do not know what “modular arithmetic” is, don’t worry about :)

**2020-08-25 Sidney** General Notes

(8) appears to be a vector of a periodic (or relative periodic orbit) through the Bernoulli map. Review Multishooting. Total number of periodic points of period  $n$  is  $N_n = s^n - 1$  but it also equals the magnitude of the determinant of the orbit Jacobian matrix. (got to page 7)

Q1 Is (??) the evolution function  $f^t(y)$  that was referenced throughout ChaosBook?

Q2 What exactly is meant by a “lattice”?

**2020-08-24 Predrag** .

A1 The whole point of the paper is that ChaosBook is obsolete - in the new formulation, there is no ‘time’ evolution, no time trajectory  $f^t(y)$ , there are only sets of fields that live on lattice points that satisfy recurrence relations. Eq. (??) is *orbit Jacobian matrix*, the stability of a lattice state, to be related to stability forward in time in section 5. This is a revolution: there is no more time, there is only spacetime.

A2 Temporal lattice  $\mathbb{Z}$  is defined in (8). Spacetime integer lattice  $\mathbb{Z}^2$ , (or more generally  $\mathbb{Z}^d$ ) in (73), (74). When you get to it, a 2-dimensional *Bravais lattice*  $\Lambda$  is defined in (82).

If this is unclear, read up on integer lattices, give your own precise definition.

**2020-08-26 Sidney** Point Lattice (integer lattice is a special case of point lattice) notes from **Wolfram**: ”A point lattice is a regularly spaced array of points.” The integer lattice is where all of these points are integers. I will look at the Barvinok lecture tomorrow, I have to finish moving to a different house today. (Stayed on page 7)

Q3 Please correct me if I am wrong, but a lattice seems to be a collection of points where are all regularly spaced, so does ”regularly” mean that it is controlled by a deterministic law? If this is the case, the  $\phi_n$  states in a periodic orbit can be grouped as a lattice and ordered by location along the periodic orbit, then the associated ”winding” number  $m_t$  can be grouped in its own lattice, which in this case is an integer lattice. What is the ”regular” spacing for the winding numbers? Have missed the point?

A3 Wolfram is right. When you have a discrete time map, time takes integer values  $t = \dots, -1, 0, 1, 2, \dots$ . That is called 1-dimensional integer lattice  $\mathbb{Z}$ . Once you are in  $d = 2$  or higher, the name makes sense, as you can visualize

$\mathbb{Z}^2$  as a ‘lattice’. It is regular, because all spacings between neighboring points are 1. There is nothing ‘deterministic’ about this, it just says that time takes its values on integers, rather than on a continuum.

There is only one lattice, but on each lattice site there is a real-valued field  $\phi_t$  and the integer valued ‘source’  $m_t$ .

**2020-08-27 Sidney** Thank you for A1, that makes complete sense now. Calculated the orbit Jacobian matrix using equation (??), matched with the paper, yay. Orbit Jacobian matrix maps the basis vectors of the unit hyper-cube into a fundamental parallelepiped basis vectors, each of which is given by a column in the orbit Jacobian matrix.  $|Det(s/\sigma)| = s^n$  because  $\sigma$  and its inverse are both unitary matrices, and if you multiply every row of an  $[n \times n]$  matrix, the determinant is multiplied by the constant raised to the power n. Periodicity  $\sigma^n = 1$  accounts for  $\bar{0}$  and  $\overline{s-1}$  fixed points being a single periodic point. (got to page 9)

Q4 I was trying to calculate the orbit Jacobian matrix using the  $\sigma$  matrix, but the delta function equation (11) for  $\sigma$  doesn’t seem to work for the Bernoulli map, I know that  $\sigma_{2,1} = 1$  and  $\sigma_{1,2} = 1$  which works with the delta function definition. However,  $\sigma_{2,1} = \delta_{3,1}$  from (11), which should equal zero. Other than just the idea of being cyclic, I don’t know why it yields one instead of zero, what am I missing?

A4 Work it out  $\sigma$  matrices for  $n = 1, 2, 3, \dots$ . It will start making sense.

Q5 So, does “lattice state” mean the set of all points (field of all points?) which running through the Bernoulli map requires the specific winding number at that lattice site?

A5 Interesting, grad students too seem to confuse coordinates (for example,  $(x, t) = (3.74, -0.02)$  in continuum,  $(n, t) = (7, -6)$  on a discretized space) and the fields  $\phi(n, t)$ . Physical “state” refers to value of field  $\phi$  over every  $(n, t)$  - is the grass high or low? rather than the coordinates of spacetime.

How would you state this precisely if you were trying to explain this paper to another student?

**2020-08-30 Sidney**

A5.1 Sidney: “ $\Phi_M$  is the set of all values the field  $\phi_z$  takes over the set of coordinates  $M$ . ”

A5.2 Predrag: Please reread 2nd paragraph of section 1.2 and explain what is wrong with your answer A5.1

Notes: For an n-periodic lattice state  $\Phi_M$  the Jacobian matrix is now a function of a  $[d \times d]$  matrix  $J$ , so the formula for the number of periodic points of period n (number of lattice states of period n) is now  $|\det(1 - J_M)|$  where  $J_M = \prod_{t=1}^n J_t$  where  $J_t$  is the one-step Jacobian matrix which is assumed to vary in time.

Note to self: look back over the topological zeta function, specifically try to understand



derivation of:

$$\frac{1}{\zeta_{top}(z)} = \exp \left( - \sum_{n=1}^{\infty} \frac{z^n}{n} N_n \right)$$

(got to page 12)

Predrag: [\(click here\)](#)

Q6 Is “there are  $s$  fundamental lattice states, and every other lattice state is built from their concatenations and repeats” is simply a restatement of the fact that the Bernoulli map is a full shift?

A6 For Bernoulli, yes. But search for word ‘fundamental’ in ChaosBook chapter *Counting*. For example, ‘We refer to the set of all non-self-intersecting loops  $\{t_{p_1}, t_{p_2}, \dots, t_{p_f}\}$  as the *fundamental cycles*’. Write up here a more nuanced statement of ‘fundamental’ cycles might be (I do not have firm grip on this either...).

Q7 Is (35) a result of expanding in a Taylor the result of the derivative (and product of  $1/\zeta_{top}$  and  $z$ )? Because the topological zeta function of the Bernoulli map is a closed form function, not an infinite sum.

**2020-08-31 Sidney** Via a finite difference method, (9) can be viewed as a first order ODE dynamical system. Back-substituted with (10) to show that with  $\Delta t = 1$  the velocity field does satisfy the diffeq (39). The Bernoulli system can be recast into a discretized ODE whose global linear stability is described by the orbit Jacobian matrix. (Stayed on page 12))

**2020-09-01 Sidney** Started reading section 2 *A kicked rotor*.

(40) and (41) describe the motion of a rotor being subjected to periodic momentum pulses. The mod is present for the  $q$  equation to make sure that the angle varies from 0 to  $2\pi$ . As in the Bernoulli map case, here mod is also added to the momentum equation to keep it bounded to a unit square. Cat maps with the stretching parameter  $s$  are the same up to a similarity transformation. An automorphism is an isomorphism of a system of objects onto itself. An isomorphism is a map that preserves sets and relations among elements.

Q8 Do the kicked rotor equations with Hooke’s law force, and bounded momentum (mod 1 added to (41)) only take the form of (42) if  $K$  is an integer?

A8 The text states: “The (mod 1) added to (41) makes the map a discontinuous ‘sawtooth,’ unless  $K$  is an integer.” How would you make that clearer?

Q9 How does (42) have a state space which is a 2-torus? I am having a hard time visualizing how this came about.

A9 Do you understand how (mod 1) operation turns unbounded stretch (2) into a circle map (3)? Circle map is 1-torus. If both  $(q_t, p_t) \in (0, 1] \times (0, 1]$  are wrapped into unit circles, the phase space  $(q_t, p_t)$  is not an infinite 2-dimensional plane, but a compact, doubly periodic unit square with opposite edges glued together, i.e., 2-torus.

**2020-09-03 Sidney** I was typing my description into "summary" textbox above the commit to master button. Obviously I was incorrect, I'll try to type in the "description" for this commit.

**2020-09-02 Predrag** "Tripping Through Fields" showed up :)

**2020-09-03 Sidney**

A5.3 Sidney: I'm not actually quite sure what's wrong with my given definition. From your answer A5 it seems that  $\mathbf{M}$  is a set of coordinates (the location of the blade of grass) and  $\Phi_{\mathbf{M}}$  is the value at that coordinate (the height of the grass at that point). Perhaps I forgot that these lattice states are for periodic orbits, so I forgot the second coordinate (period of length  $n$ ).

A5.4 Predrag: The textbook inhomogeneous *Helmoltz equation* is an elliptical equation of form

$$(\square + k^2) \phi(z) = -m(z), \quad z \in \mathbb{R}^d, \quad (10.1)$$

where the *field*  $\phi(z)$  is a  $C^2$  functions of *coordinates*  $z$ , and  $m(z)$  are *sources*. For example, charge density is a *source* of electrostatic *field*.

Suppose you are so poor, your computer lacks infinite memory, you only have miserly only 10 Tb, so you cannot store the infinitely many values that *coordinates*  $z \in \mathbb{R}^d$  take. So what do you do?

Perhaps a peak at ChaosBook [A24.1 Lattice derivatives](#) can serve as an inspiration. And once you have done what a person must do, your Helmholtz equation (hopefully) has the form of (71). What is a *field*, a *source*, a *coordinate* then?

**2020-09-03 Sidney**

A8.1 The sawtooth statement made sense, what made it unclear for me was the second sentence which started with "in this case" it was (again for me, I might not have been paying enough attention) ambiguous, I didn't know if it was talking about the integer case or the sawtooth case.

A8.2 Predrag: thanks, I rephrased that sentence.

A9.1 I understand, your explanation makes sense, thank you :).

Notes: The discrete time Hamiltonian system induces forward in time evolution on the 2-torus phase space. The orbit Jacobian matrix can take many different forms depending on the map. Despite this the Hill determinant can still count the number of periodic lattice states. (got to page [page 19](#))

**2020-09-05 Sidney**

A5.5 If I was so unlucky to only have 10Tb of memory, I would take a finite interval of points  $z$  that I was interested in, and discretize them (evenly, or unevenly) and then evaluate the field (that was probably the wrong wording) at a finite set of points, either of particular interest within the interval, or closely spaced enough so that the values were representative of the values the field took over a continuum. I think that a coordinate is a point in state space specified by

specific values of state variables (position, time, momentum etc.). To try to answer source, and field, I'll be thinking of an electric charge, a source is what generates the medium by which other sources are effected, and the field is the medium which acts upon other sources.

- A5.6 I did look at Chaosbook [A24.1 Lattice derivatives](#), but it didn't seem to address quite the fundamental confusion I seem to be facing. I'm relatively confident in my coordinate definition, but not at all in my source, and field definition.

**2020-09-05 Predrag .**

- A5.7 Expression 'state space'  $\mathcal{M}$  refers to 'states': cats, dancers, i.e., 'fields'  $\Phi$  and their names  $M$ . 'Coordinates' refer to markings on the floor that they stand on.

Does reading section [3.7 Lattice states](#) now helps in distinguish a skater from the skating ring's ice? I rewrote it for your pleasure :)

- A5.7 Re. the fundamental confusion of reading [A24.1 Lattice derivatives](#): If you mark every inch on the floor, this is 'discretization'. But the floor is still a floor, no?

**2020-09-05 Sidney**

- A5.8 I read the pink bits of section [3.7 Lattice states](#) (as I assume that was the parts that you rewrote specially). From it I (think) I understand. We're looking at two coordinates for most of the Bernoulli and cat map stuff: a spatial one, and a temporal one, the maps only effect the temporal placement, but effect it differently depending on where the point was in space when the map acted on it, because the field takes a different value at every point in space (and time). So the coordinates are the field point placement in time and space. The field is the value that is assigned to every lattice point.  $M$  keeps getting referred to as an alphabet, so that makes me think that it is similar (perhaps the multidimensional generalization) to the "alphabet" which was used to partition state space in the 1D maps of Chaosbook, such as 0 for the left half of the interval and 1 for the right, and then further partitioning the more the map is applied. Is that close at least?

**2020-09-05 Predrag .**

- A5.9 Getting hotter. Look at [\(4\)](#) and [\(47\)](#);  $\phi_t$  and  $m_t$  are the same kind of a beast,  $m_t$  is just the integer part of the "stretched" field in [\(2\)](#). In this particular, linear map setting, this integer does double duty, as a letter of an "alphabet". It cannot possibly be a "coordinate", it like saying that a dancer's head is "floor."
- A5.10 In temporal lattice formulation no "map is applied." That is the brilliance of the global spatiotemporal reformulation: there is no stepping forward in time, so there is no map - the only thing that exists is the global fixed point condition that has to be satisfied by field values everywhere on the lattice, simultaneously.

Time is dead.

**2020-09-08 Sidney**

Q11 So the temporal cat / spatiotemporal cat equations are moving around points in the lattice instead of through time?

Q12 Is something of the form of (13) an example of the “global fixed point condition”?

**2020-09-14 Predrag .**

A11 An equation does not have to be “moving around” anything: think of a quadratic equation  $x^2 + bx + c = 0$ . Does it “move” anything? No. It’s a condition that a single “field”  $x$  has to satisfy, and the solution is a root of that equation. The temporal cat / spatiotemporal cat equations are “equations” in the same sense, [bunch of terms involving  $\phi_z$ ]=0.

A12 Yes.

**2020-09-09 Sidney** Notes: Equations such as (47) can be solved using similar methods to linear odes: guessing a solution of the form  $\Lambda^t$  and finding the characteristic equation. Then assuming all terms are site independent because the difference of any two solutions of (47) solve its homogeneous counterpart (57). Got to page 20.

Notes: Topological zeta functions count prime orbits, i.e. time invariant sets of equivalent lattice states related by cyclic permutations. The “search for zeros” (49) is the “fixed point condition.” Which is a global statement which enforces (47) at every point in the lattice. Got to page 23

**2020-09-13 Sidney** The temporal cat is a special case of the spatiotemporal cat, defined on a one-dimensional lattice  $\mathbb{Z}^1$ . In this case the associated topological zeta function is known in a closed, analytic form.

*Coupled map lattices:* Starts with a review of finite difference methods for PDEs. The d dimensions in the lattice are d-1 spatial lattice points and 1 temporal one. The PDE is reduced to dynamics of a coupled map lattice, with a set of continuous fields on each site.

A5.11 I have experience with finite difference methods for solving a discretized form of a PDE, but I’m having a hard time visualizing the idea of having a discrete coordinate system in d different directions, but with a continuous field on each site. This may be valuable as it is a specific statement of where I’m getting stuck.

Q13 My current understanding is that at each point in the d-dimensional integer lattice (“point” as in a lattice node with d specified coordinates), but at each point (site) there is a continuous field. What is this field continuous over? It’s at one point in a discrete coordinate system. And why is there a continuum at each point? And finally, I assume that these continuous fields are the values of the function being solved for at that point, however, shouldn’t that just be a single value? Not a field? I’m sorry if this is a rather silly question, but

I'll keep thinking about it and I'll make a note if my understanding (or lack thereof) changes.

A13 Predrag: In figure 1 field  $x_t$  or  $\phi_t$  and  $f(\phi_t)$  on the discrete site  $t$  run over continuous values. For example, at temporal lattice site  $t = 7$  the field value is  $\phi_7 = 0.374569263952942 \dots$ . OK now?

Q13.1 Slight update, it seems that the field is the state of the system and at each discretized point there is a map acting on the state, although that conflicts with the notion that time is dead, so I'm probably still misunderstanding.

A13.1 Predrag: Yes.

Thinking of this as a spring mattress. Often starts out with chaotic on-site dynamics weakly coupled to neighboring sites. In this paper one sets the lattice spacing constant equal to one. Diffusive coupled map lattices introduced by Kaneko:

$$\phi_{n,t+1} = g(\phi_{n,t}) + \epsilon [g(\phi_{n-1,t}) - 2g(\phi_{n,t}) + g(\phi_{n+1,t})],$$

where each individual spatial site's dynamical system  $g(x)$  is a 1D map, coupled to the nearest neighbors by the discretized second order *spatial* derivative. The form of time-step map  $g(\phi_{n,t})$  is the same for all time i.e. invariant under the group of discrete time translations. Spatial stability analysis can be combined with temporal stability analysis, with orbit weights depending exponentially both on the space and the time variables:  $t_p \propto e^{-LT\lambda_p}$ .  $\sigma_i$  translates the field by one lattice spacing in the  $i^{th}$  direction.

Q14 What is a lattice period?

A14 Predrag: Does the paragraph above (79) answer your question? I would like to refer to the *set* of numbers  $\{\ell_1, \ell_2, \dots, \ell_d\}$  as the *period* of lattice  $\Lambda$ . Would that be confusing?

Q15 Is  $z$  in the definition of a lattice state both a temporal and a spatial index? So equivalent to both  $n$  and  $t$ ?

A15 Predrag: after (74) I write “a 1-dimensional spatial lattice, with field  $\phi_{nt}$  (the angle of a kicked rotor (40) at instant  $t$ ) at spatiotemporal site  $z = (n, t) \in \mathbb{Z}^2$ .” Should this “ $z = (n, t) \in \mathbb{Z}^2$ ” be repeated elsewhere. If so, where?

Q16 Often a member of the alphabet can be a negative number, which I assume means that the state is taken out of unity in the negative direction.

A16 Do you understand figure 2 and figure 3?

The spatiotemporal cat has the point-group symmetries of the square lattice. A lattice state is a set of all field values  $\Phi = \{\phi_z\}$  over the  $d$ -dimensional lattice that satisfies the spatiotemporal cat equation, with all field values constrained between zero and one. A lattice state  $\Phi_\Lambda$  is a *periodic orbit* if it satisfies  $\Phi_\Lambda(z + R) = \Phi_\Lambda(z)$  for any discrete translation  $R = n_1 \mathbf{a}_1 + n_2 \mathbf{a}_2 \in \Lambda$ . Got to page 30.

**2020-09-14 Sidney**

A13.1 I think I'm OK now. I think what I was trying to visualize was a stack of an infinite number of values at each lattice point, which was confusing, but this makes sense.

A14.1 Unfortunately I don't think I quite understand. I understand the idea of the different directions, I understand treating  $\Phi_M(\phi_z)$  as a singular fixed point, but I do not understand  $\ell_i$ .

A15.1 I think that I lost that definition of  $z$  around (80), but I think that may have been a factor of how long it takes me personally to digest this material.

A16.1 After reading the descriptions and staring at it for awhile, I think that I do.

Q17 I tried a couple days back (Thursday or Friday I think, they all blend together) to log in to your bluejeans office. But it must have been one of the times that it had logged you off due to inactivity. There was also another person their I didn't recognize, and I didn't want to step on their toes if they were waiting for you to get back, so I logged off. So, when in general would good times to try hopping into your office?

**2020-09-16 Sidney** A Bravais lattice can be denoted  $\Lambda = [L \times T]_S$  where  $L$  is the spatial lattice period,  $T$  is the temporal lattice period,  $S$  imposes the tilt to the cell. Basis vectors for the Bravais cell can be written as:

$$\mathbf{a}_1 = \begin{pmatrix} L \\ 0 \end{pmatrix}, \quad \mathbf{a}_2 = \begin{pmatrix} S \\ T \end{pmatrix}$$

Q18 If something is written as  $850[3 \times 2]_0$  what is the numerical value? More importantly, how is it found? I know it has to do with the cyclic permutations of the prime blocks, but I'm not sure how to get a numerical value.

Got to page page 33

**2020-09-17 Sidney** For the Bernoulli map its stretching uniformity allows the use of combinatorial methods for lattice points. For temporal (not spatiotemporal) the number of periodic lattice states is the same as the volume of the fundamental parallelepiped, so the magnitude of the determinant of the orbit Jacobian matrix. The block  $M$  can be used as a 2D symbolic representation of the lattice system state. For a given admissible source block  $M$ , the periodic field can be computed by:

$$\phi_{i_1 j_1} = \sum_{i_2=0}^2 \sum_{j_2=0}^1 \mathbf{g}_{i_1 j_1, i_2 j_2} M_{i_2 j_2}$$

**2020-09-19 Predrag** Sorry, I've been a bit overwhelmed with lecture preparations, so I will not answer any of the questions quite yet. But I have rewritten the abstract, and the introduction to the paper, up to the start of section 1.1 *Bernoulli map*. Can you have a critical look at the new text, report here if something does not make sense to you?

**2020-09-19 Sidney**

Update I read through, and aside from some very minor grammar issues (forgetting a "have" after "we") it all makes sense.

**2020-09-20 Predrag** .

A15.2 I now added the  $z$  definition to (80), is that clearer?

2020-09-20 Sidney

A15.3 Yes, that makes it clearer.

$$-\sum_{r=1}^{\infty} \frac{1}{r} \text{tr} \hat{\mathbf{J}}_p^r = \text{tr} \left( -\sum_{r=1}^{\infty} \frac{1}{r} \hat{\mathbf{J}}_p^r \right) = \text{tr} \ln \left( \hat{\mathbf{1}}_1 - \hat{\mathbf{J}}_p^r \right) = \ln \det \left( \hat{\mathbf{1}}_1 - \hat{\mathbf{J}}_p^r \right)$$

I liked the text cut from the introduction on page 44, it made the idea of time's death more easily digestible. Finished main paper, will look at the appendices for math.

2020-09-22 Sidney

### Math Review Part 1

Updated 9/29/20

**Bravais Lattice** From [Wikipedia](#): A Bravais lattice is an infinite array of discrete points generated by a set of discrete translation operations described in two dimensional space by:

$$\mathbf{R} = n_1 \mathbf{a}_1 + n_2 \mathbf{a}_2$$

where  $n_i$  is any integer and  $\mathbf{a}_i$  is a primitive vector, each  $\mathbf{a}_i$  lie in different directions, but are not necessarily mutually perpendicular, but they do span the lattice. A fundamental aspect of a Bravais Lattice is that no matter the direction of the primitive vectors, the lattice will look exactly the same from each of the discrete lattice points when looking in that direction. A Lattice is a periodic array of points where each point is indistinguishable from any other point and has identical surroundings. A unit cell expands the idea of the infinite array of discrete points to include the space inbetween the points, if we are looking at a physical system this includes the atoms in this space. There are two main types of unit cells: primitive unit cells and non-primitive unit cells. A unit cell is the smallest group of atoms of a substance that has the overall symmetry of a crystal of that substance, and from which the entire lattice can be built up by the repetition in three dimensions. A primitive cell must contain only one lattice point, generally, lattice points that are shared by  $n$  cells are counted as  $\frac{1}{n}$  of the lattice points contained in each of those cells. So traditional primitive cells only contain points at their corners. The most obvious way to form a primitive cell is to use the basis vectors which the lattice is constructed from:

$$C(\mathbf{a}_1, \mathbf{a}_2) = \mathbf{r} = x_1 \mathbf{a}_1 + x_2 \mathbf{a}_2$$

$$0 \leq x_i \leq 1$$

The scaling factors are to ensure that lattice points are placed on the corners of the cell. In the current paper the primitive unit cell of a d-dimensional Bravais lattice tiles the spacetime.  $C(\mathbf{a}_1, \mathbf{a}_2)$  is the Bravais cell of a Bravais Lattice spanned by basis vectors  $(\mathbf{a}_1, \mathbf{a}_2)$ . A given Bravais Lattice  $\Lambda$  can be defined

by an infinity of Bravais cells. Hermite normal form: the analogue of reduced echelon form for matrices over  $\mathbb{Z}^n$ . Each family of Bravais cells contains a unique cell of the Hermite normal form, this can be written in terms of L, T, and S, where L, and T are respectively the spatial, and temporal lattice periods, S is the "tilt" of the cell. Hence the lattice can be defined as  $[L \times T]_S$ .

**Prime Bravais Lattices** It may be possible to tile a given Bravais lattice  $\Lambda$  by a finer lattice  $\Lambda_p$ . A Bravais lattice is prime if there is no finer Bravais cell, other than the unit volume  $[1 \times 1]_0$  that can tile it. If  $\det \Lambda$  is a prime number, then  $\Lambda$  is a *prime matrix*. If  $\Lambda$  is neither prime nor unimodular (a square integer matrix having determinant of  $\pm 1$ ), it is composit can can be decomposed into a product of two non-unimodular matrices  $\Lambda = PQ$ . In order to determine all prime lattices  $\Lambda_p$  that tiles a given Bravais lattice  $\Lambda$ :

$$\mathbf{a}_1 = k\mathbf{a}_1^p + l\mathbf{a}_2^p$$

$$\mathbf{a}_2 = m\mathbf{a}_1^p + n\mathbf{a}_2^p$$

observe that a prime tile  $(\mathbf{a}_1^p, \mathbf{a}_2^p)$  tiles the large tile only if the larger tile's width L is a multiple of  $L_p$ , and the height T is a multiple of  $T_p$ , and the two tile "tilts" satisfy:

$$\mathbf{a}_2 = m\mathbf{a}_1^p + \frac{T}{T_p}\mathbf{a}_2^p \rightarrow S = mL_p + \frac{T}{T_p}S_p$$

A prime lattice only tiles the given lattice if the area spanned by the two tilted basis vectors:

$$\mathbf{a}_2 \times \mathbf{a}_2^p = ST_p - TS_p$$

is a multiple of the prime tile area  $L_p T_p$ . A lattice state is a set of all field values  $\Phi = \{\phi_z\}$  over the d-dimensional lattice  $z \in \mathbb{Z}$  that satisfies the spatiotemporal cat equation. Lattice state  $\Phi$  is a periodic orbit if  $\Phi(z + R) = \Phi(z)$  for any discrete translation  $R = n_1\mathbf{a}_1 + n_2\mathbf{a}_2$ . If a given periodic orbit over lattice  $\Lambda$  is not periodic under translations  $R \in \Lambda_p$  for any sublattice  $\Lambda_p$  (except for  $\Lambda$  itself) we shall refer to it as a prime periodic orbit: a periodic orbit of smallest periodicity in all spacetime directions.

**Shift Operator** Shift operator is a matrix:  $\sigma_{ij} = \delta_{i+1,j}$ , this along with a periodic boundary condition assuming  $[n \times n]$  matrix  $\sigma^n = I$  yields

$$\begin{pmatrix} 0 & 1 & 0 & 0 \\ 0 & 0 & 1 & 0 \\ 0 & 0 & 0 & 1 \\ 1 & 0 & 0 & 0 \end{pmatrix}$$

A lattice state is a vector with all the values that the field takes on at each point on the lattice. Shift operator is cyclic permutation of a lattice state,



changes only the coordinates of the lattice state.

$$\sigma\Phi = \begin{bmatrix} \phi_1 \\ \phi_2 \\ \vdots \\ \phi_0 \end{bmatrix}$$

$\sigma^T = \sigma^{-1}$  cyclic permutation in the opposite direction, does not destroy anything, only changes the coordinates.

**Lattice Derivatives** Hypercube in d-dimensions with unit sides. Each side is described by a unit vector in direction  $\mu$   $\hat{n}_\mu \in \{\hat{n}_1, \hat{n}_2, \hat{n}_3, \dots, \hat{n}_d\}$  unit lattice cell, points along  $\mu$ 'th direction.

Forward Lattice Derivative ( $a$  is lattice spacing):

$$(\partial_\mu \phi)_l = \frac{\phi(x + a\hat{n}_\mu) - \phi(x)}{a} = \frac{\phi_{l+\hat{n}_\mu} - \phi_l}{a}$$

Backward Lattice Derivative (transpose of forward lattice derivative):

$$(\partial_\mu \phi)^T = \frac{\phi(x - a\hat{n}_\mu) - \phi(x)}{a} = \frac{\phi_{l-\hat{n}_\mu} - \phi_l}{a}$$

**Lattice Discretization, Lattice State** Divide interval of separation  $a$  creating a discrete coordinate system. At each point read off the value of the continuous counterpart. Field has a constant value over the interval. Lattice is a coordinate, set of points, the values of the field at each lattice point is a lattice state.

field  $\phi = \phi(x)$   $x = al$   $l \in \mathbb{Z}$

Lattice State  $\phi = \{\phi_0, \phi_1, \phi_2, \dots, \phi_{n-1}\}$  "configuration".

**N-Site Periodic Lattice** After N steps, back

$$\sigma^N = I$$

eigenvalues  $\omega = e^{\frac{i2\pi}{N}}$

$$\sigma^N - I = \prod_{k=0}^{N-1} (\sigma - \omega^k I)$$

N distinct eigenvectors, N-dim space (N irrep)

N projection operators

$$P_k = \prod_{j \neq k} \frac{\sigma - \omega^j I}{\omega^k - \omega^j}$$

**Discrete Fourier Transforms** Have a lattice state  $\phi = \{\phi_0, \phi_1, \dots, \phi_{N-1}\}$

Kth Fourier Coeff=projection of  $\phi$  onto eigen vector  $\varphi$

$$\tilde{\phi}_k = \varphi_k^\dagger \cdot \phi = \frac{1}{\sqrt{N}} \sum_{l=0}^{N-1} e^{-\frac{i2\pi}{N}kl} \phi_l$$

**Q19** I think I may have gotten to the point where I can go beyond exclusively reading the paper, what should I do beyond? As well, what times would be good for me to drop in on your Bluejeans office during the week?

**Q20** I believe I've asked this before, or a form of it, but it seems that the periodic boundary condition is in direct conflict with the definition of the shift operator. Am I missing something?

**2020-10-15 Sidney** A reread.

The Bernoulli Shift map is a circle map due to the mod 1 operation for  $[1/s, 1)$  where  $s$  is the "stretching parameter" of the general Bernoulli map:  $\phi_{t+1} = s\phi_t \pmod{1}$ .  $\pmod{1}$  subtracts the integer part of  $s\phi_t$  yielding the "winding number"  $m_{t+1}$ . This keeps  $\phi_{t+1}$  in the unit interval, and divides this interval into  $s$  subintervals. The winding number is also the alphabet of the system, denoting at time  $t$ , it visits interval  $m$ . Brief note from Chaosbook: we can represent a state as a base  $s$  decimal of the resulting visitation sequence:  $\phi_0 = .m_1m_2m_3\cdots$ . The Bernoulli map operates on a state by shifting this itinerary over by one:  $\phi_0 = .m_1m_2m_3\cdots \rightarrow \phi_1 = .m_2m_3\cdots$ . The preimages of critical points (the point which when input into the map yield a maximum value on in the map) partition the map into  $s^n$  subintervals, where  $n$  is the orbit length. There is no pruning in the Bernoulli map, as its critical points are all unity, however, as it is a circle map the first and last fixed point (rightmost fixed point, and the fixed point at the origin) are the same, so they are counted as one fixed point, and thus the number of periodic orbits is  $N_n = s^n - 1$ . There can only be one periodic orbit per subinterval because each subinterval is treated as a single point where a certain orbit is possible, thus, there can only be one orbit. For the temporal Bernoulli, 'Temporal' here refers to the state (field)  $\phi_t$  and the winding number  $m_t$  (source) taking their values on the lattice sites of a 1-dimensional temporal lattice  $t \in \mathbb{Z}$ . Over a finite lattice segment they can be written as a state, and a symbol block. The Bernoulli equation can be written as a first order difference equation  $\phi_t - s\phi_{t-1} = -m_t$  where  $\phi_t$  is contained within the unit interval. This is the condition which each point on the lattice must fulfill. This can then be written in terms of the orbit Jacobian matrix, which is a sum of the identity and cyclic permutation matrix which has the condition  $\sigma^n = I$ . This permutation permutes forward in time the lattice state by one site. The temporal Bernoulli condition can be viewed as a search for zeros of the function involving the orbit Jacobian matrix operating on the lattice state summed with the symbol block  $\mathbf{M}$ . This allows the entire lattice state which solves for zero  $\Phi_M$  to be treated as a single fixed point. The orbit Jacobian matrix stretches the unit hyper cube such that every periodic point is mapped onto an integer lattice  $\mathbb{Z}^n$  site, which is then translated by the winding numbers into the origin to satisfy the fixed point condition. Therefore  $N_n$  the number of solutions to the fixed point condition is the number of lattice sites within the fundamental parallelepiped (fp), which is equivalent to the volume of the fp because each unit cell in the lattice only contains one lattice point. So  $N_n$  is the magnitude of the determinant of

the orbit Jacobian matrix, this is called Hill's Determinant, or the Fundamental Fact. The orbit Jacobian matrix maps the unit hyper cube into the basis vectors of the fundamental parallelepiped which are given by columns of the orbit Jacobian matrix.

**2020-10-18 Sidney** My notes on Barvinok [18] *Lecture notes*

The theory discussed in these lectures are inspired by a few series formulas, the first being:

$$\sum_{m=1}^n x^m = \frac{1 - x^{n+1}}{1 - x}$$

We take the interval  $[0, n)$  and for every integer point in the interval we write the monomial  $x^m$  and then take the sum over each integer point on the interval. It gives a polynomial with  $n+1$  terms, but can be written in the form given, later we will cover doing the same over a 2D plane (evaluating at each integer point on the plane and summing over every integer point  $\mathbf{m} = (m_1, m_2)$  with bivariate monomials  $\mathbf{x}^{\mathbf{m}} = x^{m_1} x^{m_2}$ . The second formula is the infinite geometric series:

$$\sum_m x^m = \frac{1}{1 - x}$$

This makes sense if  $|x| < 1$  similarly

$$\sum_{-\infty}^0 x^m = \frac{1}{1 - x^{-1}} = \frac{-x}{1 - x}$$

This converges if  $|x| > 1$

$$\sum_{m=-\infty}^{\infty} x^m$$

This converges for no values, so we will say that it equals zero, this can be reasoned through as every positive integer added to every negative integer is zero, we then subtract zero, as it was double counted:

$$\sum_{m=-\infty}^{\infty} = \sum_{m=0}^{\infty} x^m + \sum_{m=-\infty}^0 x^m - x^0 = 0$$

This suggestively agrees with

$$\frac{-x}{1 - x} + \frac{1}{1 - x} - 1 = 0$$

Geometrically, the real line  $\mathbb{R}^1$  is divided into two unbounded rays intersecting in a point. For every region (the two rays, the line and the point), we construct a rational so that the sum of  $x^m$  over the lattice points in the region converges to that rational function, if it converges at all.

**2020-10-19 Sidney**

*Inclusion-exclusion principle*

$$|A \cup B| = |A| + |B| - |A \cap B| \quad (10.2)$$

where  $|A \cap B|$  is the number of elements which are in both A and B. This avoids double counting.

If we think of a plane of points, we can draw lines which subdivide the plane, each line makes the plane two half planes, and every two lines form four angles, this forms several regions. Among these regions there are regions  $\mathcal{R}$  where the sum:

$$\sum_{m \in \mathcal{R} \cap \mathbb{Z}^2} \mathbf{x}^m$$

converges for some  $\mathbf{x}$ , and some regions where the sum will never converge.

We shall show that it is possible to assign a rational function to every region simultaneously so that each series converges to the corresponding rational function, if it converges at all, it will also satisfy the inclusion-exclusion principle.

*Definition 1* The scalar product in  $\mathbb{R}^d$  is

$$\sum_{i=1}^d x_i y_i$$

for  $x = (x_1, \dots, x_d)$  and  $y = (y_1, \dots, y_d)$ , and the same for  $\mathbb{Z}^d \subset \mathbb{R}^d$ .

*Definition* Polyhedron P is the set of solutions to finitely many linear inequalities:

$$P = \left\{ \phi \in \mathbb{R}^d : \sum_{i=1}^d a_{ij} x_j \leq b_i \right\}$$

If all  $a_{ij}$  and  $b_j$  are integers the polyhedron is rational.

Barvinok notes concern themselves with the set  $P \cap \mathbb{Z}^d$  of integer points in a rational polyhedron P. He introduces the algebra of polyhedra to account for all relations among polyhedra.

**2020-11-29 Predrag** We only need to understand parallelepipeds, not polyhedra in general. Should be easier.

*Definition 2* For a set  $\mathcal{B} \in \mathbb{R}^d$ , the function

$$[\mathcal{B}](\phi) = \begin{cases} 1 & \text{if } \phi \in \mathcal{B} \\ 0 & \text{otherwise} \end{cases} \quad (10.3)$$

is called the *indicator* of  $\mathcal{B}$ .

**2020-10-24 Sidney**

The intersection of finitely many (rational) polyhedra is a (rational) polyhedron. The union doesn't have to be, but may be a polyhedron.

Union: The union of a collection of sets is the set of all elements in the collection.

Intersection:  $A \cap B$ , is the intersection of two sets A and B, i.e., the set containing all elements of A that also belong to B.

The algebra of rational polyhedra is the vector space  $\mathcal{P}(\mathbb{Q}^d)$  spanned by the indicators  $[P]$  for all rational polyhedra  $P \subset \mathbb{R}^d$

**2020-11-29 Predrag**  $\mathbb{Q}$  is the *field of rationals*.

**2020-10-24 Sidney**

### Valuations

Let  $V$  be a vector space. A linear transformation  $\mathcal{P}(\mathbb{Q}^d) \rightarrow V$  is called a valuation. This course is on the particular valuation  $\mathcal{P}(\mathbb{Q}^d) \rightarrow \mathbb{C}(x_1, \dots, x_d)$ , where  $\mathbb{C}(x_1, \dots, x_d)$  is the space of  $d$ -variate rational functions.

**Theorem 1** There exists a unique valuation  $\chi : \mathcal{P}(\mathbb{R}^d) \rightarrow \mathbb{R}$  called the Euler characteristic, such that  $\chi([P]) = 1$  for any non-empty polyhedron  $P \subset \mathbb{R}^d$

**2020-11-30 Predrag** Klain and Rota [KlaRot97] *Introduction to Geometric Probability*:

A *valuation* on a lattice  $L$  of sets is a function  $\mu$  defined on  $L$  that takes real values, and that satisfies the following conditions:

$$\mu(A \cup B) = \mu(A) + \mu(B) - \mu(A \cap B), \quad (10.4)$$

$$\mu(\emptyset) = 0, \quad (10.5)$$

where  $\emptyset$  is the empty set. By iterating the identity (10.4) we obtain the inclusion-exclusion principle for a valuation  $\mu$  on a lattice  $L$ , namely

$$\begin{aligned} \mu(A_1 \cup A_2 \cup \dots \cup A_n) &= \sum_i \mu(A_i) - \sum_{i < j} \mu(A_i \cap A_j) \\ &\quad + \sum_{i < j < k} \mu(A_i \cap A_j \cap A_k) + \dots \end{aligned} \quad (10.6)$$

for each positive integer  $n$ .

Barvinok [18] Lecture 1, Problem 1 statement of (10.6) is less intelligible: Take sets  $A_1, A_2, \dots, A_n \in \mathbb{R}^d$ . The inclusion-exclusion formula is

$$\mu(\cup A_i) = \sum_I (-1)^{|I|-1} [\cap_{i \in I} A_i], \quad (10.7)$$

where the sum is taken over all non-empty subsets  $I \subset \{1, \dots, n\}$  and  $|I|$  is the cardinality of  $I$ .

**2020-10-25 Sidney**

### Identities in the Algebra of Polyhedra

The image of a polyhedron under a linear transformation is a polyhedron.

**Theorem 1** Let  $P \subset \mathbb{R}^d$  be a polyhedron and let  $T: \mathbb{R}^d \rightarrow \mathbb{R}^k$  be a linear transformation. Then  $T(P) \subset \mathbb{R}^k$  is a polyhedron. Furthermore, if  $P$  is a rational polyhedron and  $T$  is a rational linear transformation (that is, the matrix of  $T$  is rational), then  $T(P)$  is a rational polyhedron.

Linear transformations preserve linear relations among indicators of polyhedra.

**Theorem 2** Let  $T: \mathbb{R}^d \rightarrow \mathbb{R}^k$  be a linear transformation. Then there exists a linear transformation  $T: P(\mathbb{R}^d) \rightarrow P(\mathbb{R}^k)$  such that  $T(P) = [T(P)]$  for every polyhedron  $P \subset \mathbb{R}^d$ .

Most sensible polyhedra have vertices, but some don't.

*Definition 1* Let  $P \subset \mathbb{R}^d$  be a polyhedron. A point  $v \in P$  is called a vertex of  $P$  if whenever  $v = (x + y)/2$  for some  $x, y \in P$ , we must have  $x = y = v$ .

If  $v$  is a point in  $P$ , we define the tangent cone of  $P$  at  $v$  as:

$$co(P, v) = \{x \in \mathbb{R}^d : \epsilon x + (1 - \epsilon)v \in P \text{ for all sufficiently small } \epsilon > 0\}$$

Not all polyhedra have vertices. In fact, a non-empty polyhedron has a vertex if and only if it does not contain a line.

*Definition 2* We say that a polyhedron  $P$  contains a line if there are points  $x$  and  $y$  such that  $y \neq 0$  and  $x + ty \in P$  for all  $t \in \mathcal{R}$ .  $P_0(\mathbb{R}^d) \subset P(\mathbb{R}^d)$  is the subspace spanned by the indicators of rational polyhedra that contain lines.

*Theorem 3* Let  $P \subset \mathbb{R}^d$  be a polyhedron. Then there is a  $g \in P_0(\mathbb{R}^d)$  such that

$$[P] = g + \sum_v [co(P, v)]$$

Where the sum is taken over all vertices  $v$  of  $P$ . If  $P$  is a rational polytope then we can choose  $g \in P_0(\mathbb{Q}^d)$

*Definition 3-0* A polytope is a high dimensional generalization of a polyhedron.

*Definition 3* Let  $A \subset \mathbb{R}^d$  be a non-empty set. the set

$$A^o = \{y \in \mathbb{R}^d : \langle x, y \rangle \leq 1 \text{ for all } x \in A\}$$

is called the polar of  $A$ . Where  $\langle x, y \rangle$  is the inner product.

## 2020-10-27 Sidney

A set  $S$  in a vector space over  $\mathbb{R}^d$  is convex, if the line segment connecting any two points in  $S$  lies entirely within  $S$ . If  $P$  is a rational polyhedron then  $P^o$  is also a rational polyhedron.

**Theorem 4** There exists a linear transformation  $D: P(\mathbb{Q}^d) \rightarrow P(\mathbb{Q}^d)$  such that  $D[P] = [P^o]$  for every non-empty polyhedron  $P$ .

It follows from Theorem 4 that whenever we have a linear identity  $\sum_{i=1}^m \alpha_p [P_i] = 0$  among the indicator functions of polyhedra, we have the same identity  $\sum_{i=1}^m \alpha_p [P_i^o] = 0$  for the indicator functions of their polars.

For an integer point  $m = (m_1, \dots, m_d)$  we introduce the monomial  $\mathbf{x}^m = x_1^{m_1} \cdots x_d^{m_d}$ . Given a set  $S \subset \mathbb{R}^d$ , we consider the sum

$$f(S, \mathbf{x}) = \sum_{m \in S \cap \mathbb{Z}^d} \mathbf{x}^m$$

Our goal is to find a reasonably short expression for this sum as a rational function in  $\mathbf{x}$

**Example 1** Let  $\mathcal{R}_+^d$  be the non-negative orthant, that is the set of all points with all coordinates non-negative. We have

$$\sum_{m \in \mathbb{R}_+^d \cap \mathbb{Z}^d} \mathbf{x}^m = \left( \sum_{m_1=0}^{\infty} x_1^{m_1} \right) \cdots \left( \sum_{m_d=0}^{\infty} x_d^{m_d} \right) = \prod_{i=1}^d \frac{1}{1 - x_i}$$

provided that  $|x_i| < 1$

*Definition* Let  $u_1, \dots, u_d \in \mathbb{Z}^d$  be linearly independent integer vectors. The simple rational cone generated by  $u_1, \dots, u_d$  is the set:

$$K = \left\{ \sum_{i=1}^d \alpha_i u_i : \alpha_i \geq 0 \text{ for } i = 1, \dots, d \right\}$$

The fundamental parallelepiped of  $u_1, \dots, u_d$  is the set

$$\Pi = \left\{ \sum_{i=1}^d \alpha_i u_i : 1 > \alpha_i \geq 0 \text{ for } i = 1, \dots, d \right\}$$

**Theorem** For a simple rational cone  $K = K(u_1, \dots, u_d)$  we have

$$f(K, \mathbf{x}) = \left( \sum_{m \in \Pi \cap \mathbb{Z}^d} \mathbf{x}^m \right) \prod_{i=1}^d \frac{1}{1 - \mathbf{x}^{u_i}}$$

**Theorem** The number of integer points in the fundamental parallelepiped is equal to its volume.

**Sketch of Proof** Let  $\Lambda$  be the set of all integer combinations of  $u_1, \dots, u_d$ :

$$\Lambda = \left\{ \sum_{i=1}^d \alpha_i u_i : \alpha_i \in \mathbb{Z} \text{ for } i = 1, \dots, d \right\}$$

Let us consider all translates  $\Pi + u$  with  $u \in \Lambda$ . We claim that  $\Pi + u$  can cover all  $\mathbb{R}^d$  without overlapping, this can be extracted from the proof of theorem 1. Let us take a sufficiently large region  $X \subset \mathbb{R}^d$  and let us count the number of integer point in  $X$ , the set is roughly covered by  $\text{vol} X / \text{vol} \Pi$  translations of the parallelepiped, and each translation carries the same number of points hence we must have  $|\Pi \cap \mathbb{Z}^d| = \text{vol} \Pi$ .

**2020-11-30 Sidney** I understand your comments. Thank you, I am pretty sure that the general polyhedra stuff can be put in terms of parallelepipeds, so at least it wasn't wasted knowledge, but I'm glad that I don't need to know all of it, it's on the edge of my proof abilities.